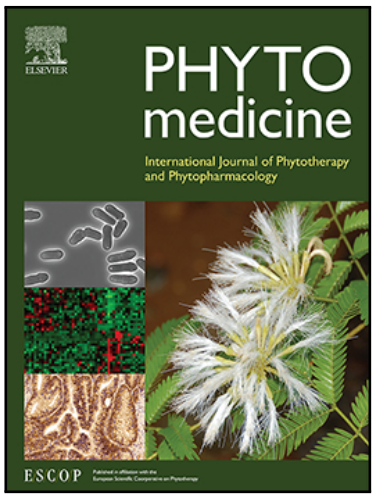

Advances in antitumor activity and mechanism of natural steroidal saponins: A review of advances, challenges, and future prospects

Fengge Wang , Lu Liang , Ma Yu , Wenjie Wang , Iftikhar Hussain Badar , Yongping Bao , Kai Zhu , Yanlin Li , Saba Shafi , Dangdang Li , Yongchao Diao , Thomas Efferth , Zheyong Xue , Xin Hua

PII: S0944-7113(24)00097-7
DOI: https://doi.org/10.1016/j.phymed.2024.155432
Reference: PHYMED 155432

To appear in: *Phytomedicine*

Received date: 12 August 2023
Revised date: 11 January 2024
Accepted date: 6 February 2024

Please cite this article as: Fengge Wang , Lu Liang , Ma Yu , Wenjie Wang , Iftikhar Hussain Badar , Yongping Bao , Kai Zhu , Yanlin Li , Saba Shafi , Dangdang Li , Yongchao Diao , Thomas Efferth , Zheyong Xue , Xin Hua , Advances in antitumor activity and mechanism of natural steroidal saponins: A review of advances, challenges, and future prospects, *Phytomedicine* (2024), doi: https://doi.org/10.1016/j.phymed.2024.155432

Advances in antitumor activity and mechanism of natural steroidal saponins: A review of advances, challenges, and future prospects

Fengge Wang[ab, &], Lu Liang[c, &], Ma Yu[d, &], Wenjie Wang[ab], Iftikhar Hussain Badar[ef], Yongping Bao[g], Kai Zhu[ab], Yanlin Li[ab], Saba Shafi[ab], Dangdang Li[ab], Yongchao Diao[ab], Thomas Efferth[h,*] Zheyong Xue[ab,*], Xin Hua[ab,*]

[a.] College of Life Science, Northeast Forestry University, Harbin, Heilongjiang 150040, China.

[b.] Key Laboratory of Saline-alkali Vegetation Ecology Restoration, Ministry of Education, Harbin, Heilongjiang 150040, China.

[c.] Guangzhou Municipal and Guangdong Provincial Key Laboratory of Molecular Target & Clinical Pharmacology, the State & NMPA Key Laboratory of Respiratory Disease, School of Pharmaceutical Sciences & The Fifth Affiliated Hospital, Guangzhou Medical University, Guangzhou, 511436, PR China.

[d.] School of Life Science and Engineering, Southwest University of Science and Technology, 59 Qinglong Road, Mianyang 621010, Sichuan, China.

[e.] College of Food Science, Northeast Agricultural University, Harbin, Heilongjiang 150030, China.

[f.] Department of Meat Science and Technology, University of Veterinary and Animal Sciences, Lahore 54000, Pakistan.

[g.] Norwich Medical School, University of East Anglia, Norwich Research Park, Norwich NR4 7UQ, United Kingdom.

[h.] Department of Pharmaceutical Biology, Institute of Pharmaceutical and Biomedical Sciences, Johannes Gutenberg University, Mainz 55128, Germany

[&]These authors contributed equally to this work

***Correspondence:**

Xin Hua

Northeast Forestry University

Hexing Rd. 26

150040 Harbin

China

Tel: +86-0451-82191535

huaxin@nefu.edu.cn

Zheyong Xue

Northeast Forestry University

Hexing Rd. 26

150040 Harbin

China

Tel: +86-0451-82191535

zyxue@nefu.edu.cn

Thomas Efferth

Johannes Gutenberg University

Staudinger Weg 5

55128 Mainz

Germany

Tel: 06131-39-25751

efferth@uni-mainz.de

Conflict Of Interest

The authors declare not to have any conflicts of interest.

Abstract：

Background: Cancer, the second leading cause of death worldwide following cardiovascular diseases, presents a formidable challenge in clinical settings due to the extensive toxic side effects associated with primary chemotherapy drugs employed for cancer treatment. Furthermore, the emergence of drug resistance against specific chemotherapeutic agents has further complicated the situation. Consequently, there exists an urgent imperative to investigate novel anticancer drugs. Steroidal saponins, a class of natural compounds, have demonstrated notable antitumor efficacy. Nonetheless, their translation into clinical applications has remained unrealized thus far. In light of this, we conducted a comprehensive systematic review elucidating the antitumor activity, underlying mechanisms, and inherent limitations of steroidal saponins. Additionally, we propose a series of strategic approaches and recommendations to augment the antitumor potential of steroidal saponin compounds, thereby offering prospective insights for their eventual clinical implementation.

Purpose: This review summarizes steroidal saponins' antitumor activity, mechanisms, and limitations.

Methods: The data included in this review are sourced from authoritative databases such as PubMed, Web of Science, ScienceDirect, and others.

Results: A comprehensive summary of over 40 steroidal saponin compounds with

proven antitumor activity, including their applicable tumor types and structural characteristics, has been compiled. These steroidal saponins can be primarily classified into five categories: spirostanol, isospirostanol, furostanol, steroidal alkaloids, and cholestanol. The isospirostanol and cholestanol saponins are found to have more potent antitumor activity. The primary antitumor mechanisms of these saponins include tumor cell apoptosis, autophagy induction, inhibition of tumor migration, overcoming drug resistance, and cell cycle arrest. However, steroidal saponins have limitations, such as higher cytotoxicity and lower bioavailability. Furthermore, strategies to address these drawbacks have been proposed.

Conclusion: In summary, isospirostanol and cholestanol steroidal saponins demonstrate notable antitumor activity and different structural categories of steroidal saponins exhibit variations in their antitumor signaling pathways. However, the clinical application of steroidal saponins in cancer treatment still faces limitations, and further research and development are necessary to advance their potential in tumor therapy.

Keywords: Antitumor mechanisms; Cancer; Phytochemistry; Phytotherapy; Steroidal saponins

Abbreviations: DA, Dioscin-6'-O-acetate; TTB2, Pennogenin 3-O-α-L-rhamnopyranosyl-(1→2) [α-L-rhamnopyranosyl-(1→4)]-β-D-glucoyranoside; DT-13, Saponin monomer 13 of the Dwarf lilyturf tuber; SPD, 5β-Spirost-25(27)-en-1β,3β-diol-1-O-α-L- rhamnopyranosyl-(1→2)-β-D-xylopyranosyl-3-O-α-L-rhamnopyranoside; A-24, Steroidal saponin from Allium; T-17, A spirostanol saponin extracted from *Rohdea chinensis*; RCE-4, A steroidal saponin isolated from *Reineckia carnea*; FSAC, 26-

O-β-d-glucopyranosyl-22α-hydroxyl-(25R)-Δ5(6)-furost-3β,26-diol-3-O-α-l-rhamnopyranosyl-(1→2)-[β-dglucopyranosyl-(1→4)-α-l-rhamnopyranosyl-(1→4)]-β-d-glucopyranoside; SL-01, Prodrug of gemcitabine; D07001-F4, Oral gemcitabine formulation; THU, 3,4,5,6-Tetrahydrouridine.

1. Introduction

According to the World Health Organization, cancer is the second most common cause of death globally, following cardiovascular ailments. Every year, over 10 million people surrender to this disease, with the most prevalent types being lung, prostate, breast, colorectal, cervical, stomach, and liver cancers (Kim and Kim, 2018; Zaimy et al., 2017). The continuous spread of cancer imposes tremendous physical, emotional, and financial stress on individuals, families, communities, and health systems. Currently, chemotherapy is the most common clinical treatment for cancer. However, common chemotherapeutic drugs like doxorubicin and cisplatin often come with significant side effects. Considering the successful clinical application of natural products, such as paclitaxel, in antitumor therapy, there is a growing recognition of the immense potential of natural compounds. Therefore, there is an urgent need to systematically screen natural compounds for their low toxicities, aiming to discover effective and safer anti-cancer treatment options (Condello and Meschini, 2021; Abu Samaan et al., 2019).

In the United States, substantial epidemiologic evidence suggests that over 50% of approved anticancer drugs, such as retinoids and podophyllotoxin, are derived from natural compounds or are derivatives of natural products derived from herbs (Ma et al., 2021). Studies have shown that natural compounds such as polyphenols, flavonoids, monoterpenes and triterpenes, sulfur compounds, cellulose, and saponins can inhibit the growth and proliferation of tumor cells (Elekofehinti et al., 2021; Ma et al., 2021). Steroidal saponins also have significant antitumor activity as natural compounds, *i.e.*,

diosgenin, rhizosgenin, anemosgenin, and some steroidal alkaloids. Notably, the anticancer activity of steroidal saponin OSW-1 isolated from *Ornithogalum caudatum* Jacq. of the lily family is 10-100 times stronger than that of gemcitabine, cisplatin, camptothecin, and other anti-cancer drugs currently used clinically, making it a potent anticancer active substance (Chiu et al., 2018; Zhang et al., 2017b).

The antitumor effects of steroids have been shown in various cancer cell lines, such as breast, colon, lung, and neuroblastoma (Yao et al., 2020). Their antitumor mechanisms include inhibition of proliferation, induction of apoptosis and autophagy, inhibition of tumor invasion and metastasis, and inhibition of tumor multidrug resistance (Liu et al., 2023).

Saponins in the field of antitumor activity possess a series of advantages, however, they also have some disadvantages. For instance, the lack of clinically applicable saponins, unclear key targets of their pharmacological actions, and high toxicity to normal cells (Tong et al., 2012). Moreover, the low content of steroidal saponins in plants with complex structures is difficult to obtain by chemical synthesis methods as well as its bioavailability is low (< 10%) (Pei et al., 2020)(Upadhyay et al., 2018; Zhang et al., 2018a). All these factors limit the further clinical application of steroid saponins. Therefore, this paper presents a detailed and critical review of the structural characteristics, antitumor activity and mechanism of steroidal saponins, and their limiting factors to provide valuable suggestions for clinical application in the future.

2. Structure and antitumor activity of steroidal saponins

A class of naturally occurring compounds known as steroidal saponins is

extensively present in medicinal plants (Sidana et al., 2016; Sparg et al., 2004; Tang et al., 2020; Thimmappa et al., 2022; Tian et al., 2017). Most monocotyledons, including Liliaceae, Agavaceae, Dioscoreaceae, and Amaryllidaceae, contain plant steroidal saponins (Pérez et al., 2013; Xu et al., 2023).

Steroidal saponin elements are six-membered ring compounds with 27 carbon atoms, primarily consisting of glycosidic elements and glycoside groups. The A, B, C, and D rings are the basic parent nuclei of steroids with perhydrocyclopentanophenanthrene structure, and the E and F rings are connected in spiroketals. Based on the structures of the sapogenins, steroidal saponins are mainly divided into different types such as spirostanol, isospirostanol, furostanol, steroidal alkaloids, and cholestanes (Chen et al., 2020; Hassani-Nezhad-Gashti et al., 2019; Xiang et al., 2019; Xu et al., 2021b; Zhang et al., 2013a; Zhang et al., 2021d).

2.1 Spirostanol type

It is a class of steroidal saponin elements in which the C-25 methyl group is located in the ring plane with an upright bond of β-type and whose absolute configuration is L-type. We mainly introduced timosaponin AIII, aspiletrein A, asparanin A, aspafilioside B, RCE-4, spicatoside A, liriopesides B, and T-17, as spirostanol-type steroidal saponins (Fig. 1) and summarized their antitumor activity and mechanisms (Table 1).

Sarsasapogenin and its derivatives, such as timosaponin AIII, aspiletrein A, asparanin A, and aspafilioside B (Mustafa et al., 2022) are representatives of spirostanol-type steroidal saponins with great antitumor activity. Timosaponin AIII is found in *Anemarrhena asphodeloides* Bunge modified by glycosylation at the C-3

position of sarsasapogenin. A disaccharide was formed by attaching D-galactose to D-glucose at the glycosyl site, with IC_{50} of 1.37 μM and 15.33 μM against K562 and A549 cells. Moreover, asparanin A, aspiletrein A, and aspafilioside B were also produced by glycosylation modification from the C-3 position of sarsasapogenin. The glycosyl of asparanin A consisted of D-glucose and had a strong inhibitory effect on uterine endometrial cancer cells and hepatocellular carcinoma cells, *e.g.,* its IC_{50} was 9.34 μM for Ishikawa cells and 6.2 μM for HepG2 cells, respectively. The glycosyl group of aspiletrein A consisted of L-rhamnose, D-xylose, and D-glucose. It also showed a significant inhibitory effect on A549 lung cancer cells with an IC_{50} of 8.78 μM. The glycosyl group of aspafilioside B consisted of D-glucose, D-xylose, and L-arabinose, and its IC_{50} for HepG2 cells, Huh7 cells, BEL7402 cells, and SMMC-7721 cells were 17.78 μM, 13.12 μM, 16.32 μM, and 21 μM, respectively.

Additionally, the saponin component of RCE-4 is derived from the hydroxylation of sarsasapogenin's C-1 position, modified by glycosylation at the C1 position. L-rhamnose and D-xylose comprise RCE-4's glycosyl portion, inhibiting cervical cancer cells, *e.g.,* its IC_{50} on Hela cells was 7.01 μM. The glycosides of spicatoside A and liriopesides B are identical, and their glycosides are sarsasapogenin hydroxylated at the C1 position as well as double-bonded between the C5 and C6 positions D-glucose, D-xylose and D-fucose makeup the glycosyl group of spicatoside A, which had a strong inhibitory effect on HCT116 colon cancer cells with an IC_{50} of 13.8 μM. The glycosyl group of liriopesides B consisted of L-rhamnose and D-fucose, and its IC_{50} against ovarian cancer A2780 cells was 29.355 μM. T-17 is one of the spirostanol-type steroidal

saponins, and its glycosyl group consists of L-rhamnose and D-xylose, strongly inhibiting gastric cancer cells. For example, its IC_{50} on SGC-7901 cells was 8.56 μM (Ramalingam and Kim, 2016; Xu et al., 2021b; You et al., 2021; Yu et al., 2020). Based on the findings presented above, it can be concluded that spirostanol-type steroidal saponins exhibit significant antitumor activity at IC_{50} concentrations, mainly below 30 mM (Fig 2a). These results suggest that spirostanol-type steroidal saponins possess great potential as antitumor agents.

2.2 Isospirostanol type

When the C-25 methyl group of steroid saponin is located under the ring plane of the flat volt bond for α type, its absolute configuration is D type, called isospiranol steroid saponin. The isospirostanol type has various derivatives with good antitumor activity, including diosgenin, pennogenin, ruscogenin, hecogenin, and tigogenin derivatives (Fig 1). Their antitumor activity and mechanisms are shown in Table 1.

The glycosylated derivatives of diosgenin include dioscin, polyphyllin I, polyphyllin II, gracillin, deltonin, progenin III, trillin, and sprengerinin C (Ali et al., 2013; Passos et al., 2022; Thapa et al., 2022; Zeng et al., 2013). All these steroidal saponins are modified by glycosylation at the C-3 position of the diosgenin, where the glycosyl groups of dioscin, gracillin, polyphyllin II, deltonin, and progenin III are composed of L-rhamnose as well as D-glucose. These five steroidal saponins have good antitumor activity. For example, the IC_{50} of dioscin against A375 melanoma cells was 1.54 μM, of gracillin against A549 lung cancer cells was 2.54 μM, of polyphyllin II against BEL7402 liver cancer cells 4.4765 μM, and of deltonin against SW-480 colon

cancer cells 1.3 μM. Progenin III had an IC_{50} of 1.59 μM against CCRF-CEM leukemia cells. Trillin is derived from the C3 position of diosgenin linked to D-glucose, and the IC_{50} of trillin against HepG2 hepatoma cells was 17.84 μM. The glycosyl group of sprengerinin C, consisting of L-rhamnose, D-glucose, and D-xylose, significantly inhibited HepG-2 hepatocellular carcinoma cells. The glycosyl group of polyphyllin I consists of L-rhamnose, D-glucose, and L-arabinose, and its IC_{50} against HGC27 gastric cancer cells was 0.55 μM.

Pennogenin is hydroxylated at the diosgenin's C-17 position, and its derived steroidal saponins, primarily polyphyllin VI, polyphyllin VII, polyphyllin H, and 3-O-α-L-rhamnopyranosyl-(1→2) [-L-rhamnopyranosyl-(1→4)]-β-D-glucoyranoside (TTB2) are also glycosylated from the C-3 position (Thapa et al., 2022; Zou and Huang, 2018). L-rhamnopyranose and D-glucose comprise the glycosyl groups of polyphyllin VI, polyphyllin VII, and TTB2. These three steroidal saponins have potent antitumor activity. For example, polyphyllin VI had an IC_{50} of 7.33 μM against U2OS osteosarcoma cells, and polyphyllin VII had an IC_{50} of 0.58 μM against K562 leukemia cells as well as TTB2 also showed significant inhibitory effects against A549 lung cancer cells. L-arabinose, L-rhamnose, and D-glucose are glycosyl groups of polyphyllin H and significantly inhibited U251 glioma cells.

Ruscogenin was modified by hydroxylation at the C-1 position of diosgenin, and its derivatives ophiopogonin-D, ophiopogonin-B, and DT-13 were all modified by glycosylation at the C-1 position (Masullo et al., 2016; Passos et al., 2022). The L-rhamnose and D-fucose make-up ophiopogonin -B glycosyl group had an IC_{50} of 10.27

μM against AGS gastric cancer cells. The ophiopogonin-D glycosyl group contained D-xylose, L-rhamnose, and D-fucose, and its IC_{50} for MDAMB-231 breast cancer cells was 10.52 μM. DT-13 is the 13th saponin extracted from the lily tuber, its glycosyl group consisted of D-glucose, D-xylose, and D-fucose, and its IC_{50} against PC3 prostate cancer cells was 4.825 μM. Moreover, some hecogenin and tigogenin derivatives are mainly terrestrosin D and macrostemonoside A (Qiu et al., 2019; Wang et al., 2013d). Terrestrosin D which is derived from the C3 position of hecogenin linked to D-glucose, D-xylose, and D-galactose strongly inhibited PC3 prostate cancer cells with an IC_{50} below 5 μM. However, macrostemonoside A derived from tigogenin at the C1 position from both D-glucose and D-galactose also showed a significant inhibitory effect on SW480 colon cancer cells.

SPD and A-24 are other isospirostanol-type steroidal saponins. A-24 is a methylation from tigogenin's C13 position to its C17 position and is linked to D-glucose and D-galactose at the C3 position with an IC_{50} of 2.18 μM against AGS gastric cancer cells. The SPD saponin element was modified by converting tigogenin's single-bond linkage between the C25 and C27 positions to a double-bond linkage and hydroxylation at the C1 position, and its glycosyl group consisted of L-rhamnose and D-xylose. SPD significantly inhibited HL-60 promyelocytes with an IC_{50} of 4.7 μM. In conclusion, isospirosteroidal saponins had significant antitumor activity with IC_{50} values mainly below 15 μM (Fig 2 a). The antitumor effect of isospirosteroidal saponins was significantly higher than that of spirosteroidal saponins, suggesting that they have excellent application potential.

2.3 Furosterol type

Furostanol steroidal saponins are spirostanol or isospirostanol-like F-ring opening compounds that introduce α-OH or α-OCH_3 at the C-22 position and have β-0H at the C-26 position to form furostanol steroidal saponins. Protodioscin, methyl protodioscin, aspidsaponins A, glauco-chinaosides A/B/E and 26-O-β-d-glucopyranosyl-22α-hydroxyl-(25R)-Δ5(6)-furost-3β,26-diol-3-O-α-l-rhamnopyranosyl-(1→2)-[β-d-glucopyranosyl-(1→4)-α-l-rhamnopyranosyl-(1 → 4)]-β-d glucopyranoside are the main furostanol-type steroidal saponins (Fig. 1) (Lee et al., 2015; Passos et al., 2022). We summarized their antitumor activity and mechanisms in Table 1. Protodioscin is mainly a proto-diosgenin that connects L-rhamnose and D-glucose at the C3 position and C26 position, whereas methyl protodioscin is derived from hydroxymethylation of protodioscin at the C22 position. It had significant inhibitory effects with an IC_{50} of 18.49 μM against HeLa cells. Aspidsaponins A mainly modified with D-glucose and D-galactose at the C3 position of its sapogenins and D-glucose at the C26 position showed a strong inhibitory effect on A549 lung cancer cells with an IC_{50} of 5.1 μM. Glauco-chinaosides A/B/E were all modified with L-rhamnose and D-glucose at the C3 position of their saponin elements and D-glucose at the C26 position of their saponin elements, and these three furostanol-types steroidal saponins inhibited SGC-7901 gastric cancer cells with IC_{50} of 2.7 μM, 11.5 μM, and 6.8 μM, respectively. In addition, 26-O-β-d-glucopyranosyl-22 α-hydroxyl-(25R)-Δ5(6)-furost-3 β,26-diol-3-O-α-l-rhamnopyranosyl-(1→2)-[β-d-glucopyranosyl-(1→4)-α-l rhamnopyranosyl-(1→4)]-β-d-glucopyranside also showed strong inhibitory effects on MHCC97H hepatocellular

carcinoma cells and H1299 lung cancer cells with IC_{50} of 4.15 μM and 5.26 μM, respectively. Furostanol steroid saponins were found frequently with IC_{50} values below 20 μM, indicating a strong antitumor effect (Fig. 2 a).

2.4 Steroidal alkaloids with cholesterol type

Steroidal alkaloids are mainly found in plants of the Solanaceae, Bufonidae, Apocynaceae, and Liliaceae families (Huang et al., 2021). As shown in Fig. 1, we have reviewed solanidine and tomatidine and their derivatives (Friedman, 2015; Hameed et al., 2017) and focused on their antitumor activities and mechanisms (Table 1). Solanidine derivatives primarily include solanine, α-solanine, and α-chaconine, synthesized by linking D-glucose and L-rhamnose at the C3 position of solanidine. These steroidal saponins have significant antitumor activity with IC_{50} against PC3 prostate cancer cells of 12 μM (α-solanine) and RL95-2 endometrial cancer cells of 4.72 μM (α-Chaconine). α-Tomatine is a derivative of tomatidine formed by linking D-xylose, D-glucose, and D-galactose at the C3 position of tomatidine. α-Tomatine inhibits PC3 cells with an IC_{50} of 1.67 μM. Considering the antitumor activity of the aforementioned steroidal alkaloids, we found that the antitumor IC_{50} of steroidal alkaloids was mainly below 40 μM (Fig 2 a), with some antitumor activity. This paper also summarizes the antitumor cholestane glycoside compounds, such as OSW-1 and Cholestane-3β-5α-6β-triol (Fig. 1) (Silvente-Poirot and Poirot, 2012; Subramaniam et al., 2021; Tang et al., 2013). We found that OSW-1 had highly significant antitumor activity compared to other types of steroidal saponins (Table 1) with IC_{50} values at the nM level (Fig 2 a); for example, the IC_{50} of OSW-1 in MCF-7 breast cancer cells was

3.72 nM. However, the IC_{50} of OSW-1 on normal mammary cells also reached the nM level, e.g., the IC_{50} of OSW-1 on MCF10A cells was 52.3 nM. In the SCID mouse tumor model, OSW-1 only reduced the tumor volume by 1-2-fold, which demonstrated the general antitumor effect of OSW-1 in the SCID mouse tumor model (Ding et al., 2020b). While OSW-1 has shown promising antitumor effects in vitro, its potent toxicity to normal cells and moderate antitumor effects in vivo suggest that further improvements are necessary before it can be considered for clinical use.

2.5 Comparison of the antitumor activity of steroidal saponins in cell lines with different types of tumors

Researchers have studied the antitumor effects of five types of steroidal saponin compounds and found that their efficacy varies. The spirostanol-type, furostanol-type, and steroidal-alkaloid types had no significant difference in antitumor effect compared to the furostanol-type. However, the isospirostanol-type had a significantly higher antitumor effect when compared to the spirostanol-type and steroidal alkaloids. OSW-1 in cholestane was found to possess significant antitumor activity. Furthermore, cholestane glycosides were found to have a significantly higher antitumor effect when compared with the other four steroidal saponins (Fig. 2 a).

The main organ-specific cancer types are leukemia, lung cancer, cervical carcinoma, skin cancer, brain cancer, colon cancer, bladder cancer, breast cancer, gastric cancer, endometrial cancer, ovarian cancer, liver cancer, and prostatic cancer. Furthermore, it was found that the IC_{50} values of steroidal saponins for these cancer types was below 30 μM, with a sensitivity of steroidal saponins for bladder cancer being

significantly higher than that for liver cancer (Fig. 2 c) compared to other cancer types where the IC_{50} values were not significantly different from each other. This indicates that steroidal saponins have a broad spectrum of anticancer effects and can target a variety of cancers.

After analyzing the IC_{50} values of tumor inhibition by steroidal saponins in each cancer type, there were no significant differences in the inhibitory effects toward carcinoma, sarcoma, and leukemia. In carcinoma, cholestane glycosides were found to be more effective in inhibiting tumor growth than spirostanol-type, furostanol-type, and steroidal alkaloids but not significantly different from isospirostanol. There was no significant difference in the antitumor effect of spirostanol-type and isospirostanol-type steroidal saponins in sarcoma and leukemia cells. Both types had IC_{50} values below 15 μM and 25 μM, respectively. Hematopoietic tumors (leukemia) and solid tumors (carcinoma and sarcoma) showed no significant difference in the inhibitory effects of steroidal saponins. The antitumor effects of steroidal saponins were essentially similar across all three types of tumors (Fig. 2 b).

Based on the findings, it can be concluded that steroidal saponins inhibit a broad spectrum of tumors, and isospirostanol-type steroidal saponins with cholestane glycosides have significant antitumor effects. Therefore, we will focus on the mechanisms of the steroidal saponin structure type, which will also be helpful for the derivatization of steroidal saponins and the design of novel antitumor drugs.

Table 1 Antitumor activity and mechanisms of action of steroidal saponins.

Structure	Chemical compound	Cells/IC_{50}	Activities/aignal pathway/affected protein	Ref
Spirostane	Aspafilioside B	HepG2: 17.780 μM (24 h) Huh7: 13.120 μM (24 h) BEL7402: 16.320 μM (24 h) SMMC-7721: 21.000 μM (24 h)	Apoptosis/cell cycle arrest, RAS/c-Raf/ERK /p38	(Liu et al., 2016)
	Asparanin A	Ishikawa (N/A)	Apoptosis/autophagy, ERK/ATF4, P53	(Zhang et al., 2021c)
	Asparanin A	Ishikawa: 10.000 μM (24 h)	Antimetastasis, RAS/ERK/MAPK	(Zhang et al., 2021b)
	Asparanin A	Ishikawa: 9.340 μM (24 h)	Apoptosis/cell cycle arrestr, PI3K/Akt/mTOR, BAK/BCL-XL, cytochrome C, caspases	(Zhang et al., 2020a)
	Asparanin A	HepG2: 6.200 μM (24 h) 4.110 μM (48 h) 2.900 μM (72 h)	Cell cycle arrest, cyclin A, CDK4, p21WAF1/C -IP1, p-CDK1, PARP, caspase-3/8/9	(Liu et al., 2009)
	Aspiletrein A	LU-1: 9.940 μM (24 h) H460: 15.130 μM (24 h) H23: 10.100 μM (24 h) A549: 8.780 μM (24 h)	Antimetastasis, PI3K/Akt	(Nguyen et al., 2021)
	Liriopesides B	A2780 (N/A)	Apoptosis/antimetastasis, E-cadherin, P21, P27, Bcl-2	(Yu et al., 2020)
	Liriopesides B	A2780: 29.355μM (48 h)	antiproliferative, CA125, AKP	(Wang et al., 2017a)
	Liriopesides B	H460; H1975 (N/A)	Apoptosis/cell cycle arrest, Bcl-2/Bcl-XL/Bax, caspase-3/8	(Sheng et al., 2020)
	RCE-4	HeLa: 7.010 μM (24 h) A549: 9.020 μM (24 h) MCF7: 10.060 μM (24 h)	Apoptosis, PI3K/AKT/mTOR, NF-κB, Bax/ Bcl2	(Bai et al., 2016)
	RCE-4	Ca-Ski (N/A)	Autophagy/apoptosis, Bcl2/Beclin 1, Lc3-II/Lc -3-I, Bax, caspase-3/7/9	(You et al., 2021)
	RCE-4	CaSki: 3.370 μM (48 h)	Apoptosis, Bax/Bcl2	(Wang et al., 2013a)
	RcE-4	CaSki: 4.180 μM (48 h)	Autophagy, AMPK/mTOR/ULK1, RAS/c-raf/E -RK1/2, PI3K/Akt/mTOR	(Xiang et al., 2020)
	T-17	SGC-7901; AGS (N/A)	Apoptosis/autophagy/antimetastasis, P53, caspa -se 3, PARP, LC3-II, MMP-2/9	(Xu et al., 2021b)
	T-17	SGC-7901: 8.560 μM (24 h) AGS: 7.350 μM (24 h) MGC-803: 8.920 μM (24 h) NCI-N87: 9.330 μM (24 h)	Apoptosis/cell cycle arrest, P21, cyclin 2, caspa -se	(Xu et al., 2020a)

	BGC-823: 8.860 μM (24 h)		
Spicatoside A	A549: 26.000 μM (72 h) HCT116: 13.800 μM (72 h) MDA-MB-231: 29.600 μM (72 h) SNU-638: 14.800 μM (72 h) SK-HEP-1: 15.500 μM (72 h)	Autophagy/apoptosis, PI3K/Akt/mTOR, MAP-K, Bcl-2/Bax, Bid, cytochrome C, PARP, LC3-I-I, p62, Beclin 1	(Kim et al., 2016b)
Sarsasapogenin	HepG2 (N/A)	Apoptosis	(Bao et al., 2007)
Sarsasapogenin	HeLa (N/A)	Apoptosis, UPR, CHOP, Bax/Bcl-2, cytochrom-e C, caspases	(Shen et al., 2013)
Timosaponin AIII	K562: 1.370 μM (24 h)	Reversing tumor resistance, PI3K/Akt, MDR1, MRP1	(Chen et al., 2016a)
Timosaponin AIII	PANC-1; BxPC-3 (N/A)	Apoptosis/cell cycle arrest, PI3K/Akt, caspase-3	(MarElia et al., 2018)
Timosaponin AIII	MG63 (N/A)	Apoptosis/antimetastasis, JNK, p38, ERK, β-ca-tenin, CREB, MMP-2/9	(Lee, 2020)
Timosaponin AIII	MG63 (N/A)	Apoptosis, FAK/Src, ERK1/2, JNK, P38, β-cate-nin, caspase-3/7	(Jung and Lee, 2019)
Timosaponin AIII	HL-60 (N/A)	Apoptosis/cell cycle arrest, PI3K/AKT, Wnt/β-catenin, cyclin D1, C-myc, caspase-3	(Zhang et al., 2017a)
Timosaponin AIII	A375-S2 (N/A)	Apoptosis/autophagy, JNK/C-Jun, ERK	(Wang et al., 2017b)
Timosaponin AIII	HepG2 (N/A)	Apoptosis, HtrA2/Omi, Smac/Diablo, cytochro-me C, IAP	(Nho et al., 2016)
Timosaponin AIII	HL-60 (N/A)	Apoptosis, JNK1/2/C-Jun	(Huang et al., 2015b)
Timosaponin AIII	A549/T: 5.120 μM (24 h) A2780/T: 4.640 μM (24 h)	Apoptosis/reversing tumor resistance, PI3K/Ak-t/mTOR, RAS/Raf/MEK/ERK	(Song et al., 2019)
Timosaponin AIII	143-B: 8.600 μM (24 h) 7.800 μM (48 h) HOS: 8.300 μM (24 h) 7.200 μM (48 h)	Antimetastasis, αVβ3/FAK/Src/F-actin, TESK1/p-cofilin/F-actin	(Hsieh et al., 2021a)
Timosaponin AIII	B16-F10; WM-115 (N/A)	Antimetastasis, NF-κB/COX-2/PGE2	(Kim et al., 2016a)
Timosaponin AIII	786-O; a-498 (N/A)	Antimetastasis, PI3K/Akt, CTSC	(Chiang et al., 2019)
Timosaponin AIII	A549: <10 μM (24 h)	Antimetastasis, ERK1/2、Src/FAK, β-catenin, MMP-2/9	(Jung et al., 2016)
Timosaponin AIII	MDA-MB-231: 2.000 μM (48 h)	Inhibit oncogenic phenotype, c-Myc/Bmi1, Pc-G	(Gergely et al., 2018)
Timosaponin AIII	AsPC-1 (N/A)	Apoptosis/cell cycle arrest, Bcl-2/Bcl-XL, Cycl	(Kim et al., 2019)

			-inD1, MMP-9, VEGF-1	
	Timosaponin AIII	MDA-MB-231; MCF-7 (N/A)	Apoptosis/cell cycle rrest, ATM/CHK2, P38, cy-clin B1, Cdc2, Cdc25c	(Zhang et al., 2020b)
	Timosaponin AIII	MDA-MB-231 (N/A)	Antimetastasis, C-Met/ERK, ATF2, Cox 2, MM-P-9	(Tsai et al., 2013)
	Timosaponin AIII	Jurkat (N/A)	Autophagy, PI3K/Akt/mTOR	(Wang et al., 2019a)
	Timosaponin AIII	A549: 15.330 μM (12 h) H1299: 20.950 μM (12 h)	Autophagy, AMPK/mTOR, MAPK/Erk1/2	(Liu et al., 2020a)
	Timosaponin AIII	HeLa: 8.5-10.100 mol/L (48 h)	Autophagy, LC3-II/LC3-I, cytochrome C, casp-ase-3	(Sy et al., 2008)
	Timosaponin AIII	HepG2; PLC/PRF/5; Hep3B (N/A)	Autophagy, AMPKα/mTOR, XIAP	(Wang et al., 2013c)
	Timosaponin AIII	HCT-15: 6.100 μM (72 h)	Apoptosis/cell cycle arrest, cyclin A, cyclin B1, CDK2, CDK4, c-Myc, Bcl-xl/Bcl-2, caspases, PARP	(Kang et al., 2011)
Isospirostane	5β-spirost-25(27)-en-1β,3β-diol-1-O-α-L- r-hamnopyranosyl-(1→2)-β-D-xylopyranosyl -3-O-α-L-rhamnopyra -noside (SPD)	HL-60: 4.700 μM (24 h) HL-60: 2.000 μM (48 h)	Autophagy/apoptosis, Akt/mTOR/P70S6K/4E-BP1, AMPK/ulk1, P62, LC3-II/LC3-I, caspases -3, Bax, PARP	(Yi et al., 2018)
	A-24	AGS; KATO-III (N/A)	Autophagy/apoptosis, ROS-PI3K/Akt/mTOR, c -aspase 3, Bax/Bcl-2	(Xu et al., 2021a)
	A-24	SGC-7901: 3.030 μM (48 h) AGS: 2.180 μM (48 h) MGC-803: 4.100 μM (48 h) NCI-N87: 4.530 μM (48 h) BGC-823: 5.110 μM (48 h)	Apoptosis/cell cycle arrest, Akt/mTOR, cyclin B1, Cdc2, Wee1, histone H3	(Xu et al., 2020b)
	Deltonin	C6: 5.100 μM (48 h)	N/A	(Shen et al., 2012)
	Deltonin	MDA-MB-231 (48 h)	Apoptosis, ERK/Akt, Bax/Bcl-2, caspase-3/8	(Zhang et al., 2013c)
	Deltonin	A549: 3.090 μM (48 h) MDA-MB-231: 1.580 μM (48 h) LL/2: 1.800 μM (48 h) SKOV3: 1.320 μM (48 h) B16: 2.590 μM (48 h) PC-3: 2.310 μM (48 h) C26: 1.210 μM (48 h)	Apoptosis, ERK1/2/Akt, Bax/bcl-2, aaspase-3/9, PARP	(Shu et al., 2011)
	Deltonin	C26: 1.220 μM (48 h)	Antiangiogenic/apoptosis, ERK1/2, Bcl-2/Bax,	(Tong et al., 2011)

	SW-620: 1.290 μM (48 h) SW-480: 1.300 μM (48 h) LOVO: 2.110 μM (48 h)	caspase-3/8/9	
Deltonin	FaDu: 3.430 μM (24 h)	Apoptosis/cell cycle arrest, CHK1/2, caspases-3/8/9	(Xie et al., 2015)
Dioscin	A375: 1.540 μM (24 h) A375: 0.570 μM (48 h)	Antimetastasis, Src/STAT3	(Liu et al., 2020b)
Dioscin	SGC-7901 (N/A)	Apoptosis, Fas/FasL, TNF-α/TNFR-1, Bid, Bcl-2, Bcl-XL, Bak, Bax, caspase-3/8	(Hu et al., 2013)
Dioscin	NCI-H520: 4.590 μM (48 h) SK-MES-1: 2.050 μM (48 h) HBE: 8.470 μM (48 h)	Apoptosis, P38 MAPK / HSP27, caspase-3, PA-RP	(Yao et al., 2020)
Dioscin	HeLa; SiHa (N/A)	Apoptosis, P53, Bak, Bax, Bid, caspase-3/9, Bc-l-2, Bcl-xl, cytochrome c	(Zhao et al., 2016)
Dioscin	MDA-MB-231; MDA-MB-453; T47D (N/A)	Apoptosis, AIF, Bcl-2, CIAP-1, Mcl-1	(Kim et al., 2014)
Dioscin	5637; T24 (N/A)	Apoptosis	(Zhou et al., 2017)
Dioscin	MNNG/HOS: 4.949 μM (24 h) MG63: 3.500 μM (24 h) U2OS: 4.212 μM (24 h)	Apoptosis, JNK/p38, Gsdme	(Ding et al., 2020a)
Dioscin	SKOV3 (N/A)	Apoptosis, VEGFR2, PI3K/Akt/MAPK, Bax, c-aspase-3/9, PARP	(Guo and Ding, 2018)
Dioscin	HepG2: 8.340 μM (24 h)	Apoptosis, PI3K/Akt/mTOR, JNK	(Zhang et al., 2018c)
Dioscin	ASPC-1; PANC-1 (N/A)	Apoptosis, Akt, Bax, Apaf-1, caspase-3/9, PAR-P, Bcl-2, cytochrome C	(Si et al., 2017)
Dioscin	H1975: 4.300 μM (48 h) H1650: 1.700 μM (48 h) PC9GR: 2.100 μM (48 h) CL97: 4.100 μM (48 h)	Reversing tumor resistance, MEK/ERK, PI3K/Akt, SHP2/Gab1	(Wang et al., 2018a)
Dioscin	A431 (N/A)	Apoptosis/Antimetastasis, ATM/p53, Bcl-2/Ba-x, caspase-3/9, PARP, MMP2/9	(Wang et al., 2021)
Dioscin	HEp-2; TU212 (N/A)	Apoptosis/antimetastasis/cell cycle arrest, JNK, ERK/p38, Bcl-2/Bax, CDK2, cyclin A, caspase-3/9, MMP-2/9	(Si et al., 2016)
Dioscin	A549; H1299 (N/A)	Antimetastasis, Akt/mTOR/GSK3β	(Mao et al., 2020)
Dioscin	C26: 7.360 μM (24 h) EA.hy926: 3.870 μM (24 h)	Antiangiogenic, VEGFR2/SRC/FAK/Akt/ERK-1/2/P38	(Tong et al., 2014)

	Dioscin	Ishikawa: 2.370 μM (24 h)	Apoptosis/cell cycle arrest, cyclin A/D/E, CDK-2/4/6, caspase3/8/9 (Li et al., 2021b)
	Dioscin	K562; HL-60; NB4 (N/A)	Apoptosis/cell cycle arrest, caspase-3/9, Bcl-2 (Liu et al., 2004)
	Dioscin	HCT116; HT29; DLD1; SW620 (N/A)	Inhibition of glycolysis, c-Myc/HK-2 (Wu et al., 2020b)
	Dioscin	HepG2 (N/A)	Reversing tumor resistance, P-gp (Sun et al., 2011)
	Dioscin	MCF-7: 6.500 μM (48 h) MCF-7/Adr: 7.300 μM (48 h)	Reversing tumor resistance, NF-κB/IκB-α, PI3-K/Akt, MDR1 (Wang et al., 2016a)
	Dioscin	Dioscin +ADR: K562: 3.400 μM (48 h) K562/ADR: 2.400 μM (48 h)	Reversing tumor resistance, NF-κB/IκB-α, MD-R1 (Wang et al., 2013b)
	Dioscin-6'-O-acetate(DA)	NCI-H460 (N/A)	Apoptosis/cell cycle arrest, JNK/P38/ERK, PI3-K/Akt (Li et al., 2019a)
	Diosgenin	HT-29; HCT-116 (N/A)	Apoptosis, COX-2, 5-LOX (Lepage et al., 2010)
	Diosgenin	DU145; LnCaP (N/A)	Apoptosis, NF-κB/STAT3 (Sikka et al., 2021)
	Diosgenin	Patu8988; Panc-1 (N/A)	Apoptosis/cell cycle arrest, EZH2, vimentin, PTEN (Guo et al., 2019)
	Diosgenin	HCT-116; HT-29 (N/A)	Apoptosis, p38 MAPK, DR5, COX-2, caspase-3/8/9 (Lepage et al., 2011)
	Diosgenin	MDA-MB-231 (N/A)	Antimetastasis, Vav2, Cdc42 (He et al., 2014)
	Diosgenin	MDA 231; MCF-7 (N/A)	Apoptosis/cell cycle arrest, Akt/NF-κB, Raf/MEK/ERK, Bcl-2, survivin, XIAP, cyclin D1, Cdk-2, Cdk-4 (Srinivasan et al., 2009)
	Diosgenin	AU565; MCF-7 (N/A)	Apoptosis, Akt/mTOR, JNK (Chiang et al., 2007)
	Diosgenin	A549: 47.000 μM (24 h) 44.000 μM (48 h) 43.000 μM (72 h)	Antiproliferative, HTERT (Rahmati-Yamchi et al., 2014)
	Diosgenin	HEp-2; M4Beu (N/A)	Apoptosis/cell cycle arrest, P53, caspase-3, AIF, PARP (Corbiere et al., 2014)
	Diosgenin	DU145: 6.757 μg/ml (48 h)	Autophagy/apoptosis, PI3K/Akt/mTOR (Nie et al., 2016)
	Diosgenin	PC-3 (N/A)	Antimetastasis, ERK, NF-κB, JNK, PI3K/Akt, MMP (Chen et al., 2011b)
	Diosgenin	MCF-7 (N/A)	Cell cycle arrest, Cdc25C/Cdc2/Chk1/cyclin B (Liao et al., 2019)
	DT-13	95D (N/A)	Antimetastasis, Raf-ERK1/2, NMIIA (Wei et al., 2016)
	DT-13	HL-60: 17.040 μM (72 h) Kasumi-1: 19.340 μM (72 h)	Apoptosis, AMPK/FOXO/KLF2, Fas/FasL/DR-5/TRAIL, Caspase-3/8 (Wang et al., 2020)
	DT-13	PC3: 4.825 μM (48 h) DU145: 5.102 μM (48 h)	Apoptosis/antimetastasis, PI3K/PDK1/Akt/mTOR/p70S6K, integrin β1, MMP2/9, Bax, Bad, Bcl-2, cytochrome C, caspase-3/9 (Wang et al., 2018b)

	DT-13	BGC-823: 23.500 μM (24h) HGC-27: 35.600 μM (24 h)	Antimetastasis, CCR5/CCL5	(Lin et al., 2014)
	DT-13	BGC-823: 84.720 μM (24 h) A549: 32.140 μM (24 h)	Autophagy, PI3k/Akt/mTOR, Beclin-1, Atg-7, Atg-3, LC3-II/LC3-I	(Li et al., 2016)
	DT -13	NCI-H460; A549; NCI-H1975 (N/A)	Reversing tumor resistance, FoxM1, Bicd2	(Li et al., 2017a)
	DT-13	HT29; MCF-7 (N/A)	Reversing tumor resistance	(Du et al., 2018)
	DT-13	MDA-MB-435 (N/A)	Antimetastasis	(Gao et al., 2020b)
	DT-13	95D (N/A)	Antimetastasis, c-Raf/ERK1/2	(Du et al., 2016)
	DT-13	NCI-H1299 (N/A)	Reversing tumor resistance, MAPK	(Li et al., 2017b)
	DT-13	HT-29: 9.050 μM (72 h) HCT-116: 8.750 μM (72 h) HCT-15: 7.530 μM (72 h) Colo205: 8.360 μM (72 h)	Apoptosis, AMPK/m-TOR	(Wei et al., 2019)
	DT-13	MDA-MB-231; MDA-MB-468 (N/A)	Antimetastasis, JAK/STAT3, PI3K/AKT, PLO-D2	(He et al., 2019a)
	Progenin III	C6: 10.300 μM (48 h)	N/A	(Shen et al., 2012)
	Progenin III	CCRF-CEM: 1.590 μM (24 h)	Apoptosis/autophagy	(Mbaveng et al., 2020)
	Gracillin	A549: 2.540 μM (24 h)	Apoptosis, Bax/bcl-2, cytochrome C, caspase-3	(Yang et al., 2021a)
	Gracillin	RKO; SW480; HCT116 (N/A)	Antimetastasis, STAT3, Bax/bcl-2, caspase-3	(Yang et al., 2021b)
	Gracillin	A549 (N/A)	Apoptosis, SDH	(Min et al., 2019)
	Gracillin	HL-60: 98.370 μM (24 h) 56.370 μM (48 h) 36.800 μM (72 h)	Apoptosis/cell cycle arrest	(Chen et al., 2015)
	Gracillin	MDA-MB-231; MCF7; H460 (N/A)	Inhibition of glycolysis, PGK1, Mitochondrial complex II	(Min et al., 2020)
	Gracillin	SGC7901: 8.900 μM (12 h) BGC823: 8.300 μM (12 h)	Apoptosis/antimetastasis, PI3K/AKT, Bcl2	(Liu et al., 2021)
	Macrostemonoside A	SW480 (N/A)	Apoptosis, Bcl-2, caspase	(Wang et al., 2013d)
	Ophiopogonin B	A549: 16.470 μM (24 h)	Pyroptosis, caspase-1/GSDMD	(Cheng et al., 2022)
	Ophiopogonin B	A549 (N/A)	Apoptosis, caspase-3, Bcl-2/Bax, survivin, XIA-P	(Chen et al., 2016b)
	Ophiopogonin B	AGS: 10.270 μM (24 h) NCI-N87: 21.320 μM (24 h)	Ferroptosis, GPX4/Xct	(Zhang et al., 2022)
	Ophiopogonin B	C666-1; HK-1 (N/A)	Apoptosis, STE20, YAP, FOXO1, Bcl-2/Bax	(Dong et al., 2021)
	Ophiopogonin B	A549 (N/A)	Apoptosis/aautophagy, TRAIL/FADD, Lc3-I/Lc3-II, P62	(Nazim et al., 2017)
	Ophiopogonin B	HT29; HCT-116 (N/A)	Autophagy/apoptosis, JNK/c-Jun, Beclin 1, P6-	(Gao et al., 2018)

		2, LC3-II/LC3-I, Bcl-2/Bax, caspases-3	
ophiopogonin B	SGC-7901 (N/A)	Apoptosis, ERK1/2 和 c-Jun N-1/2, Bax/Bcl-2, caspase-3	(Zhang et al., 2016b)
Ophiopogonin B	A549 (N/A)	Antiangiogenic/antimetastasis, EphA2/Akt	(Chen et al., 2018b)
Ophiopogonin D	A549; H1299; H460 (N/A)	Apoptosis, JAK/STAT3	(Lee et al., 2018a)
Ophiopogonin D	AMC-HN-8 (N/A)	Apoptosis, P38 MAPK, cyclin B1, MMP-9, cas-pase-3/9	(Yan et al., 2018c)
Ophiopogonin D	A549 (N/A)	Apoptosis, NF-κB/IκB, PI3K/Akt, AP-1	(Lee et al., 2018b)
Ophiopogonin D	MDAMB-231: 10.520 μM (24 h)	Antimetastasis, ITGB1/FAK/SRC/Akt/β-catenin/MMP-9	(Zhu et al., 2020)
Ophiopogonin-D	MDA-MB-435 (N/A)	Antimetastasis, P38, MMP-9	(Zhang et al., 2015)
Ophiopogonin D	MCF-7: 12.820 μM (24 h) 8.020 μM (48 h) 4.600 μM (72 h)	Apoptosis/cell cycle arrest, cyclin B1, caspase-8/9	(Zang et al., 2016)
Ruscogenin	SMC7721; HCCLM3 (N/A)	Antimetastasis, PI3K/Akt/mTOR, HIF1α/VEG-F, MMP2/9, uPA	(Hua et al., 2018)
Sprengerinin C	HepG-2 (N/A)	Antiangiogenic, HIF-α/VEGF/VEGFR2/PI3K/Akt/mTOR/MMP, MAPK/MMP	(Zeng et al., 2013)
Terrestrosin D	PC-3＜5.000 μM (24 h) DU145＜5.000 μM (24 h) PC-3MLN4＜5.000 μM (24 h) 22RV1＜5.000 μM (24 h) LNCaP＜5.000 μM (24 h)	Apoptosis	(Wei et al., 2014)
Trillin	HepG2: 17.840 μM (24 h) PLC/PRF: 18.580 μM (24 h)	Antimetastasis, MMP1/2, MUCI, VEGF, Bcl-2, survivin, PRAP	(Zhan et al., 2020)
TTB2	Rh1 (N/A)	Apoptosis, caspase-3/9, Bax/Bcl-2	(Zou and Huang, 2018)
TTB2	A549 (N/A)	Apoptosis/cell cycle arrest	(Huang and Zou, 2011)
TTB2	Rh1 (N/A)	Apoptosis, ERK	(Huang and Zou, 2015)
Polyphyllin I	A549: 4.430 μM (24 h) NCI-H1975: 4.060 μM (24 h) NCI-H820: 4.030 μM (24 h) PC9: 2.730 μM (24 h) NCI-H460: 2.600 μM (24 h) 95D: 2.480 μM (24 h)	Autophagy, AMPK/mTOR	(Wu et al., 2020a)
Polyphyllin I	GC7901: 2.48μM (48 h) SGC7901/DDP: 0.930 μM (48 h)	Reversing tumor resistance/antimetastasis, CIP-2A/PP2A/AKT, E-cadherin/vimentin	(Zhang et al., 2018b)

Polyphyllin I	HGC-27: 0.550 μM (24 h) 0.370 μM (48 h) 0.340 μM (72 h)	Autophagy/cell cycle arrest, PDK1/Akt/mTOR, LC3-II/LC3-I, cyclin B1	(He et al., 2019b)
Polyphyllin I	T24: 1.760 μM (24 h) 1.100 μM (48 h) UMUC3: 2.790 μM (24 h) 1.860 μM (48 h)	Apoptosis/cell cycle arrest, FOXO3/BIM/NOX-A	(Li et al., 2020)
Polyphyllin I	PC-9/OR; H1975/OR (N/A)	Reversing tumor resistance, PI3K/Akt	(Lai et al., 2021)
Polyphyllin II	NCI-H460; NCI-H520 (N/A)	Reversing tumor resistance, JNK	(Man et al., 2020)
Polyphyllin II	T24: 0.640 μg/ml (24 h) 5637: 0.710 μg/ml (24 h)	Antimetastasis, E-cadherin, N-cadherin, MMP-2/9	(Niu et al., 2020)
Polyphyllin II	HepG2: 4.835 μM (24 h) BEL7402: 4.477 μM (24 h)	Antimetastasis, Akt/NF-κB, MMP2/MMP9	(Pang et al., 2020)
Polyphyllin II	SKOV3: 20.990 μM (24 h) 10.440 μM (48 h) 8.830 μM (72 h) 6.980 μM (96 h)	Antiangiogenic/apoptosis, NF-κB/IKK/IκBα /VEGF, Bcl-2/Bax	(Yang et al., 2015)
Polyphyllin II	SKOV3: 7.170 μM (48 h) HOC-7: 6.440 μM (48 h)	Antiangiogenic, VEGFR2/ERK/FAK/Akt	(Xiao et al., 2014)
Polyphyllin VI	U2OS: 7.330 μM (24 h) 6.020 μM (48 h)	Autophagy/apoptosis, ROS/JNK, LC3-II/LC3-I, Atg, Bcl-2/Bax	(Yuan et al., 2019)
polyphyllin VI	4T1; MDA-MB-231 (N/A)	Antimetastasis	(Wang et al., 2019c)
Polyphyllin VI	HepaRG (N/A)	Apoptosis/cell cycle arrest, cyclin A2, CDK2, c-ytochrome C, FAS, caspase-3/8/9, PARP	(Liu et al., 2018)
Polyphyllin VII	NCI-H1299: 4.560 μM (24 h) NCI-H460: 3.160 μM (24 h) A549: 2.540 μM (24 h)	Autophagy/apoptosis, AMPK/mTOR/Ulk1, P62, LC3-II/LC3-I	(Qian et al., 2020)
Polyphyllin VII	HepG2: 1.320 μM (24 h)	Autophagy, PI3K/Akt/mTOR, AMPK/mTOR, J-NK, Bcl-2, LC3-II/LC3-I, P62	(Zhang et al., 2016a)
Polyphyllin VII	HEL: 0.667 μM (72 h) MCF-7: 3.950 μM (72 h) PC3: 2.785 μM (72 h) WM9: 5.664 μM (72 h)	Apoptosis, Bid, BIM, Bcl-2, PARP, caspase-3	(Lin et al., 2021)
Polyphyllin VII	HT-29: 1.020 μM (24 h) SW-620: 4.900 μM (24 h)	Apoptosis, MEK1/2/ERK1/2, Akt/gsk-3β, caspase-3	(Li et al., 2014b)
Polyphyllin VII	A549 (N/A)	Apoptosis, PI3K/Akt, NF-κB	(He et al., 2020)
Polyphyllin VII	MCF-7/ADR (N/A)	Reversing tumor resistance, TNFR1, Trail R1/	(Li et al., 2014a)

			DR4, trail R2/DR5, FADD, PARP, Caspases-3/8, P-gp	
	Polyphyllin VII	K562: 0.580 μM (N/A) K562/ADR: 0.910 μM (24 h) 0.920 μM (48 h) 0.970 μM (72 h)	Reversing tumor resistance, JNK, Akt/ERK1/2/p38, P-gp, Bcl-2/Bax, cytochrome C, caspase-3/9, PARP	(Yan et al., 2018b)
	Polyphyllin VII	MCF-7/ADR: 4.100 μM (24 h)	Reversing tumor resistance, MDR1	(Li et al., 2019b)
	Polyphyllin VII	SW620; LoVo (N/A)	Antimetastasis, MMP-2/9	(Fan et al., 2015b)
	Polyphyllin VII	A549 (N/A)	Antimetastasis, TIMP1/2, MMP-2/9	(Fan et al., 2015a)
	Polyphyllin VII	HepG2 (N/A)	Antiangiogenic/antimetastasis, NF-κB/MMP-9/VEGF	(Zhang et al., 2021a)
	Polyphyllin VII	U87-MG: 4.240 μM (24 h) U251: 2.170 μM (24 h)	Apoptosis/autophagy, AKT/mTORC1	(Pang et al., 2019)
	Polyphyllin H	PLC/PRF/5; Huh7 (N/A)	Antimetastasis/apoptosis, EMT, β-catenin, P-gs-k-3β	(Chen et al., 2019)
	Polyphyllin H	U251 (N/A)	Arrest cell cycle, Cyclin D1, SKP2	(Bi et al., 2021)
Furostane	Methyl Protodioscin	A7r5: 9.000 μM (24 h)		(Chung et al., 2016)
	Methyl protodioscin	SAS; SCC9 (N/A)	Apoptosis/autophagy, P38/JNK, caspase-3	(Hsieh et al., 2017)
	Methyl protodioscin	Hela: 18.490 μM (24 h)	Apoptosis, Fas, caspase-8/9	(Ma et al., 2019)
	Protodioscin	HeLa; C33A (N/A)	Apoptosis, P38/JNK, GRP78/eIF2α/ATF4/CH-OP	(Lin et al., 2018)
	Glauco-chinaosides A	SGC-7901: 2.700 μM (48 h)	N/A	(Liu et al., 2017)
	Glauco-chinaosides B	SGC-7901: 11.500 μM (48 h)	N/A	(Liu et al., 2017)
	Glauco-chinaosides E	SGC-7901: 6.800 μM (48 h)	N/A	(Liu et al., 2017)
	Aspidsaponins A	A549: 5.100 μM (48 h) Caski: 8.600 μM (48 h) HepG2: 11.100 μM (48 h) MCF-7: 13.800 μM (48 h)	N/A	(Zuo et al., 2018)
	26-O-β-d-glucopyra-nosyl-22α-hydroxyl-(25R)-Δ5(6)-furost-3β,26-diol-3-O-α-l-rha-mnopyranosyl-(1→2)-[β-dglucopyranosyl-(1→4)-α-l-rhamnopyran-osyl-(1→4)]-β-d-gluc	H1299: 5.260 μM (72 h) MHCC97H: 4.150 μM (72 h)	N/A	(Zhang et al., 2021d)

	-opyranoside (FSAC)			
Cholestane	OSW-1	LNCaP; PC3 (N/A)	Apoptosis, PI3K/AKT/mTOR2	(Elgehama, 2022)
	OSW-1	MCF-7: 3.720 nM (72 h) T47D: 5.920 nM (72 h) ZR-75-1: 10.340 nM (72 h) BT474: 6.540 nM (72 h) SKBR3: 6.670 nM (72 h) MDA-MB-231: 5.820 nM (72 h) MDA-MB-453: 8.660 nM (72 h) HCC-1937: 11.120 nM (72 h)	Antimetastasis, E-cadherin, vimentin	(Ding et al., 2020b)
	Cholestane-3β-5α-6β-triol	MDA-MB-231: HTB-26 (N/A)	Apoptosis, Lxrα, Abca 1, Abcg1	(Levy et al., 2019)
Alkaloids	α-Chaconine	RL95-2: 4.720 μM (24 h)	Antiprolifeativon, Akt, ERα	(Karaboga Arslan and Yerer, 2018)
	α-Chaconine	HT-29 (N/A)	Apoptosis, ERK, caspase-3	(Yang et al., 2006)
	Solanidine	A549 (N/A)	Apoptosis, PI3K/Akt, DFF-40	(Malojirao et al., 2018)
	Solanine	HepG2: 16.690 μM (48 h)	Apoptosis, Bcl2	(Ji et al., 2008)
	Solanine	SW1990 (N/A)	Apoptosis/antimetastasis, Bcl2/Bax, cytochrom-e c, Smac, caspase-3, MMP-2/9	(Sun et al., 2014)
	Solanine	HepG2 (N/A)	Antimetastasis, MMP	(Lin et al., 2020)
	Solanine	H22 (N/A)	Immune response, Foxp3, TGFβ	(Gao et al., 2020a)
	Solanine	DU145: 32.180 μM (24 h)	Cell cycle, P38MAPK, cyclin D1, cyclin E1, C-DK2, CDK4, CDK6, P21	(Pan et al., 2016)
	α-Solanine	EC9706; KYSE30 (N/A)	Apoptosis, miR-138/survivin, caspase-3/7	(Wu et al., 2018)
	α-Solanine	PC-3 (N/A)	Antimetastasis/apoptosis, ERK, PI3K/Akt, TIM-P-1/2/MMP-2/9	(Shen et al., 2014)
	α-Solanine	PANC-1 (N/A)	Antimetastasis, ERK1/2-HIF-1α, STAT3, VEG-F, E-cadherin	(Wen et al., 2016)
	α-Solanine	4T1: 340 μM (24 h)	Apoptosis, Bcl-2/Bax	(Mohsenikia et al., 2013)
	α-Solanine	EC9706; Eca109 (N/A)	Antimetastasis/apoptosis, E-cadherin, MMP-2/9	(Wang et al., 2016b)
	α-Solanine	A2058; A375 (N/A)	Antimetastasis, PI3K/Akt, JNK, NF-κB, MMP-2/9	(Lu et al., 2010)
	α-Solanine	RKO: 20.840 μM (72 h)	Antimetastasis/cell cycle arrest, cyclin D1, CD-K2, MMP2/9	(Yan et al., 2020)
	α-Solanine	JEG-3 (N/A)	Apoptosis/antimetastasis, Bcl-2/Bax, MMP2/9	(Gu et al., 2021)

Tomatidine	U2OS; HOS (N/A)	Antimetastasis, c-Raf/MEK/ERK, PS-1	(Hsieh et al., 2020)
Tomatidine	HT1080 (N/A)	Apoptosis/antimetastasis, P38/ERK, MMP-2	(Jeon and Kim, 2019)
Tomatidine	A549 (N/A)	Antimetastasis, Akt/ERK/NF-κB, TIMP-1, MM-P-2/9	(Yan et al., 2013)
α-Tomatine	PC-3 (N/A)	Apoptosis, NF-κB, caspase-3/8/9	(Lee et al., 2011)
α-Tomatine	HCT-116; LoVo; SW480; SW620 (N/A)	Apoptosis, RIP1/3, AIF	(Rudolf and Rudolf, 2016)
α-Tomatine	NCI-H460 (N/A)	Antimetastasis, FAK/PI3K/Akt/Iκ-B/NF-κB, M-MP-7	(Shieh et al., 2011)
α-Tomatine	PC-3: 1.670 μM (24 h)	Apoptosis, PI3K/Akt, Bcl-2, Bcl-xL, Bad	(Lee et al., 2013)
α-Tomatine	A549 (N/A)	Antimetastasis/apoptosis, PI3K/Akt, ERK1/2, NF-κB/AP-1, c-Jun, MMP2/9	(Shih et al., 2009)
α-Tomatine	CT-26: 3.500 μM (24 h)	Apoptosis, NF-κB/p65, survivin, AIF	(Kim et al., 2015)
α-Tomatine	HL-60 (N/A)	Apoptosis	(Huang et al., 2015a)
α-Tomatine	Skov3: 2.100 μM (24 h) 1.340 μM (48 h) 0.980 μM (72 h)	Apoptosis, PI3K/Akt/mTOR, Beclin-1	(Wu et al., 2021)

3. Antitumor mechanism of steroidal saponins

We will discuss the antitumor properties of five different types of steroidal saponins and how they can be classified. We aim to provide some guidance on the application of these saponins and their antitumor mechanisms.

3.1 Spirostanol type

Sarsasapogenin and its derivatives represent a classical class of spirostanol-type steroid saponins. Therefore, we mainly summarize the antitumor mechanism of sarsasapogenin and its derivatives. Among these derivatives are timosaponin AIII, aspiletrein A, and aspafilioside B. According to previous reports, sarsasapogenin and its derivatives possess various medicinal activities (Lim et al., 2015) with significant antitumor effects (Liu et al., 2020a; Sy et al., 2008; Wang et al., 2017b). Its antitumor mechanisms primarily involved the induction of programmed tumor cell death, the inhibition of tumor cell migration, the tumor cell cycle arrest, and the overcoming of drug resistance in tumor cells.

3.1.1 Induction of programmed tumor cell death

The X-linked apoptosis inhibitory protein (XIAP) of the IAP family inhibited apoptosis (Wang et al., 2004). Wang et al. (2013c) described that timosaponin AIII inhibited XIAP expression in human hepatocellular carcinoma (HCC) cells by upregulating the AMPKα/mTOR pathway to activate the autophagic pathway that triggers the lysosomal pathway to degrade XIAP, thereby inducing apoptosis. Asparanin A activated AMPK/mTOR/ULK1 signaling to promote autophagy in Ishikawa cells and inhibited ATF4 expression to suppress tumor cell growth (Zhang et al., 2021c).

Hydroxylation of the sarsasapogenin derivative RCE-4 at the C1 position enhanced the expression of LC3-II and Beclin1 in Ca-Ski cells to promote autophagy in tumor cells (You et al., 2021). Aspafilioside B induced apoptosis in A549 cells by inhibiting RAS/c-Raf/ERK signaling, and timosaponin AIII induced apoptosis by inhibiting the MAPK/Erk1/2 signaling pathway (Liu et al., 2020a; Liu et al., 2016). Huang et al. (2015b) found that timosaponin AIII dose-dependently increased the phosphorylation of JNK1/2 and p38MAPK in HL-60cells which induced apoptosis in HL-60 cells via the JNK1/2 signaling pathway. Wang et al. (2019b) found that timosaponin AIII induced apoptosis and autophagy in T-cell acute lymphoblastic leukemia (T-ALL) Jurkat cells *in vitro* by inhibiting the PI3K/Akt/mTOR signaling pathway by downregulating PI3K, Akt, and mTOR activities. RCE-4 also inhibited mTOR-dependent proteins NF-κB and Bcl-2 while increasing Bax and PARP to induce apoptosis in Hela cells (Bai et al., 2016). Asparanin A upregulated Bax, Bak, Bad, and cytochrome C in Ishikawa cells and activated the caspases, leading to apoptosis in tumor cells (Zhang et al., 2020a). Similarly, timosaponin AIII inhibited Bcl-xl expression to induce apoptosis in AsPC-1 pancreatic cancer cells and increased cytochrome C, HtrA2/Omi and Smac/Diablo in the cytoplasm of HepG2 cells to achieve tumor suppression (Kim et al., 2019; Nho et al., 2016).

3.1.2 Inhibition of tumor cell migration and invasion

Overexpression of COX-2, its metabolite prostaglandin E2 (PGE2), and PGE2 receptors (EP2 and EP4) promoted cell migration (Dohadwala et al., 2001; Mohammad et al., 2011). Kim et al. (2016a) observed that timosaponin AIII inhibited tumor cell

migration by decreasing the expression of NF-κB, the upstream transcription factor of COX-2, PGE2, and PGE2 receptors (EP2 and EP4), and *in vivo* studies showed that timosaponin A-III inhibited the expression of COX-2 and NF-κB in the lungs of melanoma-transplanted mice. Tsai et al. (2013) also showed that timosaponin AIII inhibited hepatocyte growth factor (HGF)-induced invasion of breast cancer MDA-MB-231 cells and that timosaponin AIII inhibited c-MET and ERK activity, resulting in a decrease in the activity of nuclear transcription factor ATF2, thereby reducing the expression of COX2 and MMP-9 to inhibit tumor cell migration. Chiang et al., (2019) showed that timosaponin AIII inhibited metastasis in human renal cancer cells by inhibiting PI3K/Akt activity, increasing the level of miR-129-5p, and subsequently decreasing the expression of histone protease (CTSC). Matrix metalloproteinases degrade the extracellular matrix and induce tumor cell migration (Zhang et al., 2013b). Jung et al. (2016) found that timosaponin AIII inhibited the ERK/JNK and Src/FAK signaling pathways in A549 human non-small cell lung cancer, inhibiting the effect of MMP-2 and MMP-9 from suppressing tumor cell migration and invasion. Timosaponin AIII also inhibited the TESK1/p-cofilin-mediated cytoskeletal F-actin signaling pathway to suppress tumor cell migration and invasion (Hsieh et al., 2021b).

3.1.3 Arrest of the tumor cell cycle and overcoming tumor cell drug resistance

Recently, Zhang et al. (2020b) found that timosaponin AIII caused DNA damage and activated the ATM/Chk2 and p38 MAPK pathways in breast cancer, inducing G2/M phase block and apoptosis. In HeLa cells, sarsasapogenin activated Chk1 that arrested the cell cycle in S-phase and G2/M-phase and downregulated Cyclin B1, Cdc2 and

Cdc25C (Shen et al., 2013). Similarly, Kang et al. (2011) observed that timosaponin AIII caused the down-regulation of cyclin A, cyclin B1, cell cycle protein-dependent kinase 2 (CDK2), CDK4, proliferating cell nuclear antigen, and c-Myc in human colorectal cancer HCT-15 cells, resulting in the arrest of tumor cells in G0/G1 and G2/M phases. P-glycoprotein (P-gp) and multidrug resistance protein 1 (MDR1) are ABC transporter proteins, and their overexpression in cancer cells results in multidrug resistance (Lin et al., 2003; Woodahl et al., 2009). Chen et al. (2016a) demonstrated that timosaponin AIII reversed doxorubicin resistance in human chronic granulocytic leukemia K562 cells by inhibiting the PI3K/Akt signaling pathway and causing a decrease in P-gp and MDR1 levels. Furthermore, Song et al. (2019) found that timosaponin AIII reversed paclitaxel resistance in A549 and A2780 cells by downregulating PI3K/AKT/mTOR and Ras/Raf/MEK/ERK signaling pathways, and the *in vivo* mouse model supports the *in vitro* findings that were in consistent with the results of *in vitro* experiments.

3.1.4 Summary

We found that spirostanol steroidal saponins mainly exert antitumor effects by causing apoptosis, inducing tumor cell autophagy, inhibiting tumor cell metastasis, blocking the tumor cell cycle, and overcoming tumor drug resistance. Spirostanol steroidal saponins primarily cause tumor cell apoptosis by activating the JNK/P38 signaling pathway, inhibiting the PI3K/Akt/ mTOR/NF-κB signaling pathway as well as the Ras/ERK/ATF signaling pathway (Fig 3 a). Regarding the induction of tumor cell autophagy, spirostanol steroid saponins triggered tumor cell autophagy by

inhibiting the PI3K/Akt/mTOR/ULK1 pathway and activating the AMPK/mTOR/ULK1 signaling pathway (Fig 3 c). Spirostanol steroid saponins inhibit tumor cell migration and invasion by inhibiting the Wnt/β-catenin, C-met/ERK, PI3K/Akt/NF-κB, FAK/Src/Akt, and TESK1/Cofilin/F-actin signaling pathways (Fig 3 b). Spirostanol steroid saponins mostly blocked tumor cell cycle progression by activating the ATM/CHK/P53 signaling pathway (Fig 3 e). Concerning overcoming tumor cell resistance, spirosterol steroidal saponins inhibit the Ras/ERK and PI3K/Akt/NF-κB/P-gp/MDR1 signaling pathways (Fig 3 d).

3.2 Isospirostanol type

Isospirostanol steroidal saponins have significant antitumor activities. Regarding their mechanisms of action, we categorized two major classes of isospirostanol steroidal saponin compounds: diosgenin and ruscogenin derivatives.

3.2.1 Diosgenin and its derivatives

Diosgenin is a saponin element with an isospirostanol-type structure. Its derivatives vary depending on the type and arrangement of the sugar groups they carry, mainly polyphyllins I, II, VI, VII, and H, dioscin, gracillin, deltonin, and trillin. Diosgenin compounds have a variety of therapeutic properties, including anti-infectious, anti-allergic, and antitumor activities (Yang et al., 2019). Main antitumor strategies included induction of programmed tumor cell death, suppression of tumor migration and angiogenesis, blocking the tumor cell cycle, and overcoming tumor cell drug resistance.

3.2.1.1 Induction of programmed tumor cell death

Colorectal cancer is among the most prevalent types of cancer. Polyphyllin VII induced apoptosis in colorectal cancer cells by downregulating MEK1/2 expression and MEK1/2 phosphorylation to inhibit the MAPK signaling pathway and decrease Akt and GSK-3β phosphorylation to inhibit the Akt signaling pathway, exhibiting significant antitumor activity (Li et al., 2014b). He et al. (2019b) observed that polyphyllin I reduced the phosphorylation of PDK1, Akt, and mTOR, consequently suppressing the PDK1/Akt/mTOR pathway to trigger autophagy in human gastric cancer HGC-27 cells. Polyphyllin VII can also induce autophagy in A549 cells by activating the AMPK/ULK1 pathway, and a significant accumulation of LC3II was found (Qian et al., 2020). Yuan et al. (2019) found that polyphyllin VI increased reactive oxygen species (ROS) levels and promoted JNK phosphorylation, upregulated the pro-apoptotic protein Bax and downregulated the anti-apoptotic protein Bcl-2 to induce apoptosis in U2OS cells, and also led to the accumulation of the downstream autophagy-related proteins Atg and LC3-II to induce autophagy in U2OS osteosarcoma cells.

Liu et al. (2018) discovered that polyphyllin VI acted on HepaRG cells to release cytochrome C from mitochondria into the cytoplasm and increased the levels of apoptosis-related proteins Fas, caspase-3, -8, and -9, indicating that polyphyllin VI induces apoptosis in tumor cells via the mitochondrial as well as the Fas-dependent death pathway. In addition, dioscin stimulated the production of FasL and TNFR1 proteins, which regulate death-related signaling pathways to promote apoptosis in SGC-7901 cells (Hu et al., 2013). Polyphyllin I increased the production of Bim and NOXA in BCa cells to induce apoptosis of tumor cells (Li et al., 2020). Gracillin

significantly inhibited the proliferation of colorectal cancer.Yang et al. (2021b) demonstrated that gracillin significantly inhibited tumor growth in a mouse model. Moreover, gracillin inhibited STAT3 phosphorylation, nuclear translocation of P-STAT3, and downstream gene products to inhibit the STAT3 signaling pathway, thus inducing apoptosis in colorectal cancer cells.

Recently, Ding et al. (2020a) investigated the effect of dioscin on osteosarcoma cells and reported that it exhibited a significant anti-proliferative effect. The authors found that dioscin enhanced the phosphorylation of JNK, p38, and ErK1/2, leading to apoptosis by activating intracellular JNK/p38 signaling and triggering caspase-3 mediated cleavage of GSDME. This cascade resulted in the destruction of tumor cells. In addition to increasing P38 phosphorylation, Dioscin also induced phosphorylation of HSP27, a protein downstream of P38, and increased levels of cleaved PARP, Bax/Bcl-2, and caspase-3 activation to induce apoptosis in SCC cells (Yao et al., 2020). Yang et al. (2021a) discovered that gracillin caused apoptosis in A549 lung cancer cells. Gracillin altered the mitochondrial membrane potential of tumor cells, raised the levels of cytochrome C, Bax, and activated caspase-3 in the cytoplasm, and lowered the level of Bcl-2, indicating that gracillin might trigger apoptosis in lung cancer A549 cells via the mitochondrial pathway. Additionally, dioscin decreased Bid, bcl-2, and bcl-xl levels, increased the levels of P53 in SGC-7901 cells, and induced apoptosis in tumor cells (Hu et al., 2013).

3.2.1.2 Tumor migration, invasion and angiogenesis inhibition

Polyphyllin I suppresses SGC7901 cell invasion by disrupting CIP2A/PP2A/Akt

pathway, decreasing the level of CIP2A to increase PP2A activity and decreasing Akt activity, protein phosphatase 2A (PP2A) inhibitor (CIP2A) promotes EMT and metastasis of tumor cells (Zhang et al., 2018b). Yang et al. (2015) reported that polyphyllin II reduced IKKβ kinase activity and inhibited NF-κB activation, leading to reduced expression of the downstream protein VEGF, thereby inhibiting intercellular angiogenesis in ovarian cancer. Matrix metalloproteinase inhibitors (TIMP1/2) inhibit MMP protein activity, and polyphyllin VII increases TIMP1/2 expression and inhibits MMP-2 and MMP-9 activity, consequently reducing the metastatic and invasion potential of A549 cells (Fan et al., 2015a). Similarly, Liu et al. (2021) observed that gracillin inhibited the proliferation of gastric cancer BGC-823 cells. It also inhibited tumor cell migration by blocking the PI3K/AKT pathway to promote apoptosis in gastric cancer cells and regulate EMT-related proteins (elevating E-cadherin and down-regulating N-cadherin and vimentin). Vav proteins are essential regulators of cytoskeletal rearrangement, and He et al. (2014) demonstrated that diosgenin inhibited Vav2 phosphorylation and Cdc42 activation to inhibit actin polymerization, ultimately inhibiting the migration of human breast cancer MDA-MB-231 cells. Additionally, Trillin substantially inhibited tumor vascular growth (Tong et al., 2011).Zhan et al. (2020) also found that trillin suppressed nuclear translocation of phosphorylated STAT3, regulated the expression of apoptosis-related proteins to promote apoptosis in HepG2 and PLC/PRF5 cells, and downregulated VEGF to inhibit tumor angiogenesis.

3.2.1.3 Arrest of the tumor cell cycle

Other antitumor effects of diosgenin were observed in human breast cancer cells.

Liao et al. (2019) found that diosgenin-activated Chk1 and down-regulated cyclin B expression to block human breast cancer cells in the G2/M phase. The key mechanism was the reduction of Cdc25C expression. Dioscin inhibited the proliferation of Ishikawa cells by blocking the G0/G1 cell cycle through upregulation of p16, p21, and p27 and downregulation of cyclin A/D/E and cyclin-dependent kinase (CDK2/4/6) (Li et al., 2021b). Polyphyllin H also inhibited tumor cell cycle arrest by upregulating the expression of P21 and P27 and inhibiting cyclin D1 and S-phase kinase-related protein 2 (Skp2) (Bi et al., 2021).

3.2.1.4 Overcoming tumor cell drug resistance

Resistance to current anticancer drugs such as osimertinib has emerged (Jiang et al., 2021). Lai et al. (2021) found that the combination of polyphyllin I/osimertinib significantly inhibited tumor growth compared to osimertinib alone, thereby reversing resistance to osimertinib in non-small cell lung cancer by a mechanism related to inhibition of PI3K/Akt signaling. Similarly, Yan et al. (2018a) indicated that polyphyllin VII induced apoptosis in doxorubicin-resistant human leukemia K562 cells by reducing reactive oxygen species levels, inhibiting P-glycoprotein (P-gp) expression and impeding Akt activation. Dioscin also had good inhibitory effects on drug-resistant tumor cells. Wang et al. (2018a) revealed the mechanism of dioscin's significant inhibitory effects on lung cancer cells resistant to tyrosine kinase inhibitors (TKIs). They proposed that the ROS-induced increase in P53 binding to the SHP2 promoter reduced the expression of SH2 structural domain phosphatase-2 (SHP2) and its interaction with the junction protein GAB1, thus inhibiting both MEK/ERK and

PI3K/AKT signaling pathways to block tumor cell growth. Wang et al. (2013b) found that Dioscin inhibited transcription factor NF-κB activation and downregulated MDR1 (ABC transporter protein), reversing the resistance of leukemic K562 cells to doxorubicin. MCF-7 human breast cancer cells have developed resistance to doxorubicin over time. Wang et al. (2016a) observed that dioscin inhibited NF-κB signaling from downregulating P-glycoprotein and PI3K/Akt pathway to induce autophagy in breast cancer cells, thus increasing doxorubicin toxicity. P-glycoprotein is essential for drug resistance in tumor cells, and NF-κB significantly regulated MDR1 expression. Likewise, Sun et al. (2011) revealed that dioscin inhibited the activity of MDR1 promoter pGL3 and down-regulated MDR1 (P-glycoprotein) expression, thus reversing the drug resistance of hepatocellular carcinoma HepG2 cells to doxorubicin.

3.2.2 Ruscogenin and its derivatives

Ruscogenin-like compounds of Liliaceae exhibit substantial antitumor activity, including Ophiopogonin B, Ophiopogonin D, and saponin monomer 13 (DT-13) from Lilia dwarfensis tubers (Liu et al., 2023). Its antitumor mechanism mainly includes the induction of tumor cell apoptosis and inhibiting tumor migration and angiogenesis.

3.2.2.1 Induction of apoptosis in tumor cells

JNK signaling is significant in numerous physiological and pathological processes including cell cycle, reproduction, apoptosis, and cellular stress (Jonathan Ham, 2000). In their study, Gao et al. (2018) found that ophiopogonin B inhibited the JNK/c-Jun signaling pathway to induce apoptosis in HT-29 and HCT-116 cells and significantly suppress tumor growth in a mouse transplantation model. IκB kinase, a crucial enzyme

essential for NF-κB activation, can deregulate the inhibitory effect of IκB on NF-κB. In addition to regulating apoptosis-related protein expression, ophiopogonin D induced apoptosis in lung cancer H1299 cells and A549 cells by inhibiting NF-κB activation by inhibiting IκB kinase activation and suppressing nuclear translocation of P65.

Moreover, ophiopogonin D exhibited significant antitumor effects by inhibiting the PI3K/Akt pathway by decreasing PI3K and Akt activity and inhibiting the AP-1 signaling pathway by decreasing the expression of AP-1 upstream kinase proteins (c-FOS and c-Jun) (Lee et al., 2018b). Similarly, DT-13 reduced the phosphorylation of PDK1, Akt, mTOR, and the downstream protein p70S6K to induce apoptosis in prostate cancer cells. It caused significant upregulation of Bax, Bad, cytochrome C, cleaved caspase-3, caspase-9 (Wang et al., 2018b).

3.2.2.2 Inhibition of tumor cell metastasis and angiogenesis

Lysine hydroxylase PLOD-2 is involved in extracellular matrix remodeling and epithelial-mesenchymal transition activation and is closely associated with tumor cell metastasis(Hollern et al., 2014). DT-13, a saponin monomer isolated from Lily of the Dwarf, reduced PLOD2 expression by inhibiting JAK/STAT3 and PI3K/AKT signaling pathways, thereby inhibiting the metastasis of MDA-MB-231 and MDA-MB-468 breast cancer cells (He et al., 2019a).Hua et al. (2018) demonstrated that ruscogenin suppressed the PI3K/Akt/mTOR signaling pathway to reduce the expression of MMP-2, MMP-9, and VEGF in hepatocellular carcinoma SMMC-7721 and HCCLM3 cells, exhibiting a significant anti-metastatic effect on hepatocellular carcinoma cells.

TGF-β1 can promote ITGB1 expression to induce tumor cell metastatic behavior,

and ophiopogonin D inhibits TGF-β1 induced ITGB1 expression. Thus, ophiopogonin D can resist metastasis of breast cancer MDA-MB-231 cells (Zhu et al., 2020). EphA2 signaling was involved in an essential process of angiogenesis (Baharuddin et al., 2018). Ophiopogonin B suppressed angiogenesis by downregulating EphA2 expression, phosphorylation, and Akt activity in A549 cells. Ophiopogonin B inhibited angiogenesis and downregulated hemoglobin content in the A549 cell transplantation model (Chen et al., 2018b).

3.2.3 Summary

Like spirostanol steroid saponins, the antitumor mechanism of isospirostanol steroid saponin included induction of apoptosis, autophagy in tumor cells, inhibition of tumor cell metastasis, blocking of the tumor cell cycle, and overcoming tumor drug resistance. In the induction of tumor cell apoptosis, the main mechanisms involved for inducing tumor cell apoptosis were inhibition of Jak/STAT3 signaling, Ras/ERK signaling, and PI3K/Akt/mTOR/NF-κB upstream signaling, activation of TNFR1, FasL death-related signaling, and JNK/P38 signaling (Fig 4 a). Isospirostanol steroidal saponins induced tumor cell autophagy by inhibiting PDK1/Akt/mTOR signaling and activating AMPK/mTOR/ULK1 signaling (Fig 4 c). Isospirostanol steroidal saponins inhibited tumor cell metastasis and angiogenesis by suppressing Vav2/Cdc42 signaling, Jak/STAT3 signaling, PI3K/Akt/mTOR/HIF1α signaling, PI3K/Akt/NF-κB signaling, FAK/Src/Akt signaling, EphA2/Akt signaling, and CIP2A/PP2A/Akt signaling, and by activating TIMP proteins (Fig 4 b). Like the antitumor mechanism of spirostanol steroid saponins, isospirostanol steroid saponins inhibited SKP-2 signaling and activated

ATM/CHK/P53 signaling to reduce the tumor cell progression (Fig 4 e). Isospirostanol steroid saponins mainly inhibited MEK/ERK/NF-κB signaling and PI3K/Akt/NF-κB/MDR1/P-gp signaling from overcoming tumor resistance (Fig 4 d).

3.3 Furosterol type

Furostanol steroidal saponins are found less frequently and exhibit good antitumor activity (Hu and Yao, 2003). The E/F ring of furostanol steroidal saponins is in a cleaved state compared to the structure of spirostanol steroidal saponins. This paper mainly summarizes the induction of apoptosis in tumor cells.

3.3.1 Induction of tumor cell apoptosis and inhibition of tumor cell glycolysis

Protodioscin is a furostanol steroidal saponin mostly found in Dioscoreaceae. Lin et al. (2018) observed that protodioscin promoted the upregulation of Bax, the downregulation of Bcl-2, the activation of Caspase-3 and PARP, and upstream signaling. It induced ROS generation and endoplasmic reticulum stress-mediated apoptosis in HeLa and C33A cells by activating EIF-2 and increasing the expression of stress response protein ATF4 and CCAAT enhancer binding protein CHOP. In an important study, Hsieh et al. (2017) discussed that methyl protodioscin is a methylated derivative of protodioscin. It can activate apoptosis-regulating proteins (caspase-3, etc.) associated with oral squamous cell carcinoma and induce apoptosis in OSCC cells. Combined with cathepsin S., it significantly induced apoptosis in oral squamous carcinoma cells via P38/JNK signaling. Protodioscin can induce apoptosis in Hela cells by increasing Fas expression (Ma et al., 2019). Chen et al. (2018a) used fluorodeoxyglucose as a marker in the MIA-PaCa-2 cell transplantation model and found that Methyl protodioscin

prevented fluorodeoxyglucose uptake by tumors and suppressed tumor glycolysis. The evidence above showed that protodioscin and its derivatives may soon become a potential antitumor drug.

3.3.2 Summary

Furostanol steroidal saponins are found in fewer species, resulting in fewer reported antitumor mechanisms that inhibit tumor cell growth by inducing apoptosis. To induce apoptosis in tumor cells, furostanol-type steroidal saponins primarily activated JNK/P38/eIF2/ATF4/CHOP and FasL death signals (Fig 5).

3.4 Steroidal alkaloids

The previous summary showed that steroidal alkaloids have significant antitumor activity. Regarding the antitumor mechanism of steroidal alkaloids, we have outlined two key groups of compounds such as solanidine and tomatidine derivatives.

3.4.1 Solanidine and its derivatives

Solanidine is the most common toxin found in solanaceous plants, primarily in *Solanum tuberosum* L., and their glycosylated derivatives include solanine α-Solanine and α-Chaconine. The cytotoxicity of solanidine and its derivatives towards tumor cells has been well-documented (Hameed et al., 2017). Its antitumor mechanism mainly involves inducing tumor cell apoptosis, blocking the tumor cell cycle, suppressing tumor migration, and inhibiting tumor immune escape.

3.4.1.1 Induction of apoptosis in tumor cells

DNA-breaking factor DFF-40 plays an essential role in apoptosis (Jong et al., 2012), and solanidine increased the level of DFF-40 in tumor cells' nuclei, inhibiting

the proliferation of A549 and other cells. Solanidine inhibited PI3K/Akt signaling to induce tumor cells apoptosis (Malojirao et al., 2018). α-Chaconine, a solanidine derivative, induced apoptosis in tumor cells. Yang et al. (2006) revealed that α-chaconine suppressed ERK activity, inhibiting the activation of the downstream protein caspase-3, leading to apoptosis of HT-29 cells. Similarly,Pan et al. (2016) reported that solanine derived from solanidine, induced DU145 apoptosis in prostate cancer cells by increasing ROS and activating p38 MAPK, resulting in increased levels of phosphorylated ATF-2. Solanine also induced apoptosis in pancreatic cancer cells by upregulating the Bax/Bcl-2 ratio, increasing cytochrome-C and Smac levels in the cytoplasm, and activating Caspase activation (Sun et al., 2014).

3.4.1.2 Inhibition of tumor migration and invasion

α-Solanine inhibited the migration and invasion of human choriocarcinoma JEG-3 cells mainly by the down-regulation of MMP-2/9 levels (Gu et al., 2021). α-Solanine also inhibited the phosphorylation of PI3K, Akt, and ERK to reduce the expression of MMPs and increased the expression of tissue inhibitor of metalloproteinases-1/2 (TIMP-1/2), which effectively reduced PC-3 cell invasion (Shen et al., 2014). In addition, α-solanine inhibited tumor cell migration by inhibiting ERK1/2 and HIF-1α activity, decreasing VEGF expression, and increasing E-cadherin levels (Wen et al., 2016). Immunomodulation has an important impact on tumor growth. TGFβ, a member of the TGFβ family, regulates the proliferation and differentiation of immune cells, inhibits the immune response, and plays a crucial role in tumorigenesis, development, and metastasis. Furthermore, Treg cells can inhibit tumor immunogenesis. In a mouse

model of hepatocellular carcinoma transplantation, Gao et al. (2020a) found that solanine decreased TGFβ1, phosphorylated Smad2, phosphorylated Smad3, and Treg cells in tumor peripheral blood. Thus, solanine inhibited Treg cell-mediated tumor immune escape by inhibiting the TGFβ/Smad signaling pathway.

3.4.2 Tomatidine and its derivatives

Tomatidine is a natural compound extracted from *Solanum lycopersicum* L., and its derivative α-tomatine is formed by linking tomatidine with oligosaccharide through the glycosidic bond. A-tomatine had a robust antitumor effect (Friedman, 2013; Friedman et al., 2009; Jiang et al., 2016). Its antitumor mechanism induced tumor cell apoptosis and inhibited tumor cell migration and invasion.

3.4.2.1 Inducing apoptosis and inhibiting tumor cell migration and invasion *in vitro*

Receptor-interacting protein kinase (RIP) regulates cell death and is a key regulator of cell survival and death (Meylan and Tschopp, 2005). α-Tomatine promoted apoptosis by decreasing RIP1 and increasing RIP3 in HCT116 colon cancer cells. It also relied on the mitochondrial release of apoptosis-inducing factor (AIF) for this process (Rudolf and Rudolf, 2016). α-Ttomatine also inhibited PI3K/Akt signaling and PI3K/Akt downstream proteins mTOR and NF-κB while increasing the expression of pro-apoptotic protein Bad and decreasing the expression of anti-apoptotic proteins Bcl-2 and Bcl-xL to promote tumor cell apoptosis (Kim et al., 2015; Lee et al., 2013; Wu et al., 2021).

In addition, α-tomatine was also involved in downregulating FAK/PI3K/Akt signaling and inhibiting Iκ-B phosphorylation, inhibiting the transcription factor NF-

κB activation and ultimately reducing the expression of Metallo-matrix protease MMP-7 and suppressing the migration and invasion in human non-small cell lung cancer cells NCI-H460(Shieh et al., 2011). Likewise, Jeon and Kim (2019) observed that tomatidine also inhibited tumor invasion by downregulating the survival signal ERK/P38 in HT1080 cells and reducing the activity and expression of the Metallo-matrix protease MMP-2 in HT1080 cells. Yan et al. (2013) found that tomatidine inhibited the invasion of A549 lung cancer cells by regulating MMP.

3.4.3 Summary

Steroidal alkaloids promote apoptosis in tumor cells by inhibiting Ras/ERK/P38 and PI3K/Akt/mTOR/NF-κB signaling and promoting P38/ATF2 signaling (Fig 6 a). The primary mechanism of action of steroidal alkaloids in reducing tumor cell migration and invasion is to inhibit FAK/Akt, PI3K/Akt/NF-κB, and ERK/P38/HIF1α signaling and to activate TIMP proteins to inhibit the MMP family (Fig 6 b).

3.5 Cholesterol type

Cholesterol glycosides are like steroidal saponins, and their antitumor properties are comparable to those of steroidal saponins, as discussed previously. OSW-1, which has significant antitumor activity, is mainly mentioned here, and its antitumor mechanism is primarily the induction of tumor cell apoptosis and inhibition of tumor cell migration.

3.5.1 Induction of apoptosis and inhibition of tumor cell migration and invasion

OSW-1 is a cholestane saponin isolated from *Ornithogalum caudatum* Jacq.. In their study, Iguchi et al. (2019) described that OSW-1 induced apoptosis in HL-60 cells

by producing DNA breaks and nuclear chromatin aggregates.OSW-1 also induced apoptosis in breast cancer cells by increasing cytochrome C in the cytoplasm, activating caspase-3, and cleaving PARP (Ding et al., 2020b; Zhang et al., 2017b). Moreover, OSW-1 can promote Bcl-2 cleavage via caspase-8, leading to apoptosis (Zhu et al., 2005). In addition, OSW-1 promoted LoVo and SW480 colon cancer cell apoptosis via the mitochondrial pathway and inhibited tumor proliferation in nude mice via the apoptotic pathway while exhibiting minimal adverse effects (Zhang et al., 2017b). HSP47 is known to be inhibited under Golgi stress, which can lead to Caspase-2-mediated apoptosis (Miyata et al., 2013). Kimura et al. (2019) reported that OSW-1 preferentially localizes to the Golgi and induces apoptosis by triggering the Golgi stress response through CREB3-ARF4. The mTOR signaling pathway plays a crucial role in regulating various cellular processes, and OSW-1 can also influence cellular processes through this pathway. However, unlike the previously described inhibition of mTOR signals, OSW-1 disrupts the interaction between mTOR and rictor/mTORC2. This inhibition further suppresses the growth of prostate cancer cells PC3 and LNCaP by inhibiting mTORC2 (Elgehama, 2021). Ding et al. (2020b) observed that OSW-1 inhibited the migration and invasion of triple-negative breast cancer, primarily by immunofluorescence labeling, and found a significant decrease in tumor cell migration and invasion. Protein immunoblotting analysis revealed increased E-cadherin expression and decreased vimentin expression, indicating that OSW-1 inhibited EMT-mediated migration of MDA-MB-231 and MDA-MB-453 cells.

3.5.2 Summary

The cholesteryl glycoside OSW-1 has strong antitumor activity, and the mechanism mainly represents the inhibition of PI3K/Akt/mTOR signaling and mTORC2 signaling and affection of adhesion-related protein expression to induce apoptosis and suppress tumor cell migration and invasion (Fig 7).

3.6 Summary

Steroid saponins are gaining more significance as their signaling mechanisms largely contribute to their antitumor properties. In the previous summary of the antitumor activity of steroid saponins, it was observed that isospirostanol-type steroid saponins and cholestane glycosides have better antitumor activities. The antitumor activity of isospirostanol-type steroidal saponins was considerably higher than that of spirostanol type steroidal saponins and steroidal alkaloids. In conclusion, EphA2/Akt signaling, CIP2A/PP2A/Akt signaling, FasL, and TNFR signaling mechanisms affected by isospirostanol-type steroidal saponins do not play a role in spirostanol type steroidal saponins as well as steroidal alkaloids. Furthermore, there was no difference in antitumor activity between isospirostanol steroidal saponins and furostanol-type steroidal saponins. This may be because furostanol steroidal saponins also affected the FasL death signal that was affected by isospirostanol steroidal saponins, and both types of steroidal saponins affect the same key death signal, which could be the reason for their similar antitumor activities. The antitumor activity of OSW-1 was significantly higher than that of the other four steroidal saponins because its antitumor mechanism is unique. OSW-1 damaged tumor cell DNA by direct interaction and inhibited the mTORC2 complex. These mechanisms may account for the stronger antitumor activity

of OSW-1. Therefore, targeting mechanisms or targets that can strongly inhibit tumor cell growth might aid in designing future antitumor drugs.

4. Problems and possible solutions that limit the development of steroidal saponins

The previous section highlights the noteworthy antitumor effects of steroidal saponins. Nevertheless, when developing a new anti-cancer drug, it is crucial to consider its effectiveness against tumors and its potential toxic side effects, as these are essential factors in assessing its therapeutic suitability. Therefore, we also summarized the cytotoxicity of steroidal saponins (Table 2). The IC_{50} range of steroid saponins acting on normal cells was 0.0002-33.00 μM, indicating no significant difference in the toxicity of steroid saponins on normal cells and tumor cells (Fig 8 a). Pharmacokinetics is an important part of preclinical drug studies, thus, we compiled and evaluated the steroid saponin bioavailability (Table 3) and found that steroid saponin bioavailability was lower than that of the other marketed anticancer drugs (vinorelbine, gemcitabine, etc.) (Table 4 & Fig 8 b). The steroidal saponins are secondary metabolites of medicinal plants. Their production is inadequate due to the limited availability of medicinal plants and the slow production of medicinally important secondary metabolites, limiting the clinical application of steroidal saponins (Upadhyay et al., 2018). In conclusion, steroidal saponins have disadvantages such as high cytotoxicity, low bioavailability, and insufficient sustainability to meet the market demands. Therefore, we have summarized some guidelines that may compensate for these disadvantages.

Table 2 Cytotoxicity of steroidal saponins

Structure	Chemical compound	Cells/IC_{50}	Ref
Spirostane	Asparacoside	HUVEC: 4.100 μM (N/A)	(Zhang et al., 2004)

	Suttonigenin F	HDF: 4.200 μM (N/A)	(Tran et al., 2019)
	Suttonigenin H	HDF: 8.300 μM (N/A)	(Tran et al., 2019)
	Suttonigenin I	HDF: 8.900 μM (N/A)	(Tran et al., 2019)
	Suttonigenin J	HDF: 16.500 μM (N/A)	(Tran et al., 2019)
Isospirostane	Polyphyllin I	7702: 0.847 μM (24 h) 0.544 μM (48 h) 0.500 μM (72 h)	(Wang et al., 2019d)
	Polyphyllin II	7702: 1.889 μM (24 h) 0.847 μM (48 h) 0.701 μM (72 h)	(Wang et al., 2019d)
	Polyphyllin VI	7702: 8.187 μM (24 h) 5.150 μM (48 h) 3.898 μM (72 h)	(Wang et al., 2019d)
	Polyphyllin VII	7702: 0.806 μM (24 h) 0.621 μM (48 h) 0.505 μM (72 h)	(Wang et al., 2019d)
	Deltonin	HEK293: 9.730 μM (48 h)	(Tong et al., 2012)
	Dioscin	HEK293: 6.620 μM (48 h)	(Tong et al., 2012)
	Dioscin	HUVEC: 1.600 μM (24 h)	(Tong et al., 2014)
	Terrestrosin D	HUVEC: <3.000 μM (24 h)	(Wei et al., 2014)
	Suttonigenin A	HaCat: 18.200 μM (N/A) HDF: 4.300 μM (N/A)	(Tran et al., 2019)
	Suttonigenin C	HDF: 7.500 μM (N/A)	(Tran et al., 2019)
	Suttonigenin D	HDF: 8.600 μM (N/A)	(Tran et al., 2019)
	Suttonigenin E	HDF: 6.600 μM (N/A)	(Tran et al., 2019)
	Pennogenyl saponin 1	HaCaT: 1.010 μM (24 h)	(Stefanowicz-Hajduk et al., 2015)
	Pennogenyl saponin 2	HaCaT: 0.940 μM (24 h)	(Stefanowicz-Hajduk et al., 2015)
	(22R, 25R)-spirosol-5-e-n-3β-yl O-α-L-rhamno-pyranosyl-(1-2)-β-D-gl-ucopyranosyl-(1-4)-β-D-glucopyranoside	3T3 murine fibroblast cell line: 8.200 μM (N/A)	(Esposito et al., 2013)
Furostane	(25R)-26-O-(β-D-gluco-pyranosyl)-furost-5-en-3β,22α, 26-triol 3-O-α-L-rhamnopyranosyl-(1-2)-β-D-glucopyranosyl-(1-4)-β-D-glucopyranos-ide	3T3 murine fibroblast cell line: 8.700 μM (N/A)	(Esposito et al., 2013)
	Zingiberensis saponin	HEK293: 4.150 μM (48 h)	(Tong et al., 2012)
Cholestane	OSW-1	BJ: 0.0002 μM (72h)	(Maj et al., 2011)
	OSW-1	MCF/10A: 0.052 μM (72h)	(Ding et al., 2020b)
Alkaloids	α-Tomatine	Chang: 33.000 μM (48h) Hel299: 25.000 μM (48h)	(Choi et al., 2012)
	α-Solasonine	VERO P35: 16.650 μM (48h)	(Akter et al., 2015)

β-Solamarine	NIH3T3: 11.180 μM (48h) VERO P35: 8.320 μM (48h)	(Akter et al., 2015)
(25R)-3β-{O-β-D-gluco-pyranosyl-(1→4)-O-α-L-rhamnopyranosyl-(1→4)-[O-α-L-rhamnopy-ranosyl-(1→2)]-α-L-rh-amnopyranosyl}-22αN-spirosol-5-ene	NIH3T3: 5.080 μM (48h) VERO P35: 24.030 μM (48h) NIH3T3: 22.330 μM (48h)	(Akter et al., 2015)

Table 3 Bioavailability of steroidal saponins

Structure	Compound	Bioavailability（F%）	Ref
Spirostane	Sarsasapogenin-AA13	8.82	(Pei et al., 2020)
Isospirostane	Dioscin	0.90	(Lu et al., 2020)
	DT-13	5.47	(Chen et al., 2011a)
	Gracillin	0.28	(Lu et al., 2020)
	Polyphyllin H	1.00	(Lu et al., 2020)
	Polyphyllin I	0.62	(Zhu et al., 2015)
	Polyphyllin I	0.54	(Lu et al., 2020)
	Polyphyllin II	8.20	(Yang et al., 2020)
	Polyphyllin II	7.20	(Yang et al., 2020)
	Polyphyllin II	6.10	(Yang et al., 2020)
	Polyphyllin II	0.75	(Lu et al., 2020)
	Polyphyllin S	0.35	(Lu et al., 2020)
	Polyphyllin VI	0.32	(Lu et al., 2020)
	Polyphyllin VII	0.73	(Lu et al., 2020)
	Progenin III	0.50	(Lu et al., 2020)
Furostane	Pseudoprotodioscin	5.70	(Liao et al., 2016)
	Timosaponin B-II	1.10	(Cai et al., 2008)
Cholestane	20-Hydroxyecdysone	12	(Bellahreche and Dahmani, 2023)
Alkaloids	α-Solanine	1.6	(Groen et al., 1993)
	Solasonine	1.7	(Chen et al., 2015)
	Hapepunine	22	(Chen et al., 2020)

Table 4 Bioavailability of clinical anticancer drugs

Compound	Bioavailability（F%）	Ref
Vinorelbine	20.60	(Pétain et al., 2019)
Vinorelbine	43.00	(Marty et al., 2001)
Vinorelbine	35.70	(Puozzo and Gridelli, 2004)
Vinorelbine	37.60	(Puozzo and Gridelli, 2004)
Vinorelbine	33.00	(Lush et al., 2005)
Gemcitabine	18.30	(Thompson et al., 2020)

V-Gemcitabine	16.70	(Thompson et al., 2020)
SL-01	22.39	(Zhao et al., 2013)
SL-01	32.16	(Zhao et al., 2013)
Gemcitabine	59.00	(Beumer et al., 2008b)
D07001-F4	34.00	(Hao et al., 2013)
THU	23.30	(Beumer et al., 2008a)
THU	19.10	(Beumer et al., 2008a)

4.1 Steroidal saponin cytotoxicity

Since steroid saponins have significant cytotoxicity, which is problematic in their clinical applications, however, this problem can be resolved by several approaches, including the production of steroid saponin nanocomplexes, antigen-targeted liposome complexes, and chemical modifications of steroid saponins (Fig 9 a).

The available literature suggests that drug-delivery techniques can enhance selectivity and reduce toxic side effects (Liyanage et al., 2019). Research on saponin delivery has yielded some significant results in recent years, and relevant studies have been summarized (Fuchs et al., 2009). Dioscin is a classical steroidal saponin with remarkable antitumor activity; however, its hemolytic properties and toxic side effects are also substantial. In this context, Wang et al. (2022) prepared dioscin-cholesterol nano-complexes, which effectively reduced dioscin's exposure and significantly reduced its hemolytic toxicity.

Diosgenin, a precursor of dioscin, also has good antitumor effects. Li et al. (2015) manufactured a nanoparticle platform based on polyethylene glycol-diosgenin (mPEG-DGN) conjugation, reducing toxicity and improving the antitumor effect compared to free diosgenin. Montmorillonite-human serum albumin (Mt-HSA) nanocomposites can also be used as carriers for saponins, and saponin-montmorillonite-human serum

protein nanocrystals showed excellent anti-cancer results with almost no toxicity to normal cells (Akbal et al., 2018).

Targeted delivery of steroid saponins via antigen-antibody interaction has significant advantages in reducing their cytotoxicity. CD44 is a non-kinase cell surface transmembrane glycoprotein widely used as a cancer stem cell (CSC) marker in various cancers (Hassn Mesrati et al., 2021). Lu et al. (2018) prepared anti-CD44 antibody-modified liposomes and conjugated the liposomes to timosaponin AIII for drug delivery, and this technique improved the selectivity and antitumor activity of timosaponin AIII. Therefore, targeted delivery of steroidal saponins is a promising strategy for overcoming the toxicity of steroidal saponins.

Moreover, there is a correlation between the cytotoxicity of the compounds and their chemical structures. Alteration of the side chain at the C17 position of the steroidal saponin OSW-1 significantly affected its antitumor activity, and modifications to the disaccharide component of OSW-1 significantly altered its biological activity (Shi et al., 2005; Tschamber et al., 2007). The rest of OSW-1 remained unchanged, except that the β-conformation of the hydroxyl group at position 16 was changed to the α-conformation, and its cytotoxic activity was greatly reduced (Ma et al., 2001). The cytotoxicity of the 1→3 linkage of the disaccharide in OSW-1 was greatly reduced if the 1→4 linkage was changed. Zheng and colleagues (Zheng et al., 2011; Zheng et al., 2010) synthesized a 1→4-linked derivative with at least three orders of magnitude lower cytotoxicity than OSW-1 itself and also synthesized another OSW-1 disaccharide derivative that was essentially non-cytotoxic if the linked disaccharide was 1→4-linked.

Perez-Labrada et al. (2012) also synthesized 3,6-dipivaloylated glucosides (monosaccharides) that exhibited good cytotoxicity against cancer cells without significant cytotoxicity against healthy blood cells, whereas b-chacotriosides (trisaccharides) displayed no significant difference in killing cancer and normal cells. This property shows great promise for developing cytotoxic drugs based on spirostanes scaffolds. In conclusion, the chemical structure modification of steroid saponins themselves has a great potential to reduce their cytotoxicity significantly.

4.2 Steroidal saponin bioavailability

Before their use in clinical applications, the poor bioavailability of steroidal saponins was considered as disadvantage. However, there are less reports on an improved bioavailability of steroidal saponins. To address this, we have conducted a review of some key strategies that can be employed to improve the oral bioavailability of saponins, including the use of drug nanoparticles, drug emulsions, drug absorption enhancer conjugation techniques, liposome encapsulation techniques, cyclodextrin encapsulation techniques, and osmotic capsules (Fig 9 b). These strategies also provide some implications for steroidal saponins.

The poor solubility of steroidal saponins is mainly because of their poor oral bioavailability. Nanoformulations of saponin analogues might solve this problem. In this context, Zhao et al. (2020) prepared a self-nanosolid dispersion of ginsenoside compound K(CK). This nanoformulation significantly improved the solubility of ginsenoside compound K(CK), and its area under the curve (AUC, 0-24) was also 2.02 times higher than that of pure ginsenoside compound K(CK), In addition, self-

microemulsifying drug delivery systems can also improve the oral bioavailability of drugs, and the bioavailability of ginsenoside-Rh1/2 was significantly increased to 33.25% and 48.69%, respectively, after being formulated as self-microemulsions (Mundada et al., 2021; Yang et al., 2017).

Likewise, Wang et al. (2019e) developed an Akebia saponin D (ASD)-phospholipid complex self-nanoemulsifying drug delivery system, and found that Akebia saponin D (ASD)-phospholipid complex increased the oral bioavailability of ASD primarily by increasing membrane permeability, disrupting self-micellar bundles, and inhibiting intestinal metabolism resulting in a 4.3-fold increased oral bioavailability. Drug absorption enhancers can also improve their absorption in the body. Sodium N-[8-(2-hydroxybenzoyl) amino] caprylate (SNAC) improved the bioavailability of notoginsenoside R1, and the AUC of notoginsenoside R1 with SNAC was 2.24 times that of free notoginsenoside R1 (Li et al., 2018).

Liposome encapsulation allows the drug to be encapsulated within the liposome cavity to form a drug complex with a hydrophilic surface that increases the solubility of the drug complex.Using monolayer liposome extraction, Li et al. (2013) significantly increased the intestinal absorption of notoginsenoside R1, ginsenosides Rb1/Rd1, which increased the oral bioavailability of notoginsenoside R1, ginsenosides Rb1/Rd1. Similarly, Hao et al. (2016) prepared sodium deoxycholate-containing pre-liposomes of *Ginseng* fruit saponins (GFS), which enhanced the drug's absorption in the gastrointestinal tract and raised its oral bioavailability 2.84 times compRED TO free GFS.

liposome-containing sodium glycocholate could be used as an oral nanodrug delivery system. This drug delivery system increased the oral bioavailability of notoginsenoside R1 by enhancing the water solubility and permeability of notoginsenoside R1 (Fan et al., 2018). The cyclodextrin encapsulation technique WAs similar to the liposome encapsulation technique that improved the solubility and permeability of the drug. Okawara et al. (2014) found that hydroxypropyl β-cyclodextrin increased the bioavailability of diosgenin to 49.5%, and its bioavailability was comparable to that of clinically approved anticancer drugs. In addition, γ-cyclodextrin can also improve the bioavailability of insoluble drugs. The relative bioavailability of ginsenoside (G)-Re-γ-cyclodextrin complex was 171%, which significantly improved the bioavailability of ginsenoside (G)-Re (Li et al., 2021a). Each of these techniques has its own characteristics. Huang et al. (2015c) compared drug salting, hydroxypropyl-β-cyclodextrin encapsulation, emulsification, and nanoparticles and discovered that hydroxypropyl-β-cyclodextrin encapsulation enhanced the bioavailability of saponins. The relative bioavailability of notoginsenoside colon-specific osmotic pump capsule is 487.42%, which was significantly greater compared to free notoginsenoside (Jin et al., 2018). In conclusion, drug nanoformulations, liposome encapsulation technology, cyclodextrin encapsulation technology, and self-emulsifying drug delivery systems have a great potential to enhance the bioavailability of steroidal saponins.

4.3 Steroidal saponin production

The industrial production of steroidal saponins is a prerequisite for its applications

but currently needs more natural plant resources, resulting in low yields. The mechanism of steroidal saponin synthesis is fundamental. Thus, we reviewed some steroidal saponin biosynthesis and chemical synthesis and techniques to improve their yield, such as the enumeration of high-yielding steroidal saponin natural plants, the development of microbial heterologous synthetic chassis, inducers to increase steroidal saponins yield, and artificial chemical synthesis of steroid saponins (Fig 9 c).

The biosynthesis of steroidal saponins consists of three main stages: the production of sterols, the synthesis of saponin elements, and the linkage of different sugars to synthesize steroid saponins (Chen et al., 2021). Steroidal saponins are widely distributed in plants with two synthetic pathways, the mevalonate (MVA) pathway and the methylerythritol 4 phosphate (MEP) pathway, both of which synthesize dimethylallyl diphosphate (DMAPP). Then, the three enzymes used to synthesize squalene, namely geranyl diphosphate synthase (GPS), farnesyl diphosphate synthase (FPS), and squalene synthase (SQS) act sequentially on DMAPP, next squalene is converted to 2,3-oxidosqualene catalyzed by squalene epoxidase (SE), and finally, 2,3-oxidized squalene is cyclized by different squalene oxide cyclases. The products undergo cyclization, hydroxylation, and glycosylation reactions to yield various steroidal saponins (Upadhyay et al., 2018).

However, in the *Trigonella foenum-graecum* L., the yield of diosgenin reached 164.44 mg/L, indicating that *Trigonella foenum-graecum* L. represents a natural resource with a significant advantage in the production of diosgenin despite the yield of steroidal saponins synthesized by the plant itself is limited and has a considerable disadvantage

compared to other steroidal saponin synthesis methods (Jasim et al., 2017). Nevertheless, advances in metabolic engineering have greatly facilitated the re-establishment of plant secondary metabolic pathways in yeast cells, thus enabling the heterologous production of steroidal saponins in yeast and significantly increasing the yield of steroidal saponins. Xu et al. (2022) constructed the diosgenin synthesis pathway in *Saccharomyces cerevisiae*, screened the optimal ratio of cytochrome P450 monooxygenase (CYP) to cytochrome P450 reductase (CPR) associated with diosgenin synthesis, and attenuated the expression of *ERG6* gene, which significantly increased the synthesis of diosgenin and reduced the formation of by-products under high-density fermentation conditions. A DSG titer of 2.03 g/L was obtained under the conditions of high-density fermentation. In addition to optimizing steroidal saponin synthesis pathways to increase steroidal saponin production, inducers can also increase steroidal saponin content in plants, particularly in the more dominant *Trigonella foenum-graecum* L. plants. For example, diosgenin production increased from 164.44 mg/L to 214 mg/L in *Trigonella foenum-graecum* L. seedlings treated with silver nanoparticles (Ag-NPs). Accordingly, chemical inducers can also significantly increase the synthesis of steroidal saponins in plants (Jasim et al., 2017).

Its chemical synthesis is a promising method compared to the biosynthesis of steroidal saponins. Xiao and Yu (2013) achieved the entire synthesis of goniopectenoside B using inexpensive materials in 70 steps. This is the first artificial synthesis of the complex asterosaponin.Dai and Yu (2015) synthesized astrosterioside A with a total yield of 6.8% using 24-step linear convergence.Iga et al. (2005) used

2,3,4,6-tetra-O-acetyl-DD-galactopyranosyl bromide as a sugar group donor and obtained β-DD-galactopyranoside by alkaline hydrolysis..Normandin and Boudreault (2021) utilized the chemical synthesis of tomatidine, specifically using the Suzuki-Miyaura-type coupling reaction as a key step to link the enantiomerically pure F-ring side to the steroid scaffold of the natural product, using Lewis acid-mediated opening of the helical ketone followed by azide substitution and reduction sequences to generate helical amino ketone motif of the natural product in a total reaction of 15 steps with a yield of 15.2%.

In summary, among the abovementioned methodologies for steroid saponin biosynthesis, the natural plant *Trigonella foenum-graecum* L. showed significant advantages, and diosgenin yields exceeded 100 mg/L under natural conditions. However, the heterologous production of steroid saponins in brewer's yeast was more favorable than others, and steroid saponins reached gram levels, resulting in a significant increase in the yield of steroid saponins. Secondly, Ag nanoparticles also improved diosgenin yield up to 200 mg/L. Moreover, the chemical synthesis of steroid saponins is free from natural conditions, and synthetic raw materials are inexpensive. Although the numerous steps of *ab initio* synthesis are a drawback that needs to be improved, the chemical synthesis of steroid saponins lays a solid foundation for the industrial production of steroid saponins.

5. Conclusion and future prospects

In this review paper, we divided more than 40 steroidal saponins into five categories of steroidal saponins: spirostanol type, isospirostanol type, furostanol type,

steroidal alkaloids, and cholesterol type, and summarized the antitumor activity of these five categories of steroidal saponins. We found that isospirostanol type steroidal saponin and cholesterol-type steroidal saponin OSW-1 have better antitumor effects compared to the others. We also discussed the antitumor mechanisms of each of the five classes of steroidal saponins mentioned above. Seroidal saponins mainly display the five major mechanisms of inducing apoptosis, inducing autophagy in tumor cells, inhibiting tumor migration and invasion, blocking tumor cell cycle progression, and overcoming drug resistance in tumor cells by affecting the signaling network in tumor cells. Moreover, the antitumor mechanisms of different classes of steroidal saponins also differ slightly. Possibly, the antitumor mechanisms of each class of steroidal saponins are responsible for the differences in antitumor activity among each class of steroidal saponins. We summarized the antitumor activity of steroid saponins while observing their shortcomings. Besides, we determined that steroid saponins have greater cytotoxicity, lower bioavailability, and the lack of natural medicinal plant resources. We proposed strategies to overcome these disadvantages and promote the clinical application of steroid saponins. In conclusion, steroidal saponins have excellent antitumor activity and antitumor mechanisms, and steroidal saponins have the potential to be developed into novel antitumor drugs. However, compared to mature drugs, steroidal saponins also have some drawbacks that must be addressed: (1) steroidal saponins not only have tumor-inhibiting activity but also have inhibitory effects on normal cells, indicating high cytotoxicity, (2) the bioavailability of steroidal saponins is around 10%, which is less than that of established clinical drugs, (3) due to the lack

of medicinal plant resources, the production of steroidal saponins is insufficient to meet market demand. Addressing the above shortcomings will play a role in expanding the application of steroidal saponins.

Funding

This work was supported by the National Key Research and Development Program of China (Grant No.2023YFA0915800), Key project at central government level: The ability establishment of sustainable use for valuable Chinese medicine resources (2060302).

References

Abu Samaan, T.M., Samec, M., Liskova, A., Kubatka, P., Busselberg, D., 2019. Paclitaxel's Mechanistic and Clinical Effects on Breast Cancer. Biomolecules 9, 789.

Akbal, O., Vural, T., Malekghasemi, S., Bozdoğan, B., Denkbaş, E.B., 2018. Saponin loaded montmorillonite-human serum albumin nanocomposites as drug delivery system in colorectal cancer therapy. Applied Clay Science 166, 214-222.

Akter, R., Uddin, S.J., Tiralongo, J., Grice, I.D., Tiralongo, E., 2015. A New Cytotoxic Steroidal Glycoalkaloid from the Methanol Extract of Blumea lacera Leaves. J Pharm Pharm Sci 18, 616-633.

Ali, Z., Smillie, T. J., Khan, I. A., 2013. Two spirostan steroid glycoside fatty esters from Dioscorea cayenensis. Nat Prod Commun 8, 323–326.

Baharuddin, W.N.A., Yusoff, A.A.M., Abdullah, J.M., Osman, Z.F., Ahmad, F., 2018. Roles of EphA2 Receptor in Angiogenesis Signaling Pathway of Glioblastoma Multiforme. Malays J Med Sci 25, 22-27.

Bai, C., Yang, X., Zou, K., He, H., Wang, J., Qin, H., Yu, X., Liu, C., Zheng, J., Cheng,

F., Chen, J., 2016. Anti-proliferative effect of RCE-4 from Reineckia carnea on human cervical cancer HeLa cells by inhibiting the PI3K/Akt/mTOR signaling pathway and NF-kappaB activation. Naunyn Schmiedebergs Arch Pharmacol 389, 573-584.

Bao, W., Pan, H., Lu, M., Ni, Y., Zhang, R., Gong, X., 2007. The apoptotic effect of sarsasapogenin from Anemarrhena asphodeloides on HepG2 human hepatoma cells. Cell Biol Int 31, 887-892.

Bellahreche, Z., Dahmani, Y., 2023. 20-Hydroxyecdysone bioavailability and pharmacokinetics in Gerbillus tarabuli, a gerbil model for metabolic syndrome studies. Steroids 198, 109262.

Beumer, J.H., Eiseman, J.L., Parise, R.A., Florian, J.A., Jr., Joseph, E., D'Argenio, D.Z., Parker, R.S., Kay, B., Covey, J.M., Egorin, M.J., 2008a. Plasma pharmacokinetics and oral bioavailability of 3,4,5,6-tetrahydrouridine, a cytidine deaminase inhibitor, in mice. Cancer Chemother Pharmacol 62, 457-464.

Beumer, J.H., Eiseman, J.L., Parise, R.A., Joseph, E., Covey, J.M., Egorin, M.J., 2008b. Modulation of gemcitabine (2',2'-difluoro-2'-deoxycytidine) pharmacokinetics, metabolism, and bioavailability in mice by 3,4,5,6-tetrahydrouridine. Clin Cancer Res 14, 3529-3535.

Bi, L., Liu, Y., Yang, Q., Zhou, X., Li, H., Liu, Y., Li, J., Lu, Y., Tang, H., 2021. Paris saponin H inhibits the proliferation of glioma cells through the A1 and A3 adenosine receptor-mediated pathway. Int J Mol Med 47, 30.

Cai, F., Sun, L., Gao, S., Yang, Y., Yang, Q., Chen, W., 2008. A rapid and sensitive liquid

chromatography-tandem mass spectrometric method for the determination of timosaponin B-II in blood plasma and a study of the pharmacokinetics of saponin in the rat. J Pharm Biomed Anal 48, 1411-1416.

Chen, C. R., Zhang, J., Wu, K. W., Liu, P. Y., Wang, S. J., Chen, D. Y., Ji, Z. N., 2015. Gracillin induces apoptosis in HL60 human leukemic cell line via oxidative stress and cell cycle arrest of G1. Pharmazie 70, 199–204.

Chen, J.R., Jia, X.H., Wang, H., Yi, Y.J., Wang, J.Y., Li, Y.J., 2016a. Timosaponin A-III reverses multi-drug resistance in human chronic myelogenous leukemia K562/ADM cells via downregulation of MDR1 and MRP1 expression by inhibiting PI3K/Akt signaling pathway. Int J Oncol 48, 2063-2070.

Chen, L., Cheng, C.S., Gao, H., Zhan, L., Wang, F., Qu, C., Li, Y., Wang, P., Chen, H., Meng, Z., Liu, L., Chen, H., Chen, Z., 2018a. Natural Compound Methyl Protodioscin Suppresses Proliferation and Inhibits Glycolysis in Pancreatic Cancer. Evid Based Complement Alternat Med 2018, 7343090.

Chen, L.L., Yuan, W.W., Hu, Z.F., Qi, J., Zhu, D.N., Yu, B.Y., 2011a. Determination and pharmacokinetics of DT-13 in rat plasma by LC-MS. J Pharm Biomed Anal 56, 650-654.

Chen, L., Zhang, Q., Lin, Y., Lu, X., Zhong, Z., Ma, J., Wen, C., Ding, C., 2020. Pharmacokinetics and bioavailability of hapepunine in mice by ultra-performance liquid chromatography–tandem mass spectrometry. Acta Chromatographica 32, 44-48.

Chen, M., Guo, Y., Zhao, R., Wang, X., Jiang, M., Fu, H., Zhang, X., 2016b.

Ophiopogonin B induces apoptosis, mitotic catastrophe and autophagy in A549 cells. Int J Oncol 49, 316-324.

Chen, M., Hu, C., Guo, Y., Jiang, R., Jiang, H., Zhou, Y., Fu, H., Wu, M., Zhang, X., 2018b. Ophiopogonin B suppresses the metastasis and angiogenesis of A549 cells in vitro and in vivo by inhibiting the EphA2/Akt signaling pathway. Oncol Rep 40, 1339-1347.

Chen, P.S., Shih, Y.W., Huang, H.C., Cheng, H.W., 2011b. Diosgenin, a steroidal saponin, inhibits migration and invasion of human prostate cancer PC-3 cells by reducing matrix metalloproteinases expression. PLoS One 6, e20164.

Chen, Q.W., Gong, T., Zhang, P.C., Kong, J.Q., 2020. Seven new 1-oxygenated cholestane glycosides from Ornithogalum saundersiae. J Asian Nat Prod Res 22, 201-216.

Chen, T., Lin, J., Tang, D., Zhang, M., Wen, F., Xue, D., Zhang, H., 2019. Paris saponin H suppresses human hepatocellular carcinoma (HCC) by inactivation of Wnt/β-catenin pathway in vitro and in vivo. Int J Clin Exp Pathol 12, 2875–2886.

Chen, Y., Wu, J., Yu, D., Du, X., 2021. Advances in steroidal saponins biosynthesis. Planta 254, 91.

Chen, Y., Zhang, S., Chen, D., Zhou, M., Zheng, J., Xiang, Z., 2015. An UPLC-MS/MS method for determination of solasonine in rat plasma and its application of a pharmacokinetic and bioavailability study. J Chromatogr B Analyt Technol Biomed Life Sci 985, 1-5.

Cheng, Z., Li, Z., Gu, L., Li, L., Gao, Q., Zhang, X., Fu, J., Guo, Y., Li, Q., Shen, X.,

Chen, M., Zhang, X., 2022. Ophiopogonin B alleviates cisplatin resistance of lung cancer cells by inducing Caspase-1/GSDMD dependent pyroptosis. J Cancer 13, 715-727.

Chiang, C.T., Way, T.D., Tsai, S.J., Lin, J.K., 2007. Diosgenin, a naturally occurring steroid, suppresses fatty acid synthase expression in HER2-overexpressing breast cancer cells through modulating Akt, mTOR and JNK phosphorylation. FEBS Lett 581, 5735-5742.

Chiang, K.C., Lai, C.Y., Chiou, H.L., Lin, C.L., Chen, Y.S., Kao, S.H., Hsieh, Y.H., 2019. Timosaponin AIII inhibits metastasis of renal carcinoma cells through suppressing cathepsin C expression by AKT/miR-129-5p axis. J Cell Physiol 234, 13332-13341.

Chiu, Y.H., Hsu, S.H., Hsu, H.W., Huang, K.C., Liu, W., Wu, C.Y., Huang, W.P., Chen, J.Y., Chen, B.H., Chiu, C.C., 2018. Human non-small cell lung cancer cells can be sensitized to camptothecin by modulating autophagy. Int J Oncol 53, 1967-1979.

Choi, S.H., Ahn, J.B., Kozukue, N., Kim, H.J., Nishitani, Y., Zhang, L., Mizuno, M., Levin, C.E., Friedman, M., 2012. Structure-activity relationships of alpha-, beta(1)-, gamma-, and delta-tomatine and tomatidine against human breast (MDA-MB-231), gastric (KATO-III), and prostate (PC3) cancer cells. J Agric Food Chem 60, 3891-3899.

Chung, Y.L., Pan, C.H., Wang, C.C., Hsu, K.C., Sheu, M.J., Chen, H.F., Wu, C.H., 2016. Methyl Protodioscin, a Steroidal Saponin, Inhibits Neointima Formation in Vitro and in Vivo. J Nat Prod 79, 1635-1644.

Condello, M., Meschini, S., 2021. Role of Natural Antioxidant Products in Colorectal Cancer Disease: A Focus on a Natural Compound Derived from Prunus spinosa, Trigno Ecotype. Cells 10, 3326.

Corbiere, C., Liagre, B., Terro, F., Beneytout, J. L., 2004. Induction of antiproliferative effect by diosgenin through activation of p53, release of apoptosis-inducing factor (AIF) and modulation of caspase-3 activity in different human cancer cells. Cell Res 14, 188–196.

Dai, Y., Yu, B., 2015. Total synthesis of astrosterioside A, an anti-inflammatory asterosaponin. Chem Commun (Camb) 51, 13826-13829.

Ding, Q., Zhang, W., Cheng, C., Mo, F., Chen, L., Peng, G., Cai, X., Wang, J., Yang, S., Liu, X., 2020a. Dioscin inhibits the growth of human osteosarcoma by inducing G2/M-phase arrest, apoptosis, and GSDME-dependent cell death in vitro and in vivo. J Cell Physiol 235, 2911-2924.

Ding, X., Li, Y., Li, J., Yin, Y., 2020b. OSW-1 inhibits tumor growth and metastasis by NFATc2 on triple-negative breast cancer. Cancer Med 9, 5558-5569.

Dohadwala, M., Luo, J., Zhu, L., Lin, Y., Dougherty, G.J., Sharma, S., Huang, M., Pold, M., Batra, R.K., Dubinett, S.M., 2001. Non-small cell lung cancer cyclooxygenase-2-dependent invasion is mediated by CD44. J Biol Chem 276, 20809-20812.

Dong, W., Dong, Q., Ding, H., 2021. Ophiopogonin B induces reactive oxygen species-dependent apoptosis through the Hippo pathway in nasopharyngeal carcinoma. Mol Med Rep 24, 534.

Du, H., Huang, Y., Hou, X., Yu, X., Lin, S., Wei, X., Li, R., Khan, G.J., Yuan, S., Sun, L., 2016. DT-13 inhibits cancer cell migration by regulating NMIIA indirectly in the tumor microenvironment. Oncol Rep 36, 721-728.

Du, H., Liu, Y., Chen, X., Yu, X., Hou, X., Li, H., Zhan, M., Lin, S., Lu, L., Yuan, S., Sun, L., 2018. DT-13 synergistically potentiates the sensitivity of gastric cancer cells to topotecan via cell cycle arrest in vitro and in vivo. Eur J Pharmacol 818, 124-131.

Elekofehinti, O.O., Iwaloye, O., Olawale, F., Ariyo, E.O., 2021. Saponins in Cancer Treatment: Current Progress and Future Prospects. Pathophysiology 28, 250-272.

Elgehama, A., 2022. Selective obstruction of the mTORC2 complex by a naturally occurring cholestane saponin (OSW-1) for inhibiting prostate cancer cell growth. J Asian Nat Prod Res 24, 663-672.

Esposito, D., Munafo, J.P., Jr., Lucibello, T., Baldeon, M., Komarnytsky, S., Gianfagna, T.J., 2013. Steroidal glycosides from the bulbs of Easter lily (Lilium longiflorum Thunb.) promote dermal fibroblast migration in vitro. J Ethnopharmacol 148, 433-440.

Fan, L., Li, Y., Sun, Y., Han, J., Yue, Z., Meng, J., Zhang, X., Zhang, F., Mei, Q., 2015a. Paris Saponin VII Inhibits the Migration and Invasion in Human A549 Lung Cancer Cells. Phytother Res 29, 1366-1372.

Fan, L., Li, Y., Sun, Y., Yue, Z., Meng, J., Zhang, X., Zhang, R., Zhang, D., Zhang, F., Mei, Q., 2015b. Paris saponin VII inhibits metastasis by modulating matrix metalloproteinases in colorectal cancer cells. Mol Med Rep 11, 705-711.

Fan, Q., Zhang, Y., Hou, X., Li, Z., Zhang, K., Shao, Q., Feng, N., 2018. Improved oral bioavailability of notoginsenoside R1 with sodium glycocholate-mediated liposomes: Preparation by supercritical fluid technology and evaluation in vitro and in vivo. Int J Pharm 552, 360-370.

Friedman, M., 2013. Anticarcinogenic, cardioprotective, and other health benefits of tomato compounds lycopene, alpha-tomatine, and tomatidine in pure form and in fresh and processed tomatoes. J Agric Food Chem 61, 9534-9550.

Friedman, M., 2015. Chemistry and anticarcinogenic mechanisms of glycoalkaloids produced by eggplants, potatoes, and tomatoes. J Agric Food Chem 63, 3323-3337.

Friedman, M., Levin, C.E., Lee, S.U., Kim, H.J., Lee, I.S., Byun, J.O., Kozukue, N., 2009. Tomatine-containing green tomato extracts inhibit growth of human breast, colon, liver, and stomach cancer cells. J Agric Food Chem 57, 5727-5733.

Fuchs, H., Bachran, D., Panjideh, H., Schellmann, N., Weng, A., Melzig, M. F., Sutherland, M., Bachran, C., 2009. Saponins as tool for improved targeted tumor therapies. Curr Drug Targets 10, 140–151.

Gao, G.Y., Ma, J., Lu, P., Jiang, X., Chang, C., 2018. Ophiopogonin B induces the autophagy and apoptosis of colon cancer cells by activating JNK/c-Jun signaling pathway. Biomed Pharmacother 108, 1208-1215.

Gao, J., Ying, Y., Wang, J., Cui, Y., 2020a. Solanine Inhibits Immune Escape Mediated by Hepatoma Treg Cells via the TGFbeta/Smad Signaling Pathway. Biomed Res Int 2020, 9749631.

Gao, Y., Khan, G.J., Wei, X., Zhai, K.F., Sun, L., Yuan, S., 2020b. DT-13 inhibits breast

cancer cell migration via non-muscle myosin II-A regulation in tumor microenvironment synchronized adaptations. Clin Transl Oncol 22, 1591-1602.

Gergely, J.E., Dorsey, A.E., Dimri, G.P., Dimri, M., 2018. Timosaponin A-III inhibits oncogenic phenotype via regulation of PcG protein BMI1 in breast cancer cells. Mol Carcinog 57, 831-841.

Groen, K., Pereboom-de Fauw, D.P., Besamusca, P., Beekhof, P.K., Speijers, G.J., Derks, H.J., 1993. Bioavailability and disposition of 3H-solanine in rat and hamster. Xenobiotica 23, 995-1005.

Gu, T., Yuan, W., Li, C., Chen, Z., Wen, Y., Zheng, Q., Yang, Q., Xiong, X., Yuan, A., 2021. alpha-Solanine Inhibits Proliferation, Invasion, and Migration, and Induces Apoptosis in Human Choriocarcinoma JEG-3 Cells In Vitro and In Vivo. Toxins (Basel) 13, 210.

Guo, W., Chen, Y., Gao, J., Zhong, K., Wei, H., Li, K., Tang, M., Zhao, X., Liu, X., Nie, C., Yuan, Z., 2019. Diosgenin exhibits tumor suppressive function via down-regulation of EZH2 in pancreatic cancer cells. Cell Cycle 18, 1745-1758.

Guo, X., Ding, X., 2018. Dioscin suppresses the viability of ovarian cancer cells by regulating the VEGFR2 and PI3K/AKT/MAPK signaling pathways. Oncol Lett 15, 9537-9542.

Hameed, A., Ijaz, S., Mohammad, I.S., Muhammad, K.S., Akhtar, N., Khan, H.M.S., 2017. Aglycone solanidine and solasodine derivatives: A natural approach towards cancer. Biomed Pharmacother 94, 446-457.

Hao, F., He, Y., Sun, Y., Zheng, B., Liu, Y., Wang, X., Zhang, Y., Lee, R.J., Teng, L.,

Xie, J., 2016. Improvement of oral availability of ginseng fruit saponins by a proliposome delivery system containing sodium deoxycholate. Saudi J Biol Sci 23, S113-125.

Hao, W.H., Wang, J.J., Hsueh, S.P., Hsu, P.J., Chang, L.C., Hsu, C.S., Hsu, K.Y., 2013. In vitro and in vivo studies of pharmacokinetics and antitumor efficacy of D07001-F4, an oral gemcitabine formulation. Cancer Chemother Pharmacol 71, 379-388.

Hassani-Nezhad-Gashti, F., Kummu, O., Karpale, M., Rysa, J., Hakkola, J., 2019. Nutritional status modifies pregnane X receptor regulated transcriptome. Sci Rep 9, 16728.

Hassn Mesrati, M., Syafruddin, S.E., Mohtar, M.A., Syahir, A., 2021. CD44: A Multifunctional Mediator of Cancer Progression. Biomolecules 11, 1850.

He, H., Xu, C., Zheng, L., Wang, K., Jin, M., Sun, Y., Yue, Z., 2020. Polyphyllin VII induces apoptotic cell death via inhibition of the PI3K/Akt and NF-kappaB pathways in A549 human lung cancer cells. Mol Med Rep 21, 597-606.

He, J., Wei, X., Li, S., Quan, X., Li, R., Du, H., Yuan, S., Sun, L., 2019a. DT-13 suppresses breast cancer metastasis by modulating PLOD2 in the adipocytes microenvironment. Phytomedicine 59, 152778.

He, J., Yu, S., Guo, C., Tan, L., Song, X., Wang, M., Wu, J., Long, Y., Gong, D., Zhang, R., Cao, Z., Li, Y., Peng, C., 2019b. Polyphyllin I induces autophagy and cell cycle arrest via inhibiting PDK1/Akt/mTOR signal and downregulating cyclin B1 in human gastric carcinoma HGC-27 cells. Biomed Pharmacother 117, 109189.

He, Z., Chen, H., Li, G., Zhu, H., Gao, Y., Zhang, L., Sun, J., 2014. Diosgenin inhibits

the migration of human breast cancer MDA-MB-231 cells by suppressing Vav2 activity. Phytomedicine 21, 871-876.

Hollern, D.P., Honeysett, J., Cardiff, R.D., Andrechek, E.R., 2014. The E2F transcription factors regulate tumor development and metastasis in a mouse model of metastatic breast cancer. Mol Cell Biol 34, 3229-3243.

Hsieh, M.H., Yang, J.S., Lin, R.C., Hsieh, Y.H., Yang, S.F., Chang, H.R., Lu, K.H., 2020. Tomatidine Represses Invasion and Migration of Human Osteosarcoma U2OS and HOS Cells by Suppression of Presenilin 1 and c-Raf-MEK-ERK Pathway. Molecules 25, 326.

Hsieh, M.J., Lin, C.W., Chen, M.K., Chien, S.Y., Lo, Y.S., Chuang, Y.C., Hsi, Y.T., Lin, C.C., Chen, J.C., Yang, S.F., 2017. Inhibition of cathepsin S confers sensitivity to methyl protodioscin in oral cancer cells via activation of p38 MAPK/JNK signaling pathways. Sci Rep 7, 45039.

Hsieh, Y.-H., Hsu, W.-H., Yang, S.-F., Liu, C.-J., Lu, K.-H., Wang, P.-H., Lin, R.-C., 2021a. Potential Antimetastatic Effect of Timosaponin AIII against Human Osteosarcoma Cells through Regulating the Integrin/FAK/Cofilin Axis. Pharmaceuticals 14, 260.

Hsieh, Y.H., Hsu, W.H., Yang, S.F., Liu, C.J., Lu, K.H., Wang, P.H., Lin, R.C., 2021b. Potential Antimetastatic Effect of Timosaponin AIII against Human Osteosarcoma Cells through Regulating the Integrin/FAK/Cofilin Axis. Pharmaceuticals (Basel) 14, 260.

Hu, K., Yao, X., 2003. The cytotoxicity of methyl protoneogracillin (NSC-698793) and

gracillin (NSC-698787), two steroidal saponins from the rhizomes of Dioscorea collettii var. hypoglauca, against human cancer cells in vitro. Phytother Res 17, 620-626.

Hu, M., Xu, L., Yin, L., Qi, Y., Li, H., Xu, Y., Han, X., Peng, J., Wan, X., 2013. Cytotoxicity of dioscin in human gastric carcinoma cells through death receptor and mitochondrial pathways. J Appl Toxicol 33, 712-722.

Hua, H., Zhu, Y., Song, Y.H., 2018. Ruscogenin suppressed the hepatocellular carcinoma metastasis via PI3K/Akt/mTOR signaling pathway. Biomed Pharmacother 101, 115-122.

Huang, H., Chen, S., Van Doren, J., Li, D., Farichon, C., He, Y., Zhang, Q., Zhang, K., Conney, A.H., Goodin, S., Du, Z., Zheng, X., 2015a. alpha-Tomatine inhibits growth and induces apoptosis in HL-60 human myeloid leukemia cells. Mol Med Rep 11, 4573-4578.

Huang, H.L., Chiang, W.L., Hsiao, P.C., Chien, M.H., Chen, H.Y., Weng, W.C., Hsieh, M.J., Yang, S.F., 2015b. Timosaponin AIII mediates caspase activation and induces apoptosis through JNK1/2 pathway in human promyelocytic leukemia cells. Tumour Biol 36, 3489-3497.

Huang, J., Liu, Y., Li, X., Song, Y., Li, W., Liu, K., Su, D., Feng, Y., Yang, S., 2015c. Comparative pharmacokinetic profiles of five poorly soluble pulchinenosides in different formulations from Pulsatilla chinensis saponins extracts for enhanced bioavailability. Biomed Chromatogr 29, 1885-1892.

Huang, W., Zou, K., 2011. Cytotoxicity of a plant steroidal saponin on human lung

cancer cells. Asian Pac J Cancer Prev 12, 513–517.

Huang, W., Zou, K., 2015. Cytotoxicity of the saponin TTB2 on Ewing sarcoma cells. Exp Ther Med 10, 625-628.

Huang, Y., Li, G., Hong, C., Zheng, X., Yu, H., Zhang, Y., 2021. Potential of Steroidal Alkaloids in Cancer: Perspective Insight Into Structure-Activity Relationships. Front Oncol 11, 733369.

Iga, D.P., Iga, S., Schmidt, R.R., Buzas, M.C., 2005. Chemical synthesis of cholesteryl beta-D-galactofuranoside and -pyranoside. Carbohydr Res 340, 2052-2054.

Iguchi, T., Kuroda, M., Naito, R., Watanabe, T., Matsuo, Y., Yokosuka, A., Mimaki, Y., 2019. Cholestane glycosides from Ornithogalum saundersiae bulbs and the induction of apoptosis in HL-60 cells by OSW-1 through a mitochondrial-independent signaling pathway. J Nat Med 73, 131-145.

Jasim, B., Thomas, R., Mathew, J., Radhakrishnan, E.K., 2017. Plant growth and diosgenin enhancement effect of silver nanoparticles in Fenugreek (Trigonella foenum-graecum L.). Saudi Pharm J 25, 443-447.

Jeon, S., Kim, M.M., 2019. Tomatidine inhibits cell invasion through the negative modulation of gelatinase and inactivation of p38 and ERK. Chem Biol Interact 313, 108826.

Ji, Y.B., Gao, S.Y., Ji, C.F., Zou, X., 2008. Induction of apoptosis in HepG2 cells by solanine and Bcl-2 protein. J Ethnopharmacol 115, 194-202.

Jiang, Q.W., Chen, M.W., Cheng, K.J., Yu, P.Z., Wei, X., Shi, Z., 2016. Therapeutic Potential of Steroidal Alkaloids in Cancer and Other Diseases. Med Res Rev 36,

119-143.

Jiang, Y., Zhuo, X., Wu, Y., Fu, X., Mao, C., 2021. PAR2 blockade reverses osimertinib resistance in non-small-cell lung cancer cells via attenuating ERK-mediated EMT and PD-L1 expression. Biochim Biophys Acta Mol Cell Res 1869, 119144.

Jin, D., Wang, B., Hu, R., Su, D., Chen, J., Zhou, H., Lu, W., Guo, Y., Fang, W., Gao, S., 2018. A Novel Colon-Specific Osmotic Pump Capsule of Panax notoginseng Saponins (PNS): Formulation, Optimization, and In Vitro-In Vivo Evaluation. AAPS PharmSciTech 19, 2322-2329.

Jonathan Ham, A.E., Jonathan Whitfield, Stephen J., 2000. c-Jun and the Transcriptional Control of Neuronal Apoptosis. Biochemical Pharmacology 60, 1015–1021.

Jong, J.E., Jeong, K.W., Shin, H., Hwang, L.R., Lee, D., Seo, T., 2012. Human papillomavirus type 16 E6 protein inhibits DNA fragmentation via interaction with DNA fragmentation factor 40. Cancer Lett 324, 109-117.

Jung, O., Lee, J., Lee, Y.J., Yun, J.M., Son, Y.J., Cho, J.Y., Ryou, C., Lee, S.Y., 2016. Timosaponin AIII inhibits migration and invasion of A549 human non-small-cell lung cancer cells via attenuations of MMP-2 and MMP-9 by inhibitions of ERK1/2, Src/FAK and beta-catenin signaling pathways. Bioorg Med Chem Lett 26, 3963-3967.

Jung, O., Lee, S.Y., 2019. Synergistic anticancer effects of timosaponin AIII and ginsenosides in MG63 human osteosarcoma cells. J Ginseng Res 43, 488-495.

Kang, Y.J., Chung, H.J., Nam, J.W., Park, H.J., Seo, E.K., Kim, Y.S., Lee, D., Lee, S.K.,

2011. Cytotoxic and antineoplastic activity of timosaponin A-III for human colon cancer cells. J Nat Prod 74, 701-706.

Karaboga Arslan, A.K., Yerer, M.B., 2018. alpha-Chaconine and alpha-Solanine Inhibit RL95-2 Endometrium Cancer Cell Proliferation by Reducing Expression of Akt (Ser473) and ERalpha (Ser167). Nutrients 10, 672.

Kim, C., Kim, B., 2018. Anti-Cancer Natural Products and Their Bioactive Compounds Inducing ER Stress-Mediated Apoptosis: A Review. Nutrients 10, 1021.

Kim, E.A., Jang, J.H., Lee, Y.H., Sung, E.G., Song, I.H., Kim, J.Y., Kim, S., Sohn, H.Y., Lee, T.J., 2014. Dioscin induces caspase-independent apoptosis through activation of apoptosis-inducing factor in breast cancer cells. Apoptosis 19, 1165-1175.

Kim, K.M., Im, A.R., Kim, S.H., Hyun, J.W., Chae, S., 2016a. Timosaponin AIII inhibits melanoma cell migration by suppressing COX-2 and in vivo tumor metastasis. Cancer Sci 107, 181-188.

Kim, S.P., Nam, S.H., Friedman, M., 2015. The Tomato Glycoalkaloid alpha-Tomatine Induces Caspase-Independent Cell Death in Mouse Colon Cancer CT-26 Cells and Transplanted Tumors in Mice. J Agric Food Chem 63, 1142-1150.

Kim, W.K., Pyee, Y., Chung, H.J., Park, H.J., Hong, J.Y., Son, K.H., Lee, S.K., 2016b. Antitumor Activity of Spicatoside A by Modulation of Autophagy and Apoptosis in Human Colorectal Cancer Cells. J Nat Prod 79, 1097-1104.

Kim, Y., Kim, K.H., Lee, I.S., Park, J.Y., Na, Y.C., Chung, W.S., Jang, H.J., 2019. Apoptosis and G2/M cell cycle arrest induced by a timosaponin A3 from Anemarrhena asphodeloides Bunge on AsPC-1 pancreatic cancer cells.

Phytomedicine 56, 48-56.

Kimura, M., Sasaki, K., Fukutani, Y., Yoshida, H., Ohsawa, I., Yohda, M., Sakurai, K., 2019. Anticancer saponin OSW-1 is a novel class of selective Golgi stress inducer. Bioorg Med Chem Lett 29, 1732-1736.

Lai, L., Shen, Q., Wang, Y., Chen, L., Lai, J., Wu, Z., Jiang, H., 2021. Polyphyllin I reverses the resistance of osimertinib in non-small cell lung cancer cell through regulation of PI3K/Akt signaling. Toxicol Appl Pharmacol 419, 115518.

Lee, J.H., Kim, C., Lee, S.G., Sethi, G., Ahn, K.S., 2018a. Ophiopogonin D, a Steroidal Glycoside Abrogates STAT3 Signaling Cascade and Exhibits Anti-Cancer Activity by Causing GSH/GSSG Imbalance in Lung Carcinoma. Cancers (Basel) 10, 427.

Lee, J.H., Kim, C., Lee, S.G., Yang, W.M., Um, J.Y., Sethi, G., Ahn, K.S., 2018b. Ophiopogonin D modulates multiple oncogenic signaling pathways, leading to suppression of proliferation and chemosensitization of human lung cancer cells. Phytomedicine 40, 165-175.

Lee, J.H., Lim, H.J., Lee, C.W., Son, K.H., Son, J.K., Lee, S.K., Kim, H.P., 2015. Methyl Protodioscin from the Roots of Asparagus cochinchinensis Attenuates Airway Inflammation by Inhibiting Cytokine Production. Evid Based Complement Alternat Med 2015, 640846.

Lee, S.T., Wong, P.F., Cheah, S.C., Mustafa, M.R., 2011. Alpha-tomatine induces apoptosis and inhibits nuclear factor-kappa B activation on human prostatic adenocarcinoma PC-3 cells. PLoS One 6, e18915.

Lee, S.T., Wong, P.F., Hooper, J.D., Mustafa, M.R., 2013. Alpha-tomatine synergises

with paclitaxel to enhance apoptosis of androgen-independent human prostate cancer PC-3 cells in vitro and in vivo. Phytomedicine 20, 1297-1305.

Lee, S.Y., 2020. Ginsenoside Rg1 Drives Stimulations of Timosaponin AIII-Induced Anticancer Effects in Human Osteosarcoma Cells. Evid Based Complement Alternat Med 2020, 8980124.

Lepage, C., Leger, D.Y., Bertrand, J., Martin, F., Beneytout, J.L., Liagre, B., 2011. Diosgenin induces death receptor-5 through activation of p38 pathway and promotes TRAIL-induced apoptosis in colon cancer cells. Cancer Lett 301, 193-202.

Lepage, C., Liagre, B., Cook-Moreau, J., Pinon, A., Beneytout, J.L., 2010. Cyclooxygenase-2 and 5-lipoxygenase pathways in diosgenin-induced apoptosis in HT-29 and HCT-116 colon cancer cells. Int J Oncol 36, 1183-1191.

Levy, D., de Melo, T.C., Oliveira, B.A., Paz, J.L., de Freitas, F.A., Reichert, C.O., Rodrigues, A., Bydlowski, S.P., 2019. 7-Ketocholesterol and cholestane-triol increase expression of SMO and LXRalpha signaling pathways in a human breast cancer cell line. Biochem Biophys Rep 19, 100604.

Li, C., Dai, L., Liu, K., Deng, L., Pei, T., Lei, J., 2015. A self-assembled nanoparticle platform based on poly(ethylene glycol)–diosgenin conjugates for co-delivery of anticancer drugs. RSC Advances 5, 74828-74834.

Li, H., Sun, L., de Carvalho, E.L., Li, X., Lv, X., Khan, G.J., Semukunzi, H., Yuan, S., Lin, S., 2016. DT-13, a saponin monomer of dwarf lilyturf tuber, induces autophagy and potentiates anti-cancer effect of nutrient deprivation. Eur J

Pharmacol 781, 164-172.

Li, H., Sun, L., Li, H., Lv, X., Semukunzi, H., Li, R., Yu, J., Yuan, S., Lin, S., 2017a. DT-13 synergistically enhanced vinorelbine-mediated mitotic arrest through inhibition of FOXM1-BICD2 axis in non-small-cell lung cancer cells. Cell Death Dis 8, e2810.

Li, H., Sun, L., Li, H., Lv, X., Semukunzi, H., Li, R., Yu, J., Yuan, S., Lin, S., 2017b. DT-13, a saponin monomer 13 of the Dwarf lilyturf tuber, synergized with vinorelbine to induce mitotic arrest via activation of ERK signaling pathway in NCI-H1299 cells. Biomed Pharmacother 89, 1277-1285.

Li, H., Zhang, G., Wang, W., Chen, C., Jiao, L., Wu, W., 2021a. Preparation, Characterization, and Bioavailability of Host-Guest Inclusion Complex of Ginsenoside Re with Gamma-Cyclodextrin. Molecules 26, 7227.

Li, J., Ma, W., Cheng, X., Zhang, X., Xie, Y., Ji, Z., Wu, S., 2020. Activation of FOXO3 pathway is involved in polyphyllin I-induced apoptosis and cell cycle arrest in human bladder cancer cells. Arch Biochem Biophys 687, 108363.

Li, S.X., Mu, Y., Zheng, F.Y., 2013. Influence of gastrointestinal digestion and edible plant combination on oral bioavailability of triterpene saponins, using a biomimetic digestion and absorption system and determination by HPLC. J Agric Food Chem 61, 10599-10603.

Li, X., Qu, Z., Jing, S., Li, X., Zhao, C., Man, S., Wang, Y., Gao, W., 2019a. Dioscin-6'-O-acetate inhibits lung cancer cell proliferation via inducing cell cycle arrest and caspase-dependent apoptosis. Phytomedicine 53, 124-133.

Li, X.L., Ma, R.H., Ni, Z.J., Thakur, K., Cespedes-Acuna, C.L., Wang, S., Zhang, J.G., Wei, Z.J., 2021b. Dioscin inhibits human endometrial carcinoma proliferation via G0/G1 cell cycle arrest and mitochondrial-dependent signaling pathway. Food Chem Toxicol 148, 111941.

Li, Y., Fan, L., Sun, Y., Miao, X., Zhang, F., Meng, J., Han, J., Zhang, D., Zhang, R., Yue, Z., Mei, Q., 2014a. Paris saponin VII from trillium tschonoskii reverses multidrug resistance of adriamycin-resistant MCF-7/ADR cells via P-glycoprotein inhibition and apoptosis augmentation. J Ethnopharmacol 154, 728-734.

Li, Y., Sun, Y., Fan, L., Zhang, F., Meng, J., Han, J., Guo, X., Zhang, D., Zhang, R., Yue, Z., Mei, Q., 2014b. Paris saponin VII inhibits growth of colorectal cancer cells through Ras signaling pathway. Biochem Pharmacol 88, 150-157.

Li, Y., Sun, Y., Tang, T., Niu, Y., Li, X., Xie, M., Jin, H., Mei, Q., 2019b. Paris saponin VII reverses chemoresistance in breast MCF-7/ADR cells. J Ethnopharmacol 232, 47-54.

Li, Y., Yang, D., Zhu, C., 2018. Impact of Sodium N-[8-(2-Hydroxybenzoyl)amino]-caprylate on Intestinal Permeability for Notoginsenoside R1 and Salvianolic Acids in Caco-2 Cells Transport and Rat Pharmacokinetics. Molecules 23, 2990.

Liao, M., Chen, X., Chen, J., Liu, M., Wang, J., Chen, Z., Xie, Z., Yao, M., 2016. Determination of pseudoprotodioscin in rat plasma by UPLC–MS/MS: Assay development and application to pharmacokinetic study. Journal of Chromatography B 1026, 97-104.

Liao, W.L., Lin, J.Y., Shieh, J.C., Yeh, H.F., Hsieh, Y.H., Cheng, Y.C., Lee, H.J., Shen,

C.Y., Cheng, C.W., 2019. Induction of G2/M Phase Arrest by Diosgenin via Activation of Chk1 Kinase and Cdc25C Regulatory Pathways to Promote Apoptosis in Human Breast Cancer Cells. Int J Mol Sci 21, 172.

Lim, S.M., Jeong, J.J., Kang, G.D., Kim, K.A., Choi, H.S., Kim, D.H., 2015. Timosaponin AIII and its metabolite sarsasapogenin ameliorate colitis in mice by inhibiting NF-kappaB and MAPK activation and restoring Th17/Treg cell balance. Int Immunopharmacol 25, 493-503.

Lin, C.L., Lee, C.H., Chen, C.M., Cheng, C.W., Chen, P.N., Ying, T.H., Hsieh, Y.H., 2018. Protodioscin Induces Apoptosis Through ROS-Mediated Endoplasmic Reticulum Stress via the JNK/p38 Activation Pathways in Human Cervical Cancer Cells. Cell Physiol Biochem 46, 322-334.

Lin, J. H., Yamazaki, M., 2003. Role of P-glycoprotein in pharmacokinetics: clinical implications. Clin Pharmacokinet 42, 59-98.

Lin, L.T., Choong, C.Y., Tai, C.J., 2020. Solanine Attenuated Hepatocarcinoma Migration and Invasion Induced by Acetylcholine. Integr Cancer Ther 19, 1534735420909895.

Lin, S.S., Fan, W., Sun, L., Li, F.F., Zhao, R.P., Zhang, L.Y., Yu, B.Y., Yuan, S.T., 2014. The saponin DT-13 inhibits gastric cancer cell migration through down-regulation of CCR5-CCL5 axis. Chin J Nat Med 12, 833-840.

Lin, X., Gajendran, B., Varier, K.M., Liu, W., Song, J., Rao, Q., Wang, C., Qiu, J., Ni, W., Qin, X., Wen, M., Liu, H., Li, Y., 2021. Paris Saponin VII Induces Apoptosis and Cell Cycle Arrest in Erythroleukemia Cells by a Mitochondrial Membrane

Signaling Pathway. Anticancer Agents Med Chem 21, 498-507.

Liu, J., Deng, X., Sun, X., Dong, J., Huang, J., 2020a. Inhibition of autophagy enhances timosaponin AIII-induced lung cancer cell apoptosis and anti-tumor effect in vitro and in vivo. Life Sci 257, 118040.

Liu, M. J., Wang, Z., Ju, Y., Zhou, J. B., Wang, Y., Wong, R. N., 2004. The mitotic-arresting and apoptosis-inducing effects of diosgenyl saponins on human leukemia cell lines. Biol Pharm Bull 27, 1059–1065.

Liu, Q., Lu, J. J., Hong, H. J., Yang, Q., Wang, Y., Chen, X. J., 2023. Ophiopogon japonicus and its active compounds: A review of potential anticancer effects and underlying mechanisms. Phytomedicine 113, 154718.

Liu, W., Huang, X.F., Qi, Q., Dai, Q.S., Yang, L., Nie, F.F., Lu, N., Gong, D.D., Kong, L.Y., Guo, Q.L., 2009. Asparanin A induces G(2)/M cell cycle arrest and apoptosis in human hepatocellular carcinoma HepG2 cells. Biochem Biophys Res Commun 381, 700-705.

Liu, W., Ning, R., Chen, R.N., Huang, X.F., Dai, Q.S., Hu, J.H., Wang, Y.W., Wu, L.L., Xiong, J., Hu, G., Guo, Q.L., Yang, J., Wang, H., 2016. Aspafilioside B induces G2/M cell cycle arrest and apoptosis by up-regulating H-Ras and N-Ras via ERK and p38 MAPK signaling pathways in human hepatoma HepG2 cells. Mol Carcinog 55, 440-457.

Liu, W., Wang, Y., Chen, J., Lin, Z., Lin, M., Lin, X., Fan, Y., 2021. Beneficial Effects of Gracillin From Rhizoma Paridis Against Gastric Carcinoma via the Potential TIPE2-Mediated Induction of Endogenous Apoptosis and Inhibition of Migration

in BGC823 Cells. Front Pharmacol 12, 669199.

Liu, X., Liang, J., Pan, L.L., Chen, J.Y., Liu, R.H., Zhu, G.H., Huang, H.L., Shu, J.C., Shao, F., Liang, Y.H., Yu, J.L., 2017. Six new furostanol glycosides from Smilax glauco-china and their cytotoxic activity. J Asian Nat Prod Res 19, 754-765.

Liu, Y., Dong, X., Wang, W., You, L., Yin, X., Yang, C., Sai, N., Leng, X., Ni, J., 2018. Molecular Mechanisms of Apoptosis in HepaRG Cell Line Induced by Polyphyllin VI via the Fas Death Pathway and Mitochondrial-Dependent Pathway. Toxins (Basel) 10, 201.

Liu, Y.X., Xu, B.W., Chen, Y.J., Fu, X.Q., Zhu, P.L., Bai, J.X., Chou, J.Y., Yin, C.L., Li, J.K., Wang, Y.P., Wu, J.Y., Wu, Y., Chan, K.K., Liang, C., Yu, Z.L., 2020b. Inhibiting the Src/STAT3 signaling pathway contributes to the anti-melanoma mechanisms of dioscin. Oncol Lett 19, 2508-2514.

Liu, Z., Cao, Y., Guo, X., Chen, Z., 2023. The Potential Role of Timosaponin-AIII in Cancer Prevention and Treatment. Molecules 28, 5500.

Liyanage, P.Y., Hettiarachchi, S.D., Zhou, Y., Ouhtit, A., Seven, E.S., Oztan, C.Y., Celik, E., Leblanc, R.M., 2019. Nanoparticle-mediated targeted drug delivery for breast cancer treatment. Biochim Biophys Acta Rev Cancer 1871, 419-433.

Lu, L., Ding, Y., Zhang, Y., Ho, R.J., Zhao, Y., Zhang, T., Guo, C., 2018. Antibody-modified liposomes for tumor-targeting delivery of timosaponin AIII. Int J Nanomedicine 13, 1927-1944.

Lu, M. K., Shih, Y. W., Chang Chien, T. T., Fang, L. H., Huang, H. C., Chen, P. S., 2010. α-Solanine inhibits human melanoma cell migration and invasion by reducing

matrix metalloproteinase-2/9 activities. Biol Pharm Bull 33, 1685–1691.

Lu, W., Pan, M., Zhang, P., Zheng, T., Huang, L., Ye, F., Lei, P., 2020. The Pharmacokinetics and Tissue Distributions of Nine Steroidal Saponins from Paris polyphylla in Rats. Eur J Drug Metab Pharmacokinet 45, 665-673.

Lush, R.M., McCune, J.S., Tetteh, L., Thompson, J.A., Mahany, J.J., Garland, L., Suttle, A.B., Sullivan, D.M., 2005. The absolute bioavailability of oral vinorelbine in patients with solid tumors. Cancer Chemother Pharmacol 56, 578-584.

Ma, L., Zhang, M., Zhao, R., Wang, D., Ma, Y., Li, A., 2021. Plant Natural Products: Promising Resources for Cancer Chemoprevention. Molecules 26, 933.

Ma, X., Yu, B., Hui, Y., Miao, Z., Ding, J., 2001. Synthesis of OSW-1 analogues and a dimer and their antitumor activities. Bioorg Med Chem Lett 11, 2153–2156.

Ma, Y.L., Zhang, Y.S., Zhang, F., Zhang, Y.Y., Thakur, K., Zhang, J.G., Wei, Z.J., 2019. Methyl protodioscin from Polygonatum sibiricum inhibits cervical cancer through cell cycle arrest and apoptosis induction. Food Chem Toxicol 132, 110655.

Maj, J., Morzycki, J.W., Rarova, L., Oklest'kova, J., Strnad, M., Wojtkielewicz, A., 2011. Synthesis and biological activity of 22-deoxo-23-oxa analogues of saponin OSW-1. J Med Chem 54, 3298-3305.

Malojirao, V.H., Vigneshwaran, V., Thirusangu, P., Mahmood, R., Prabhakar, B.T., 2018. The tumor antagonistic steroidal alkaloid Solanidine prompts the intrinsic suicidal signal mediated DFF-40 nuclear import and nucleosomal disruption. Life Sci 199, 139-150.

Man, S., Lv, P., Cui, J., Liu, F., Peng, L., Ma, L., Liu, C., Gao, W., 2020. Paris saponin

II-induced paraptosis-associated cell death increased the sensitivity of cisplatin. Toxicol Appl Pharmacol 406, 115206.

Mao, W., Yin, H., Chen, W., Zhao, T., Wu, S., Jin, H., Du, B., Tan, Y., Zhang, R., He, Y., 2020. Network Pharmacology and Experimental Evidence Reveal Dioscin Suppresses Proliferation, Invasion, and EMT via AKT/GSK3b/mTOR Signaling in Lung Adenocarcinoma. Drug Des Devel Ther 14, 2135-2147.

MarElia, C.B., Sharp, A.E., Shemwell, T.A., Clare Zhang, Y., Burkhardt, B.R., 2018. Anemarrhena asphodeloides Bunge and its constituent timosaponin-AIII induce cell cycle arrest and apoptosis in pancreatic cancer cells. FEBS Open Bio 8, 1155-1166.

Marty, M., Fumoleau, P., Adenis, A., Rousseau, Y., Merrouche, Y., Robinet, G., Senac, I., Puozzo, C., 2001. Oral vinorelbine pharmacokinetics and absolute bioavailability study in patients with solid tumors. Ann Oncol 12, 1643–1649.

Masullo, M., Pizza, C., Piacente, S., 2016. Ruscus Genus: A Rich Source of Bioactive Steroidal Saponins. Planta Med 82, 1513-1524.

Mbaveng, A.T., Chi, G.F., Nguenang, G.S., Abdelfatah, S., Tchangna Sop, R.V., Ngadjui, B.T., Kuete, V., Efferth, T., 2020. Cytotoxicity of a naturally occuring spirostanol saponin, progenin III, towards a broad range of cancer cell lines by induction of apoptosis, autophagy and necroptosis. Chem Biol Interact 326, 109141.

Meylan, E., Tschopp, J., 2005. The RIP kinases: crucial integrators of cellular stress. Trends Biochem Sci 30, 151-159.

Min, H.Y., Jang, H.J., Park, K.H., Hyun, S.Y., Park, S.J., Kim, J.H., Son, J., Kang, S.S., Lee, H.Y., 2019. The natural compound gracillin exerts potent antitumor activity by targeting mitochondrial complex II. Cell Death Dis 10, 810.

Min, H.Y., Pei, H., Hyun, S.Y., Boo, H.J., Jang, H.J., Cho, J., Kim, J.H., Son, J., Lee, H.Y., 2020. Potent Anticancer Effect of the Natural Steroidal Saponin Gracillin Is Produced by Inhibiting Glycolysis and Oxidative Phosphorylation-Mediated Bioenergetics. Cancers (Basel) 12, 913.

Miyata, S., Mizuno, T., Koyama, Y., Katayama, T., Tohyama, M., 2013. The endoplasmic reticulum-resident chaperone heat shock protein 47 protects the Golgi apparatus from the effects of O-glycosylation inhibition. PLoS One 8, e69732.

Mohammad, S., Ram, H., Gupta, P.N., Husain, N., Bhatt, M.L., 2011. Overexpression of COX-2 in oral squamous cell carcinoma patients undergoing chemoradiotherapy. Natl J Maxillofac Surg 2, 17-21.

Mohsenikia, M., Alizadeh, A.M., Khodayari, S., Khodayari, H., Kouhpayeh, S.A., Karimi, A., Zamani, M., Azizian, S., Mohagheghi, M.A., 2013. The protective and therapeutic effects of alpha-solanine on mice breast cancer. Eur J Pharmacol 718, 1-9.

Mundada, V.P., Patel, M.H., Mundada, P.K., Sawant, K.K., 2021. Development of Self-Microemulsifying Drug Delivery System to Improve Nisoldipine Bioavailability: Cell Line and In Vivo Evaluations : Development of Self-Microemulsifying Drug Delivery System. AAPS PharmSciTech 22, 256.

Mustafa, N.H., Sekar, M., Fuloria, S., Begum, M.Y., Gan, S.H., Rani, N., Ravi, S., Chidambaram, K., Subramaniyan, V., Sathasivam, K.V., Jeyabalan, S., Uthirapathy, S., Ponnusankar, S., Lum, P.T., Bhalla, V., Fuloria, N.K., 2022. Chemistry, Biosynthesis and Pharmacology of Sarsasapogenin: A Potential Natural Steroid Molecule for New Drug Design, Development and Therapy. Molecules 27, 2032.

Nazim, U. M., Jeong, J. K., Park, S. Y., 2017. Ophiopogonin B sensitizes TRAIL-induced apoptosis through activation of autophagy flux and downregulates cellular FLICE-like inhibitory protein. Oncotarget 9, 4161–4172.

Nguyen, H.M., Nguyen, H.T., Seephan, S., Do, H.B., Nguyen, H.T., Ho, D.V., Pongrakhananon, V., 2021. Antitumor activities of Aspiletrein A, a steroidal saponin from Aspidistra letreae, on non-small cell lung cancer cells. BMC Complement Med Ther 21, 87.

Nho, K.J., Chun, J.M., Kim, H.K., 2016. Induction of mitochondria-dependent apoptosis in HepG2 human hepatocellular carcinoma cells by timosaponin A-III. Environ Toxicol Pharmacol 45, 295-301.

Nie, C., Zhou, J., Qin, X., Shi, X., Zeng, Q., Liu, J., Yan, S., Zhang, L., 2016. Diosgenin-induced autophagy and apoptosis in a human prostate cancer cell line. Mol Med Rep 14, 4349-4359.

Niu, W., Xu, L., Li, J., Zhai, Y., Sun, Z., Shi, W., Jiang, Y., Ma, C., Lin, H., Guo, Y., Liu, Z., 2020. Polyphyllin II inhibits human bladder cancer migration and invasion by regulating EMT-associated factors and MMPs. Oncol Lett 20, 2928-2936.

Normandin, C., Boudreault, P.L., 2021. Concise Large-Scale Synthesis of Tomatidine, A Potent Antibiotic Natural Product. Molecules 26, 6008.

Okawara, M., Tokudome, Y., Todo, H., Sugibayashi, K., Hashimoto, F., 2014. Effect of β-cyclodextrin derivatives on the diosgenin absorption in Caco-2 cell monolayer and rats. Biol Pharm Bull 37, 54–59.

Pan, B., Zhong, W., Deng, Z., Lai, C., Chu, J., Jiao, G., Liu, J., Zhou, Q., 2016. Inhibition of prostate cancer growth by solanine requires the suppression of cell cycle proteins and the activation of ROS/P38 signaling pathway. Cancer Med 5, 3214-3222.

Pang, D., Li, C., Yang, C., Zou, Y., Feng, B., Li, L., Liu, W., Geng, Y., Luo, Q., Chen, Z., Huang, C., 2019. Polyphyllin VII Promotes Apoptosis and Autophagic Cell Death via ROS-Inhibited AKT Activity, and Sensitizes Glioma Cells to Temozolomide. Oxid Med Cell Longev 2019, 1805635.

Pang, D., Yang, C., Li, C., Zou, Y., Feng, B., Li, L., Liu, W., Luo, Q., Chen, Z., Huang, C., 2020. Polyphyllin II inhibits liver cancer cell proliferation, migration and invasion through downregulated cofilin activity and the AKT/NF-kappaB pathway. Biol Open 9, bio046854.

Passos, F.R.S., Araujo-Filho, H.G., Monteiro, B.S., Shanmugam, S., Araujo, A.A.S., Almeida, J., Thangaraj, P., Junior, L.J.Q., Quintans, J.S.S., 2022. Anti-inflammatory and modulatory effects of steroidal saponins and sapogenins on cytokines: A review of pre-clinical research. Phytomedicine 96, 153842.

Pei, L., Ye, Y., Zhao, W., Ye, Q., Ge, S., Jiang, Z.W., Liang, X.Q., Gan, H.X., Ma, L.,

2020. A validated UPLC-MS/MS method for quantitative determination of a potent neuroprotective agent Sarsasapogenin-AA13 in rat plasma: Application to pharmacokinetic studies. Biomed Chromatogr 34, e4775.

Pérez, A.J., Calle, J.M., Simonet, A.M., Guerra, J.O., Stochmal, A., Macías, F.A., 2013. Bioactive steroidal saponins from Agave offoyana flowers. Phytochemistry 95, 298-307.

Perez-Labrada, K., Brouard, I., Estevez, S., Marrero, M.T., Estevez, F., Rivera, D.G., 2012. Effect of C-ring modifications on the cytotoxicity of spirostan saponins and related glycosides. Bioorg Med Chem 20, 4522-4531.

Pétain, A., Zhong, D., Chen, X., Li, Z., Zhimin, S., Zefei, J., Zorza, G., Ferré, P., 2019. Effect of ethnicity on vinorelbine pharmacokinetics: a population pharmacokinetics analysis. Cancer Chemotherapy and Pharmacology 84, 373-382.

Puozzo, C., Gridelli, C., 2004. Non-small-cell lung cancer in elderly patients: influence of age on vinorelbine oral pharmacokinetics. Clin Lung Cancer 5, 237-242.

Qian, S., Tong, S., Wu, J., Tian, L., Qi, Z., Chen, B., Zhu, D., Zhang, Y., 2020. Paris saponin VII extracted from Trillium tschonoskii induces autophagy and apoptosis in NSCLC cells. J Ethnopharmacol 248, 112304.

Qiu, M., An, M., Bian, M., Yu, S., Liu, C., Liu, Q., 2019. Terrestrosin D from Tribulus terrestris attenuates bleomycin-induced inflammation and suppresses fibrotic changes in the lungs of mice. Pharm Biol 57, 694-700.

Rahmati-Yamchi, M., Ghareghomi, S., Haddadchi, G., Milani, M., Aghazadeh, M., Daroushnejad, H., 2014. Fenugreek extract diosgenin and pure diosgenin inhibit

the hTERT gene expression in A549 lung cancer cell line. Mol Biol Rep 41, 6247-6252.

Ramalingam, M., Kim, S.J., 2016. Pharmacological Activities and Applications of Spicatoside A. Biomol Ther (Seoul) 24, 469-474.

Rudolf, K., Rudolf, E., 2016. Antiproliferative effects of α-tomatine are associated with different cell death modalities in human colon cancer cells. Journal of Functional Foods 27, 491-502.

Shen, K.H., Liao, A.C., Hung, J.H., Lee, W.J., Hu, K.C., Lin, P.T., Liao, R.F., Chen, P.S., 2014. alpha-Solanine inhibits invasion of human prostate cancer cell by suppressing epithelial-mesenchymal transition and MMPs expression. Molecules 19, 11896-11914.

Shen, S., Li, G., Huang, J., Chen, C., Ren, B., Lu, G., Tan, Y., Zhang, J., Li, X., Wang, J., 2012. Steroidal saponins from Fritillaria pallidiflora Schrenk. Fitoterapia 83, 785-794.

Shen, S., Zhang, Y., Zhang, R., Gong, X., 2013. Sarsasapogenin induces apoptosis via the reactive oxygen species-mediated mitochondrial pathway and ER stress pathway in HeLa cells. Biochemical and Biophysical Research Communications 441, 519-524.

Sheng, H., Lv, W., Zhu, L., Wang, L., Wang, Z., Han, J., Hu, J., 2020. Liriopesides B induces apoptosis and cell cycle arrest in human non-small cell lung cancer cells. Int J Mol Med 46, 1039–1050.

Shi, B., Tang, P., Hu, X., Liu, J. O., Yu, B., 2005. OSW saponins: facile synthesis toward

a new type of structures with potent antitumor activities. J Org Chem 70, 10354–10367.

Shieh, J.M., Cheng, T.H., Shi, M.D., Wu, P.F., Chen, Y., Ko, S.C., Shih, Y.W., 2011. alpha-Tomatine suppresses invasion and migration of human non-small cell lung cancer NCI-H460 cells through inactivating FAK/PI3K/Akt signaling pathway and reducing binding activity of NF-kappaB. Cell Biochem Biophys 60, 297-310.

Shih, Y.W., Shieh, J.M., Wu, P.F., Lee, Y.C., Chen, Y.Z., Chiang, T.A., 2009. Alpha-tomatine inactivates PI3K/Akt and ERK signaling pathways in human lung adenocarcinoma A549 cells: effect on metastasis. Food Chem Toxicol 47, 1985-1995.

Shu, D., Qing, Y., Tong, Q., He, Y., Xing, Z., Zhao, Y., Li, Y., Wei, Y., Huang, W., Wu, X., 2011. Deltonin isolated from Dioscorea zingiberensis inhibits cancer cell growth through inducing mitochondrial apoptosis and suppressing Akt and mitogen activated protein kinase signals. Biol Pharm Bull 34, 1231–1239.

Si, L., Xu, L., Yin, L., Qi, Y., Han, X., Xu, Y., Zhao, Y., Liu, K., Peng, J., 2017. Potent effects of dioscin against pancreatic cancer via miR-149-3P-mediated inhibition of the Akt1 signalling pathway. Br J Pharmacol 174, 553-568.

Si, L., Zheng, L., Xu, L., Yin, L., Han, X., Qi, Y., Xu, Y., Wang, C., Peng, J., 2016. Dioscin suppresses human laryngeal cancer cells growth via induction of cell-cycle arrest and MAPK-mediated mitochondrial-derived apoptosis and inhibition of tumor invasion. Eur J Pharmacol 774, 105-117.

Sidana, J., Singh, B., Sharma, O.P., 2016. Saponins of Agave: Chemistry and bioactivity.

Phytochemistry 130, 22-46.

Sikka, S., Shanmugam, M.K., Siveen, K.S., Ong, T.H., Yang, M.H., Lee, J.H., Rajendran, P., Chinnathambi, A., Alharbi, S.A., Alahmadi, T.A., Vali, S., Kumar, A.P., Sethi, G., Wang, L., Hui, K.M., Ahn, K.S., 2021. Diosgenin attenuates tumor growth and metastasis in transgenic prostate cancer mouse model by negatively regulating both NF-kappaB/STAT3 signaling cascades. Eur J Pharmacol 906, 174274.

Silvente-Poirot, S., Poirot, M., 2012. Cholesterol epoxide hydrolase and cancer. Curr Opin Pharmacol 12, 696-703.

Song, X.Y., Han, F.Y., Chen, J.J., Wang, W., Zhang, Y., Yao, G.D., Song, S.J., 2019. Timosaponin AIII, a steroidal saponin, exhibits anti-tumor effect on taxol-resistant cells in vitro and in vivo. Steroids 146, 57-64.

Sparg, S.G., Light, M.E., van Staden, J., 2004. Biological activities and distribution of plant saponins. J Ethnopharmacol 94, 219-243.

Srinivasan, S., Koduru, S., Kumar, R., Venguswamy, G., Kyprianou, N., Damodaran, C., 2009. Diosgenin targets Akt-mediated prosurvival signaling in human breast cancer cells. Int J Cancer 125, 961-967.

Stefanowicz-Hajduk, J., Bartoszewski, R., Bartoszewska, S., Kochan, K., Adamska, A., Kosinski, I., Ochocka, J.R., 2015. Pennogenyl Saponins from Paris quadrifolia L. Induce Extrinsic and Intrinsic Pathway of Apoptosis in Human Cervical Cancer HeLa Cells. PLoS One 10, e0135993.

Subramaniam, Y., Subban, K., Chelliah, J., 2021. A novel synergistic anticancer effect

of fungal cholestanol glucoside and paclitaxel: Apoptosis induced by an intrinsic pathway through ROS generation in cervical cancer cell line (HeLa). Toxicol In Vitro 72, 105079.

Sun, B.T., Zheng, L.H., Bao, Y.L., Yu, C.L., Wu, Y., Meng, X.Y., Li, Y.X., 2011. Reversal effect of Dioscin on multidrug resistance in human hepatoma HepG2/adriamycin cells. Eur J Pharmacol 654, 129-134.

Sun, H., Lv, C., Yang, L., Wang, Y., Zhang, Q., Yu, S., Kong, H., Wang, M., Xie, J., Zhang, C., Zhou, M., 2014. Solanine induces mitochondria-mediated apoptosis in human pancreatic cancer cells. Biomed Res Int 2014, 805926.

Sy, L.K., Yan, S.C., Lok, C.N., Man, R.Y., Che, C.M., 2008. Timosaponin A-III induces autophagy preceding mitochondria-mediated apoptosis in HeLa cancer cells. Cancer Res 68, 10229-10237.

Tang, G.H., Lu, N., Li, W., Wu, M., Chen, Y.Y., Zhang, H.Y., He, S.Y., 2020. Mannosylxylarinolide, a new 3,4-seco-ergostane-type steroidal saponin featuring a beta-d-mannose from the endophytic fungus Xylaria sp. J Asian Nat Prod Res 22, 397-403.

Tang, Y., Li, N., Duan, J.A., Tao, W., 2013. Structure, bioactivity, and chemical synthesis of OSW-1 and other steroidal glycosides in the genus Ornithogalum. Chem Rev 113, 5480-5514.

Thapa, C.B., Paudel, M.R., Bhattarai, H.D., Pant, K.K., Devkota, H.P., Adhikari, Y.P., Pant, B., 2022. Bioactive secondary metabolites in Paris polyphylla Sm. and their biological activities: A review. Heliyon 8, e08982.

Thimmappa, R., Wang, S., Zheng, M., Misra, R.C., Huang, A.C., Saalbach, G., Chang, Y., Zhou, Z., Hinman, V., Bao, Z., Osbourn, A., 2022. Biosynthesis of saponin defensive compounds in sea cucumbers. Nat Chem Biol 18, 774-781.

Thompson, B.R., Shi, J., Zhu, H.J., Smith, D.E., 2020. Pharmacokinetics of gemcitabine and its amino acid ester prodrug following intravenous and oral administrations in mice. Biochem Pharmacol 180, 114127.

Tian, L.W., Zhang, Z., Long, H.L., Zhang, Y.J., 2017. Steroidal Saponins from the Genus Smilax and Their Biological Activities. Nat Prod Bioprospect 7, 283-298.

Tong, Q., Qing, Y., Wu, Y., Hu, X., Jiang, L., Wu, X., 2014. Dioscin inhibits colon tumor growth and tumor angiogenesis through regulating VEGFR2 and AKT/MAPK signaling pathways. Toxicol Appl Pharmacol 281, 166-173.

Tong, Q.Y., He, Y., Zhao, Q.B., Qing, Y., Huang, W., Wu, X.H., 2012. Cytotoxicity and apoptosis-inducing effect of steroidal saponins from Dioscorea zingiberensis Wright against cancer cells. Steroids 77, 1219-1227.

Tong, Q. Y., Qing, Y., Shu, D., He, Y., Zhao, Y. L., Li, Y., Wang, Z. L., Zhang, S. Y., Xing, Z. H., Xu, C., Wei, Y. Q., Huang, W., Wu, X. H., 2011. Deltonin, a steroidal saponin, inhibits colon cancer cell growth in vitro and tumor growth in vivo via induction of apoptosis and antiangiogenesis. Cell Physiol Biochem 27, 233–242.

Tran, T.D., Olsson, M.A., Choudhury, M.A., McMillan, D.J., Cullen, J.K., Parsons, P.G., Bernhardt, P.V., Reddell, P.W., Ogbourne, S.M., 2019. Antibacterial 5alpha-Spirostane Saponins from the Fruit of Cordyline manners-suttoniae. J Nat Prod 82, 2809-2817.

Tsai, C.H., Yang, C.W., Wang, J.Y., Tsai, Y.F., Tseng, L.M., King, K.L., Chen, W.S., Chiu, J.H., Shyr, Y.M., 2013. Timosaponin AIII Suppresses Hepatocyte Growth Factor-Induced Invasive Activity through Sustained ERK Activation in Breast Cancer MDA-MB-231 Cells. Evid Based Complement Alternat Med 2013, 421051.

Tschamber, T., Adam, S., Matsuya, Y., Masuda, S., Ohsawa, N., Maruyama, S., Kamoshita, K., Nemoto, H., Eustache, J., 2007. OSW-1 analogues: modification of the carbohydrate moiety. Bioorg Med Chem Lett 17, 5101-5106.

Upadhyay, S., Jeena, G.S., Shikha, Shukla, R.K., 2018. Recent advances in steroidal saponins biosynthesis and in vitro production. Planta 248, 519-544.

Wang, C., He, H., Liu, G., Ma, H., Li, L., Jiang, M., Lu, Q., Li, P., Qi, H., 2020. DT-13 induced apoptosis and promoted differentiation of acute myeloid leukemia cells by activating AMPK-KLF2 pathway. Pharmacol Res 158, 104864.

Wang, C., Huo, X., Wang, L., Meng, Q., Liu, Z., Liu, Q., Sun, H., Sun, P., Peng, J., Liu, K., 2016a. Dioscin strengthens the efficiency of adriamycin in MCF-7 and MCF-7/ADR cells through autophagy induction: More than just down-regulation of MDR1. Sci Rep 6, 28403.

Wang, D., Sha, L., Xu, C., Huang, Y., Tang, C., Xu, T., Li, X., Di, D., Liu, J., Yang, L., 2022. Natural saponin and cholesterol assembled nanostructures as the promising delivery method for saponin. Colloids Surf B Biointerfaces 214, 112448.

Wang, G., Huang, W., He, H., Fu, X., Wang, J., Zou, K., Chen, J., 2013a. Growth inhibition and apoptosis-inducing effect on human cancer cells by RCE-4, a

spirostanol saponin derivative from natural medicines. Int J Mol Med 31, 219-224.

Wang, H., Dong, R., Fan, W.W., Zheng, X.C., Li, A.M., Wang, W.D., 2019a. Timosaponin A-III induces autophagy of T-cell acute lymphoblastic leukemia Jurkat cells via inhibition of the PI3K/Akt/mTOR pathway. Oncol Rep 41, 2937-2944.

Wang, H., Dong, R., Fan, W.W., Zheng, X.C., Li, A.M., Wang, W.D., 2019b. Timosaponin AIII induces autophagy of Tcell acute lymphoblastic leukemia Jurkat cells via inhibition of the PI3K/Akt/mTOR pathway. Oncol Rep 41, 2937-2944.

Wang, H., Yu, H., Sun, Y., Zhao, H., Guo, Z., Yu, B., 2017a. Liriopesides B inhibited cell growth and decreased CA125 level in human ovarian cancer A2780 cells. Nat Prod Res 31, 2198-2202.

Wang, L., Meng, Q., Wang, C., Liu, Q., Peng, J., Huo, X., Sun, H., Ma, X., Liu, K., 2013b. Dioscin restores the activity of the anticancer agent adriamycin in multidrug-resistant human leukemia K562/adriamycin cells by down-regulating MDR1 via a mechanism involving NF-kappaB signaling inhibition. J Nat Prod 76, 909-914.

Wang, L., Sun, Q.Q., Zhang, S.J., Du, Y.W., Wang, Y.Y., Zang, W.Q., Chen, X.N., Zhao, G.Q., 2016b. Inhibitory effect of alpha-solanine on esophageal carcinoma in vitro. Exp Ther Med 12, 1525-1530.

Wang, N., Feng, Y., Zhu, M., Siu, F.M., Ng, K.M., Che, C.M., 2013c. A novel mechanism of XIAP degradation induced by timosaponin AIII in hepatocellular carcinoma. Biochim Biophys Acta 1833, 2890-2899.

Wang, P., Wang, C., Liu, C., 2021. Antitumor effects of dioscin in A431 cells via adjusting ATM/p53-mediated cell apoptosis, DNA damage and migration. Oncol Lett 21, 59.

Wang, P., Yang, Q., Du, X., Chen, Y., Zhang, T., 2019c. Targeted regulation of Rell2 by microRNA-18a is implicated in the anti-metastatic effect of polyphyllin VI in breast cancer cells. Eur J Pharmacol 851, 161-173.

Wang, W., Liu, Y., Sun, M., Sai, N., You, L., Dong, X., Yin, X., Ni, J., 2019d. Hepatocellular Toxicity of Paris Saponins I, II, VI and VII on Two Kinds of Hepatocytes-HL-7702 and HepaRG Cells, and the Underlying Mechanisms. Cells 8, 690.

Wang, X., Zhu, C., Wang, X., Hagberg, H., Korhonen, L., Sandberg, M., Lindholm, D., Blomgren, K., 2004. X-linked inhibitor of apoptosis (XIAP) protein protects against caspase activation and tissue loss after neonatal hypoxia-ischemia. Neurobiol Dis 16, 179-189.

Wang, Y., Shen, J., Yang, X., Jin, Y., Yang, Z., Wang, R., Zhang, F., Linhardt, R.J., 2019e. Mechanism of enhanced oral absorption of akebia saponin D by a self-nanoemulsifying drug delivery system loaded with phospholipid complex. Drug Dev Ind Pharm 45, 124-129.

Wang, Y., Tang, Q., Jiang, S., Li, M., Wang, X., 2013d. Anti-colorectal cancer activity of macrostemonoside A mediated by reactive oxygen species. Biochem Biophys Res Commun 441, 825-830.

Wang, Y., Xu, L., Lou, L.L., Song, S.J., Yao, G.D., Ge, M.Y., Hayashi, T., Tashiro, S.I.,

Onodera, S., Ikejima, T., 2017b. Timosaponin AIII induces apoptosis and autophagy in human melanoma A375-S2 cells. Arch Pharm Res 40, 69-78.

Wang, Y.C., Wu, D.W., Wu, T.C., Wang, L., Chen, C.Y., Lee, H., 2018a. Dioscin overcome TKI resistance in EGFR-mutated lung adenocarcinoma cells via down-regulation of tyrosine phosphatase SHP2 expression. Int J Biol Sci 14, 47-56.

Wang, Z., Wang, Y., Zhu, S., Liu, Y., Peng, X., Zhang, S., Zhang, Z., Qiu, Y., Jin, M., Wang, R., Zhong, Y., Kong, D., 2018b. DT-13 Inhibits Proliferation and Metastasis of Human Prostate Cancer Cells Through Blocking PI3K/Akt Pathway. Front Pharmacol 9, 1450.

Wei, S., Fukuhara, H., Chen, G., Kawada, C., Kurabayashi, A., Furihata, M., Inoue, K., Shuin, T., 2014. Terrestrosin D, a steroidal saponin from Tribulus terrestris L., inhibits growth and angiogenesis of human prostate cancer in vitro and in vivo. Pathobiology 81, 123-132.

Wei, X., Mao, T., Li, S., He, J., Hou, X., Li, H., Zhan, M., Yang, X., Li, R., Xiao, J., Yuan, S., Sun, L., 2019. DT-13 inhibited the proliferation of colorectal cancer via glycolytic metabolism and AMPK/mTOR signaling pathway. Phytomedicine 54, 120-131.

Wei, X.H., Lin, S.S., Liu, Y., Zhao, R.P., Khan, G.J., Du, H.Z., Mao, T.T., Yu, B.Y., Li, R.M., Yuan, S.T., Sun, L., 2016. DT-13 attenuates human lung cancer metastasis via regulating NMIIA activity under hypoxia condition. Oncol Rep 36, 991-999.

Wen, Z., Huang, C., Xu, Y., Xiao, Y., Tang, L., Dai, J., Sun, H., Chen, B., Zhou, M., 2016. alpha-Solanine inhibits vascular endothelial growth factor expression by

down-regulating the ERK1/2-HIF-1alpha and STAT3 signaling pathways. Eur J Pharmacol 771, 93-98.

Woodahl, E. L., Crouthamel, M. H., Bui, T., Shen, D. D., Ho, R. J., 2009. MDR1 (ABCB1) G1199A (Ser400Asn) polymorphism alters transepithelial permeability and sensitivity to anticancer agents. Cancer Chemother Pharmacol 64, 183-188.

Wu, H., Li, W., Wang, T., Rong, Y., He, Z., Huang, S., Zhang, L., Wu, Z., Liu, C., 2021. alpha-Tomatine, a novel early-stage autophagy inhibitor, inhibits autophagy to enhance apoptosis via Beclin-1 in Skov3 cells. Fitoterapia 152, 104911.

Wu, J., Wang, L., Du, X., Sun, Q., Wang, Y., Li, M., Zang, W., Liu, K., Zhao, G., 2018. alpha-solanine enhances the chemosensitivity of esophageal cancer cells by inducing microRNA-138 expression. Oncol Rep 39, 1163-1172.

Wu, Y., Si, Y., Xiang, Y., Zhou, T., Liu, X., Wu, M., Li, W., Zhang, T., Xiang, K., Zhang, L., Zhao, H., Liu, Y., 2020a. Polyphyllin I activates AMPK to suppress the growth of non-small-cell lung cancer via induction of autophagy. Arch Biochem Biophys 687, 108285.

Wu, Z., Han, X., Tan, G., Zhu, Q., Chen, H., Xia, Y., Gong, J., Wang, Z., Wang, Y., Yan, J., 2020b. Dioscin Inhibited Glycolysis and Induced Cell Apoptosis in Colorectal Cancer via Promoting c-myc Ubiquitination and Subsequent Hexokinase-2 Suppression. Onco Targets Ther 13, 31-44.

Xiang, L., Wang, Y., Yi, X., He, X., 2019. Steroidal alkaloid glycosides and phenolics from the immature fruits of Solanum nigrum. Fitoterapia 137, 104268.

Xiang, W., Zhang, R.J., Jin, G.L., Tian, L., Cheng, F., Wang, J.Z., Xing, X.F., Xi, W.,

Tang, S.J., Chen, J.F., 2020. RCE-4, a potential anti-cervical cancer drug isolated from Reineckia carnea, induces autophagy via the dual blockade of PI3K and ERK pathways in cervical cancer CaSki cells. Int J Mol Med 45, 245-254.

Xiao, G., Yu, B., 2013. Total synthesis of starfish saponin goniopectenoside B. Chemistry 19, 7708-7712.

Xiao, X., Yang, M., Xiao, J., Zou, J., Huang, Q., Yang, K., Zhang, B., Yang, F., Liu, S., Wang, H., Bai, P., 2014. Paris Saponin II suppresses the growth of human ovarian cancer xenografts via modulating VEGF-mediated angiogenesis and tumor cell migration. Cancer Chemother Pharmacol 73, 807-818.

Xie, Y.L., Fan, M., Jiang, R.M., Wang, Z.L., Li, Y., 2015. Deltonin induced both apoptosis and autophagy in head and neck squamous carcinoma FaDu cell. Neoplasma 62, 419-431.

Xu, C., Xia, B., Zhang, Z., Lin, Y., Li, C., Lin, L., 2023. Research progress in steroidal saponins from the genus Polygonatum: Chemical components, biosynthetic pathways and pharmacological effects. Phytochemistry 213, 113731.

Xu, J., Wang, Y., Wang, Y., Wang, Z., He, X., 2021a. A-24, a steroidal saponin from Allium chinense, induced apoptosis, autophagy and migration inhibition in p53 wild-type and p53-deficient gastric cancer cells. Chem Biol Interact 348, 109648.

Xu, J., Wang, Y., Wang, Z., Wang, Y., He, X., 2021b. T-17, a spirostanol saponin, inhibits p53-independent proliferation and p53-dependent migration of gastric cancer cells. Steroids 170, 108828.

Xu, J., Wang, Z., Huang, Y., Wang, Y., Xiang, L., He, X., 2020a. A spirostanol saponin

isolated from Tupistra chinensis Baker simultaneously induces apoptosis and autophagy by regulating the JNK pathway in human gastric cancer cells. Steroids 164, 108737.

Xu, J., Zhang, M., Lin, X., Wang, Y., He, X., 2020b. A steroidal saponin isolated from Allium chinense simultaneously induces apoptosis and autophagy by modulating the PI3K/Akt/mTOR signaling pathway in human gastric adenocarcinoma. Steroids 161, 108672.

Xu, L., Wang, D., Chen, J., Li, B., Li, Q., Liu, P., Qin, Y., Dai, Z., Fan, F., Zhang, X., 2022. Metabolic engineering of Saccharomyces cerevisiae for gram-scale diosgenin production. Metab Eng 70, 115-128.

Yan, K.H., Lee, L.M., Yan, S.H., Huang, H.C., Li, C.C., Lin, H.T., Chen, P.S., 2013. Tomatidine inhibits invasion of human lung adenocarcinoma cell A549 by reducing matrix metalloproteinases expression. Chem Biol Interact 203, 580-587.

Yan, T., Hu, G., Wang, A., Sun, X., Yu, X., Jia, J., 2018a. Paris saponin VII induces cell cycle arrest and apoptosis by regulating Akt/MAPK pathway and inhibition of P-glycoprotein in K562/ADR cells. Phytotherapy Research 32, 898-907.

Yan, T., Hu, G., Wang, A., Sun, X., Yu, X., Jia, J., 2018b. Paris saponin VII induces cell cycle arrest and apoptosis by regulating Akt/MAPK pathway and inhibition of P-glycoprotein in K562/ADR cells. Phytother Res 32, 898-907.

Yan, X., Li, M., Chen, L., Peng, X., Que, Z.J., An, H.M., Shen, K.P., Hu, B., 2020. alpha-Solanine inhibits growth and metastatic potential of human colorectal cancer cells. Oncol Rep 43, 1387-1396.

Yan, Z., Liu, G., Liang, M., Xu, Y., 2018c. Ophiopogonin D inhibits cell proliferation and induces apoptosis of human laryngocarcinoma through downregulation of cyclin B1 and MMP-9 and upregulation of p38-MAPK signaling. Oncology Letters 17, 1877–1882.

Yang, F., Zhou, J., Hu, X., Yu, S.K., Liu, C., Pan, R., Chang, Q., Liu, X., Liao, Y., 2017. Preparation and evaluation of self-microemulsions for improved bioavailability of ginsenoside-Rh1 and Rh2. Drug Deliv Transl Res 7, 731-737.

Yang, J., Cao, L., Li, Y., Liu, H., Zhang, M., Ma, H., Wang, B., Yuan, X., Liu, Q., 2021a. Gracillin Isolated from Reineckia carnea Induces Apoptosis of A549 Cells via the Mitochondrial Pathway. Drug Des Devel Ther 15, 233-243.

Yang, L., Ren, S., Xu, F., Ma, Z., Liu, X., Wang, L., 2019. Recent Advances in the Pharmacological Activities of Dioscin. Biomed Res Int 2019, 5763602.

Yang, L., Zhu, T., Ye, H., Shen, Y., Li, Z., Chen, L., Wang, C., Chen, X., Zhao, H., Xiang, Y., Xiao, Z., Zhao, C., Li, J., Hu, W., 2021b. Gracillin shows potent efficacy against colorectal cancer through inhibiting the STAT3 pathway. J Cell Mol Med 25, 801-812.

Yang, M., Zou, J., Zhu, H., Liu, S., Wang, H., Bai, P., Xiao, X., 2015. Paris saponin II inhibits human ovarian cancer cell-induced angiogenesis by modulating NF-kappaB signaling. Oncol Rep 33, 2190-2198.

Yang, Q., Li, H., Gui, M., Li, Z., Sun, H., 2020. Development and validation of a rapid and sensitive LC-MS/MS method for the determination of polyphyllin II in rat plasma and its application in a pharmacokinetic study. Biomed Chromatogr 34,

e4780.

Yang, S.A., Paek, S.H., Kozukue, N., Lee, K.R., Kim, J.A., 2006. Alpha-chaconine, a potato glycoalkaloid, induces apoptosis of HT-29 human colon cancer cells through caspase-3 activation and inhibition of ERK 1/2 phosphorylation. Food Chem Toxicol 44, 839-846.

Yao, M., Li, R., Yang, Z., Ding, Y., Zhang, W., Li, W., Liu, M., Zhao, C., Wang, Y., Tang, H., Wang, J., Wen, A., 2020. PP9, a steroidal saponin, induces G2/M arrest and apoptosis in human colorectal cancer cells by inhibiting the PI3K/Akt/GSK3β pathway. Chem Biol Interact 331, 109246.

Yao, Y., Cui, L., Ye, J., Yang, G., Lu, G., Fang, X., Zeng, Z., Zhou, J., 2020. Dioscin facilitates ROS-induced apoptosis via the p38-MAPK/HSP27-mediated pathways in lung squamous cell carcinoma. Int J Biol Sci 16, 2883-2894.

Yi, X., Xiang, L., Huang, Y., Wang, Y., He, X., 2018. Apoptosis and pro-death autophagy induced by a spirostanol saponin isolated from Rohdea chinensis (Baker) N. Tanaka (synonym Tupistra chinensis Baker) on HL-60 cells. Phytomedicine 42, 83-89.

You, F.F., Zhang, J., Cheng, F., Zou, K., Zhang, X.Q., Chen, J.F., 2021. ATG 4B Serves a Crucial Role in RCE-4-Induced Inhibition of the Bcl-2-Beclin 1 Complex in Cervical Cancer Ca Ski Cells. Int J Mol Sci 22, 12302.

Yu, H., Wang, H., Yin, Y., Wang, Z., 2020. Liriopesides B from Liriope spicata var. prolifera inhibits metastasis and induces apoptosis in A2780 human ovarian cancer cells. Mol Med Rep 22, 1747-1758.

Yuan, Y.L., Jiang, N., Li, Z.Y., Song, Z.Z., Yang, Z.H., Xue, W.H., Zhang, X.J., Du, Y., 2019. Polyphyllin VI induces apoptosis and autophagy in human osteosarcoma cells by modulation of ROS/JNK activation. Drug Des Devel Ther 13, 3091-3103.

Zaimy, M.A., Saffarzadeh, N., Mohammadi, A., Pourghadamyari, H., Izadi, P., Sarli, A., Moghaddam, L.K., Paschepari, S.R., Azizi, H., Torkamandi, S., Tavakkoly-Bazzaz, J., 2017. New methods in the diagnosis of cancer and gene therapy of cancer based on nanoparticles. Cancer Gene Ther 24, 233-243.

Zang, Q.Q., Zhang, L., Gao, N., Huang, C., 2016. Ophiopogonin D inhibits cell proliferation, causes cell cycle arrest at G2/M, and induces apoptosis in human breast carcinoma MCF-7 cells. J Integr Med 14, 51-59.

Zeng, K.W., Li, N., Dong, X., Ma, Z.Z., Jiang, Y., Jin, H.W., Tu, P.F., 2013. Sprengerinin C exerts anti-tumorigenic effects in hepatocellular carcinoma via inhibition of proliferation and angiogenesis and induction of apoptosis. Eur J Pharmacol 714, 261-273.

Zhan, G., Hu, J., Xiao, B., Wang, X., Yang, Z., Yang, G., Lu, L., 2020. Trillin prevents proliferation and induces apoptosis through inhibiting STAT3 nuclear translocation in hepatoma carcinoma cells. Med Oncol 37, 44.

Zhang, C., Feng, S., Zhang, L., Ren, Z., 2013a. A new cytotoxic steroidal saponin from the rhizomes and roots of Smilax scobinicaulis. Nat Prod Res 27, 1255-1260.

Zhang, C., Jia, X., Wang, K., Bao, J., Li, P., Chen, M., Wan, J.B., Su, H., Mei, Z., He, C., 2016a. Polyphyllin VII Induces an Autophagic Cell Death by Activation of the JNK Pathway and Inhibition of PI3K/AKT/mTOR Pathway in HepG2 Cells. PLoS

One 11, e0147405.

Zhang, C., Li, Q., Qin, G., Zhang, Y., Li, C., Han, L., Wang, R., Wang, S., Chen, H., Liu, K., He, C., 2021a. Anti-angiogenesis and anti-metastasis effects of Polyphyllin VII on Hepatocellular carcinoma cells in vitro and in vivo. Chin Med 16, 41.

Zhang, F., Ni, Z.J., Ye, L., Zhang, Y.Y., Thakur, K., Cespedes-Acuna, C.L., Han, J., Zhang, J.G., Wei, Z.J., 2021b. Asparanin A inhibits cell migration and invasion in human endometrial cancer via Ras/ERK/MAPK pathway. Food Chem Toxicol 150, 112036.

Zhang, F., Zhang, Y.Y., Ma, R.H., Thakur, K., Han, J., Hu, F., Zhang, J.G., Wei, Z.J., 2021c. Multi-omics reveals the anticancer mechanism of asparagus saponin-asparanin A on endometrial cancer Ishikawa cells. Food Funct 12, 614-632.

Zhang, F., Zhang, Y.Y., Sun, Y.S., Ma, R.H., Thakur, K., Zhang, J.G., Wei, Z.J., 2020a. Asparanin A from Asparagus officinalis L. Induces G0/G1 Cell Cycle Arrest and Apoptosis in Human Endometrial Carcinoma Ishikawa Cells via Mitochondrial and PI3K/AKT Signaling Pathways. J Agric Food Chem 68, 213-224.

Zhang, H. J., Sydara, K., Tan, G. T., Ma, C., Southavong, B., Soejarto, D. D., Pezzuto, J. M., Fong, H. H., 2004. Bioactive constituents from Asparagus cochinchinensis. J Nat Prod 67, 194–200.

Zhang, L., Li, C., Zhang, Y., Zhang, J., Yang, X., 2022. Ophiopogonin B induces gastric cancer cell death by blocking the GPX4/xCT-dependent ferroptosis pathway. Oncol Lett 23, 104.

Zhang, M., Qu, J., Gao, Z., Qi, Q., Yin, H., Zhu, L., Wu, Y., Liu, W., Yang, J., Huang, X., 2020b. Timosaponin AIII Induces G2/M Arrest and Apoptosis in Breast Cancer by Activating the ATM/Chk2 and p38 MAPK Signaling Pathways. Front Pharmacol 11, 601468.

Zhang, M., Teng, X.D., Guo, X.X., Li, Z.G., Han, J.G., Yao, L., 2013b. Expression of tissue levels of matrix metalloproteinases and their inhibitors in breast cancer. Breast 22, 330-334.

Zhang, Q.W., Lin, L.G., Ye, W.C., 2018a. Techniques for extraction and isolation of natural products: a comprehensive review. Chin Med 13, 20.

Zhang, R.S., Liu, Y.Y., Zhu, P.F., Jin, Q., Dai, Z., Luo, X.D., 2021d. Furostanol Saponins from Asparagus cochinchinensis and Their Cytotoxicity. Nat Prod Bioprospect 11, 651-658.

Zhang, S., He, Y., Tong, Q., Chen, Q., Wu, X., Huang, W., 2013c. Deltonin induces apoptosis in MDA-MB-231 human breast cancer cells via reactive oxygen species-mediated mitochondrial dysfunction and ERK/AKT signaling pathways. Mol Med Rep 7, 1038-1044.

Zhang, S., Pang, H., Sun, M., Li, H., 2017a. Timosaponin AIII inhibits the growth of human leukaemia cells HL-60 by down-regulation of PI3K/AKT and Wnt/β-catenin pathways. Biotechnology & Biotechnological Equipment 32, 150-155.

Zhang, W., Zhang, Q., Jiang, Y., Li, F., Xin, H., 2016b. Effects of ophiopogonin B on the proliferation and apoptosis of SGC-7901 human gastric cancer cells. Mol Med Rep 13, 4981-4986.

Zhang, Y., Fang, F., Fan, K., Zhang, Y., Zhang, J., Guo, H., Yu, P., Ma, J., 2017b. Effective cytotoxic activity of OSW-1 on colon cancer by inducing apoptosis in vitro and in vivo. Oncol Rep 37, 3509-3519.

Zhang, Y., Han, Y., Zhai, K., Sun, M., Liu, J., Yu, B., Kou, J., 2015. Ophiopogonin-D suppresses MDA-MB-435 cell adhesion and invasion by inhibiting matrix metalloproteinase-9. Mol Med Rep 12, 1493-1498.

Zhang, Y., Huang, P., Liu, X., Xiang, Y., Zhang, T., Wu, Y., Xu, J., Sun, Z., Zhen, W., Zhang, L., Si, Y., Liu, Y., 2018b. Polyphyllin I inhibits growth and invasion of cisplatin-resistant gastric cancer cells by partially inhibiting CIP2A/PP2A/Akt signaling axis. J Pharmacol Sci 137, 305-312.

Zhang, Y.S., Ma, Y.L., Thakur, K., Hussain, S.S., Wang, J., Zhang, Q., Zhang, J.G., Wei, Z.J., 2018c. Molecular mechanism and inhibitory targets of dioscin in HepG2 cells. Food Chem Toxicol 120, 143-154.

Zhao, C., Li, Y., Qin, Y., Wang, R., Li, G., Sun, C., Qu, X., Li, W., 2013. Pharmacokinetics and metabolism of SL-01, a prodrug of gemcitabine, in rats. Cancer Chemother Pharmacol 71, 1541-1550.

Zhao, L., Wang, L., Chang, L., Hou, Y., Wei, C., Wu, Y., 2020. Ginsenoside CK-loaded self-nanomicellizing solid dispersion with enhanced solubility and oral bioavailability. Pharm Dev Technol 25, 1127-1138.

Zhao, X., Tao, X., Xu, L., Yin, L., Qi, Y., Xu, Y., Han, X., Peng, J., 2016. Dioscin Induces Apoptosis in Human Cervical Carcinoma HeLa and SiHa Cells through ROS-Mediated DNA Damage and the Mitochondrial Signaling Pathway.

Molecules 21, 730.

Zheng, D., Guan, Y., Chen, X., Xu, Y., Chen, X., Lei, P., 2011. Synthesis of cholestane saponins as mimics of OSW-1 and their cytotoxic activities. Bioorg Med Chem Lett 21, 3257-3260.

Zheng, D., Zhou, L., Guan, Y., Chen, X., Zhou, W., Chen, X., Lei, P., 2010. Synthesis of cholestane glycosides bearing OSW-1 disaccharide or its 1-->4-linked analogue and their antitumor activities. Bioorg Med Chem Lett 20, 5439-5442.

Zhou, Q., Song, W., Xiao, W., 2017. Dioscin induces demethylation of DAPK-1 and RASSF-1alpha genes via the antioxidant capacity, resulting in apoptosis of bladder cancer T24 cells. EXCLI J 16, 101-112.

Zhu, H., Zhu, S.C., Shakya, S., Mao, Q., Ding, C.H., Long, M.H., Li, S.L., 2015. Study on the pharmacokinetics profiles of polyphyllin I and its bioavailability enhancement through co-administration with P-glycoprotein inhibitors by LC-MS/MS method. J Pharm Biomed Anal 107, 119-124.

Zhu, J., Xiong, L., Yu, B., Wu, J., 2005. Apoptosis Induced by a New Member of Saponin Family Is Mediated through Caspase-8-Dependent Cleavage of Bcl-2. Molecular Pharmacology 68, 1831-1838.

Zhu, X., Wang, K., Chen, Y., 2020. Ophiopogonin D suppresses TGF-beta1-mediated metastatic behavior of MDA-MB-231 breast carcinoma cells via regulating ITGB1/FAK/Src/AKT/beta-catenin/MMP-9 signaling axis. Toxicol In Vitro 69, 104973.

Zou, X., Huang, W., 2018. TTB2 induces apoptosis in Ewing sarcoma cells. Exp Ther

Med 16, 1021-1025.

Zuo, S.-Q., Liu, Y.-N., Yang, Y., Guo, Z.-Q., Liu, C.-X., Guo, Z.-Y., He, H.-B., Tu, X., Zou, K., 2018. Aspidsaponins A–D, Four new steroidal saponins from the rhizomes of Aspidistra elatior Blume and their cytotoxicity. Phytochemistry Letters 25, 126-131.

Figure legends

Figure 1. Structural diagram of steroidal saponins.

Figure 2. Summary of IC_{50} of steroidal saponins for tumor suppression (Duncan analysis method, the presence of different letters between each two groups indicates significant differences, while the presence of a common letter between each two groups indicates no significant differences, $p<0.05$).

a. IC_{50} of five types of steroidal saponins on tumor cells. **b.** IC_{50} of steroidal saponins against carcinoma, sarcoma as well as leukemia. **c.** IC_{50} of steroidal saponins against cell lines from 14 cancers.

Figure 3. Antitumor mechanisms of spirostanol type steroidal saponins (Proteins circled by red dashed lines represent distinct signals of the same antitumor mechanism).

a. Mechanism of apoptosis of tumor cells induced by spirostanol steroidal saponins. **b**. Mechanism of inhibition of tumor migration and invasion by spirostanol steroidal saponins. **c**. Mechanism of tumor cell autophagy induced by spirostanol type steroidal saponins. **d**. Overcoming mechanisms of drug resistance in tumor cells by spirostanol type steroidal saponins. **e**. Mechanism of cell cycle arrest induced by spirostanol type steroidal saponins in tumors.

Figure 4. Antitumor mechanisms of isospirostanol type steroidal saponins (Proteins circled by red dashed lines represent distinct signals of the same antitumor mechanism).

a. Mechanism of tumor cell apoptosis induced by isospirostanol type steroidal saponins.

b. Mechanisms of tumor migration, invasion and angiogenesis inhibition by isospirosterol steroidal saponins. **c.** Mechanism of tumor cell autophagy induced by isospirostanol type steroidal saponins. **d.** Overcoming mechanisms of drug resistance in tumor cells by isospirostanol type steroidal saponins. **e.** Mechanism of cell cycle arrest induced by isospirostanol type steroidal saponins in tumors.

Figure 5. Antitumor mechanism of furostanol steroidal saponins (Proteins circled by red dashed lines represent distinct signals of the same antitumor mechanism).

Mechanism of tumor cell apoptosis induced by furostanol type steroidal saponins.

Figure 6. Antitumor mechanism of steroidal alkaloids (Proteins circled by red dashed lines represent distinct signals of the same antitumor mechanism).

a. Mechanism of tumor cell apoptosis induced by steroidal alkaloids. **b.** Mechanism of inhibition of tumor migration and invasion by steroidal alkaloids.

Figure 7. Antitumor mechanisms of cholestane glycosides (Proteins circled by red dashed lines represent distinct signals of the same antitumor mechanism).

Mechanism of cholestane glycosides induced cell apoptosis and inhibition of tumor migration and invasion.

Figure 8. Cytotoxicity and bioavailability of steroidal saponins (Independent Samples t-test, **p＜0.01).

a. Comparison of cytotoxicity and antitumor activity of steroidal saponins. **b.** Comparison of steroidal saponin bioavailability and clinical drug bioavailability.

Figure 9. Strategies to improve the shortcomings of steroidal saponins.

a. Strategies for reducing the cytotoxicity of steroidal saponins. **b.** Strategies to improve

the bioavailability of steroidal saponins. **c.** Strategies for improving the yields of steroidal saponins.

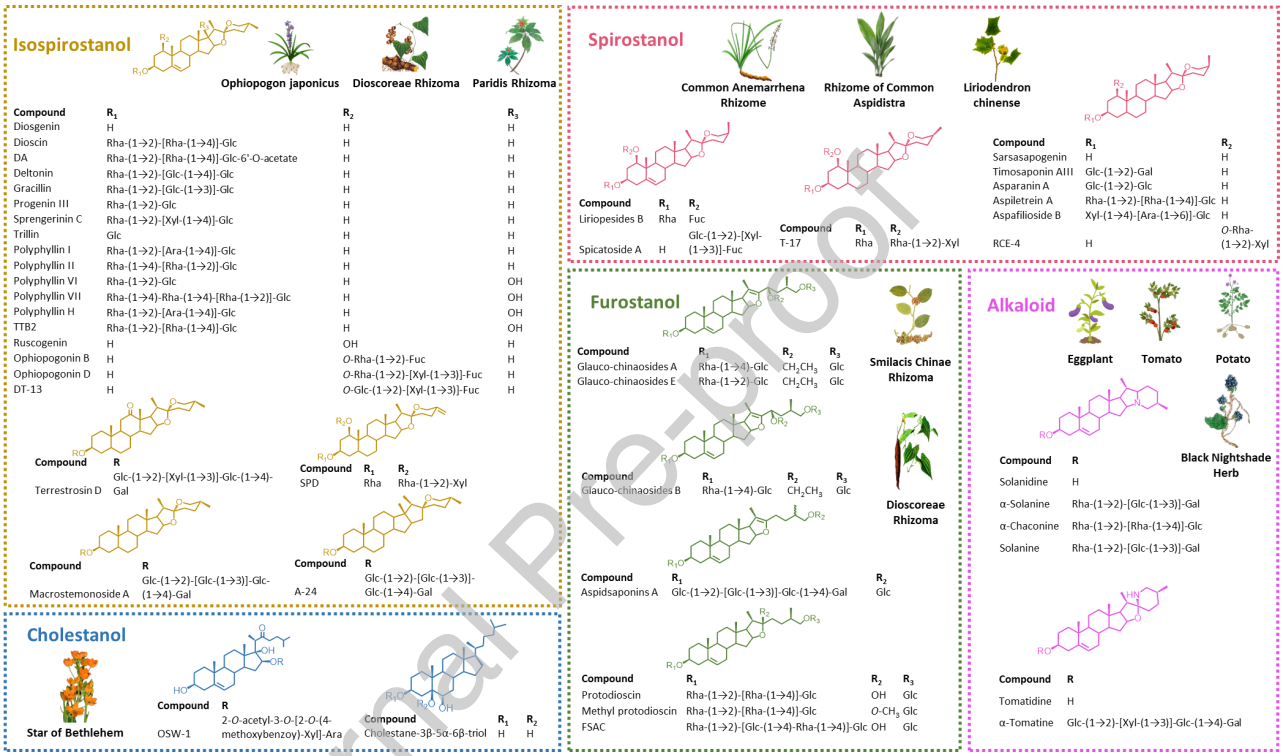

Figure 1

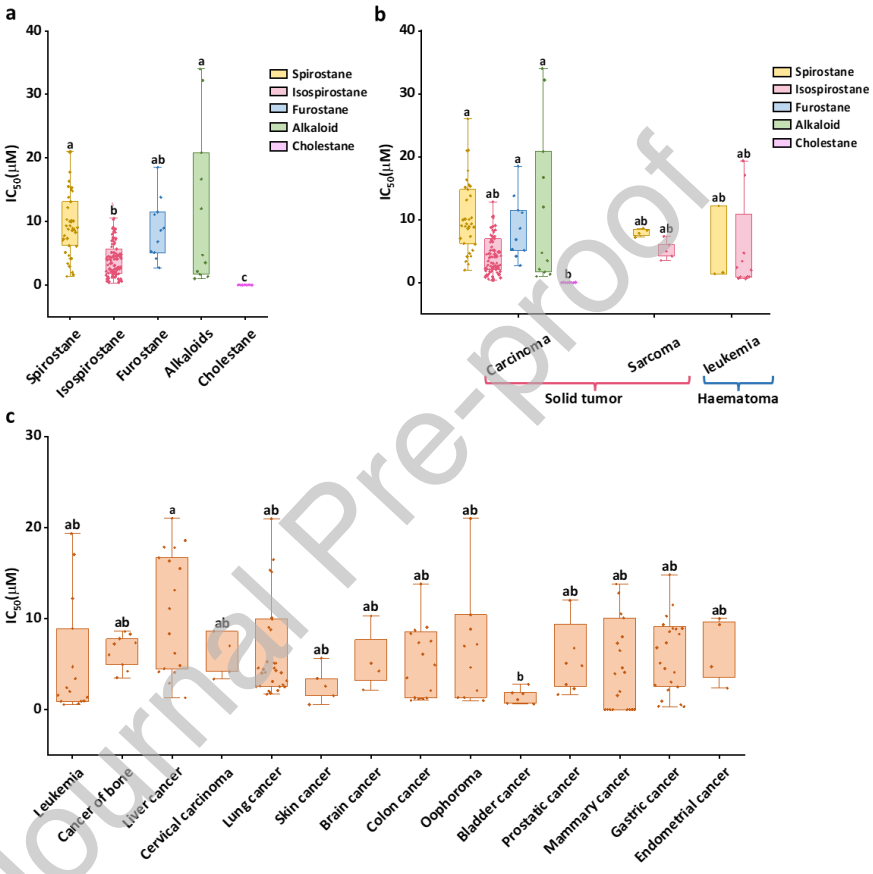

Figure 2

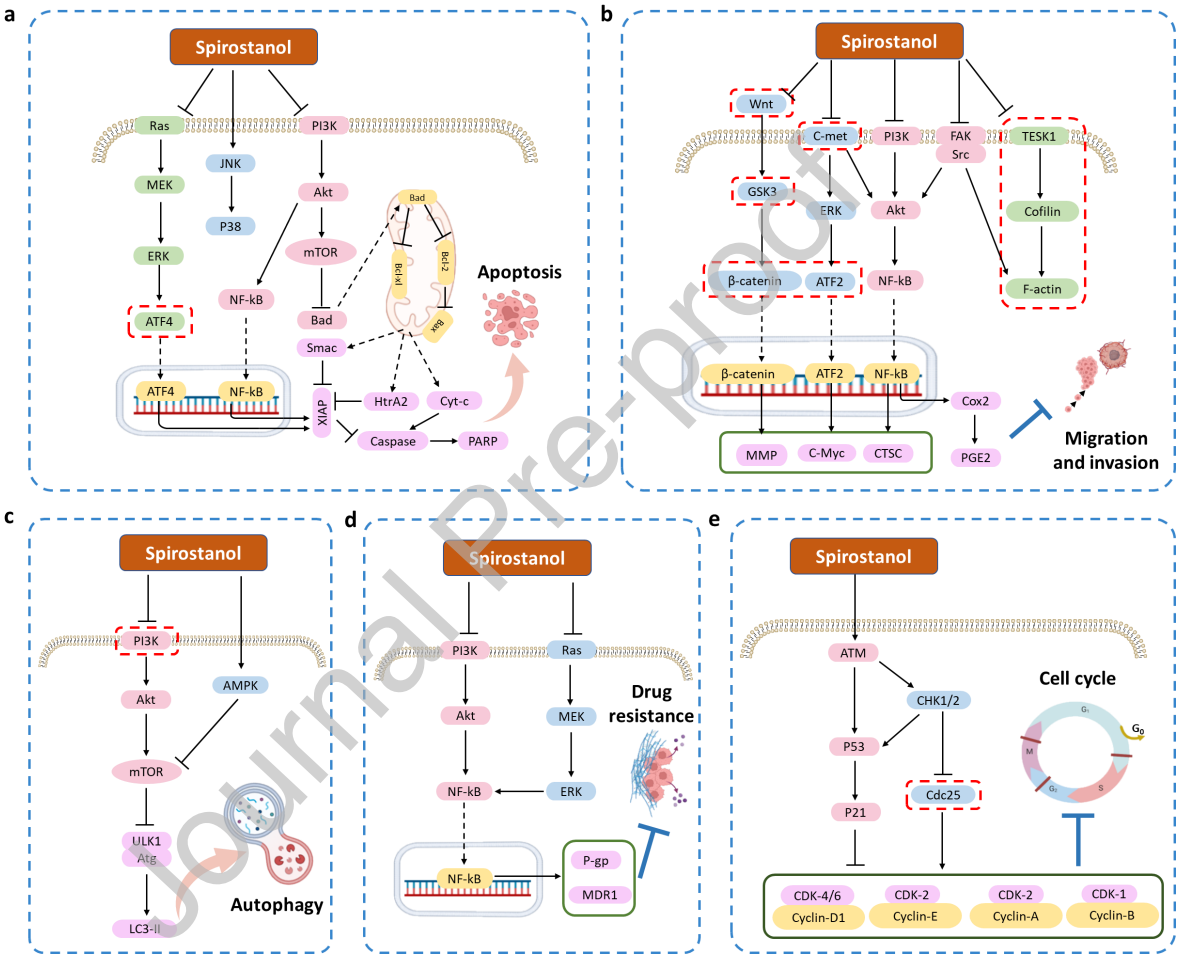
a
Spirostanol
Ras
PI3K
JNK
MEK
Akt
P38
ERK
mTOR
NF-kB
ATF4
Bad
Smac
Bad
Bcl-xl
Bcl-2
Bax
Apoptosis
ATF4
NF-kB
XIAP
HtrA2
Cyt-c
Caspase
PARP
b
Spirostanol
Wnt
C-met
PI3K
FAK
Src
TESK1
GSK3
ERK
Akt
Cofilin
β-catenin
ATF2
NF-kB
F-actin
β-catenin
ATF2
NF-kB
Cox2
MMP
C-Myc
CTSC
PGE2
Migration
and invasion
c
Spirostanol
PI3K
AMPK
Akt
mTOR
ULK1
Atg
LC3-II
Autophagy
d
Spirostanol
PI3K
Ras
Akt
MEK
ERK
NF-kB
Drug
resistance
NF-kB
P-gp
MDR1
e
Spirostanol
ATM
CHK1/2
P53
P21
Cdc25
Cell cycle
CDK-4/6
Cyclin-D1
CDK-2
Cyclin-E
CDK-2
Cyclin-A
CDK-1
Cyclin-B

Figure 3

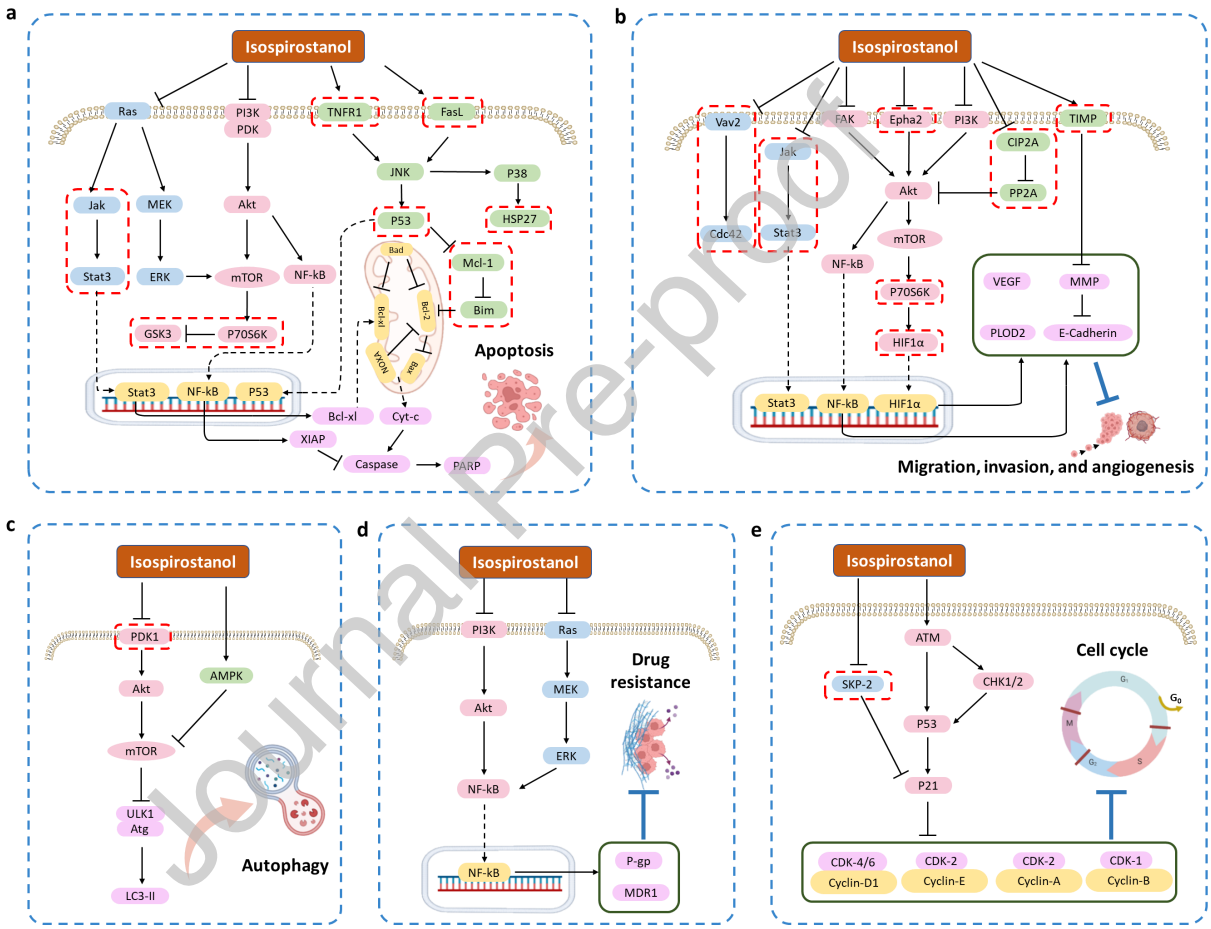
a
Isospirostanol
Ras
PI3K
PDK
TNFR1
FasL
JNK
P38
Jak
MEK
Akt
P53
HSP27
Stat3
ERK
mTOR
NF-kB
Mcl-1
Bad
Bcl-xl
Bcl-2
Bim
GSK3
P70S6K
NOXA
Bax
Apoptosis
Stat3
NF-kB
P53
Bcl-xl
Cyt-c
XIAP
Caspase
PARP
b
Isospirostanol
Vav2
FAK
Epha2
PI3K
TIMP
CIP2A
Jak
Akt
PP2A
Cdc42
Stat3
mTOR
NF-kB
VEGF
MMP
P70S6K
PLOD2
E-Cadherin
HIF1α
Stat3
NF-kB
HIF1α
Migration, invasion, and angiogenesis
c
Isospirostanol
PDK1
Akt
AMPK
mTOR
ULK1
Atg
LC3-II
Autophagy
d
Isospirostanol
PI3K
Ras
MEK
Akt
ERK
NF-kB
NF-kB
Drug resistance
P-gp
MDR1
e
Isospirostanol
ATM
SKP-2
CHK1/2
P53
P21
Cell cycle
CDK-4/6
Cyclin-D1
CDK-2
Cyclin-E
CDK-2
Cyclin-A
CDK-1
Cyclin-B

Figure 4

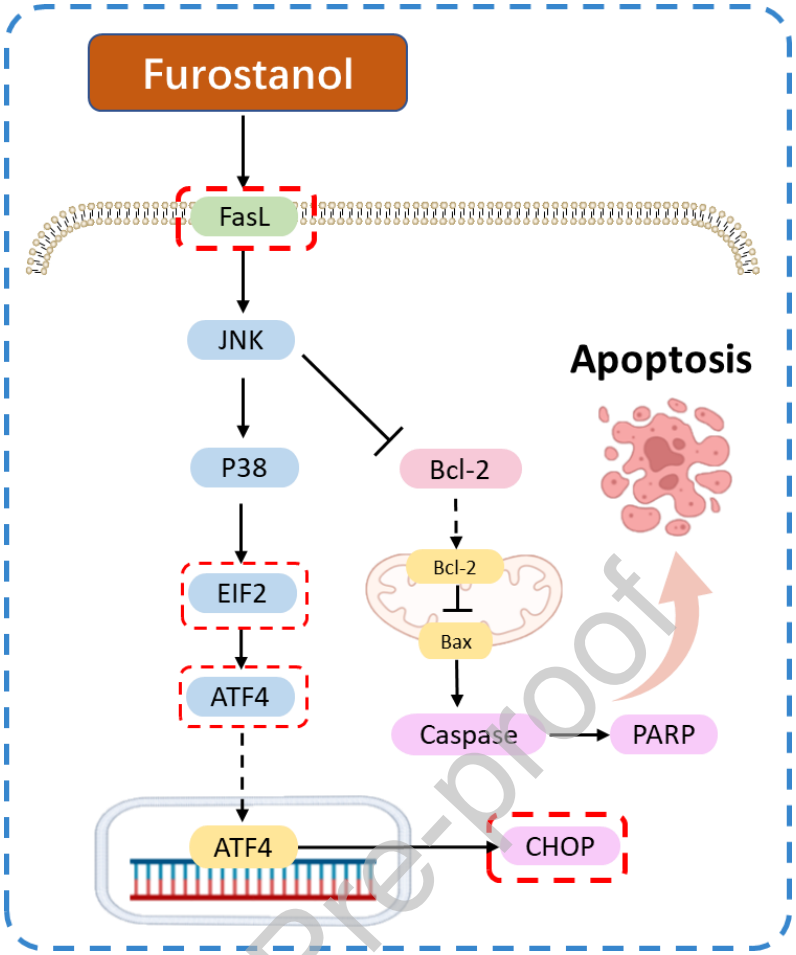

Figure 5

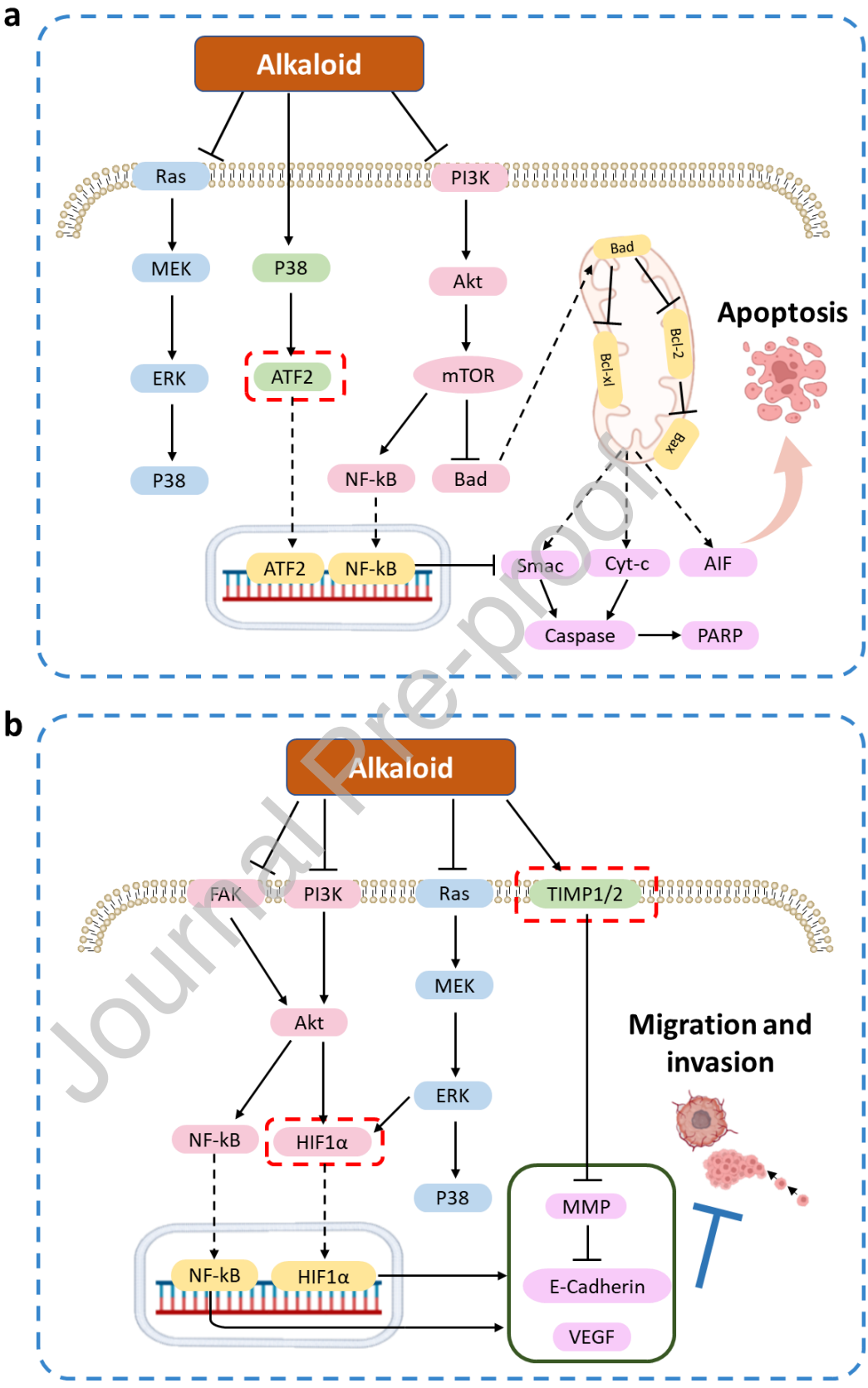

Figure 6

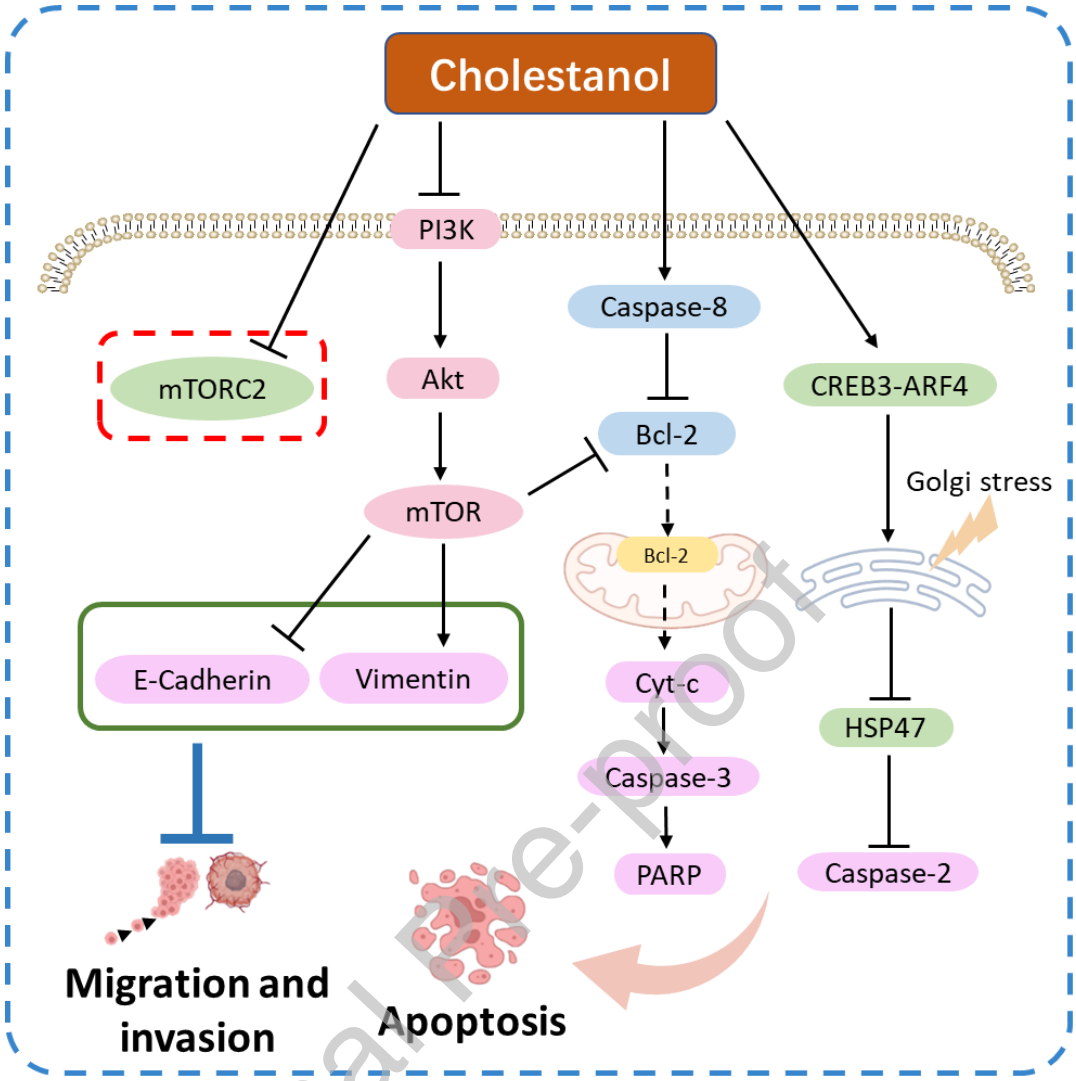

Figure 7

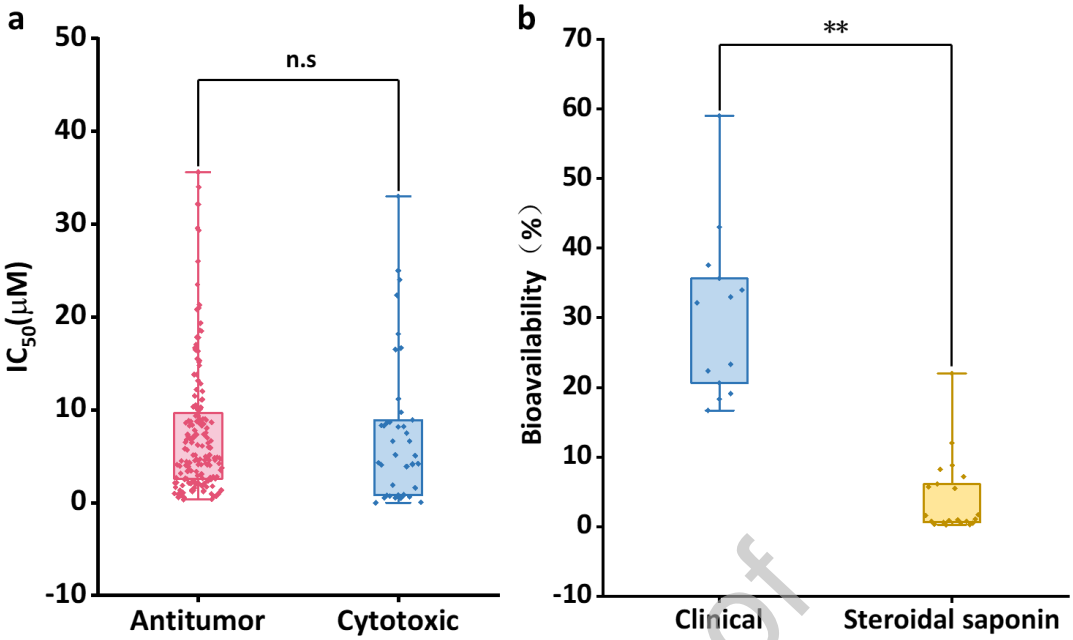

Figure 8

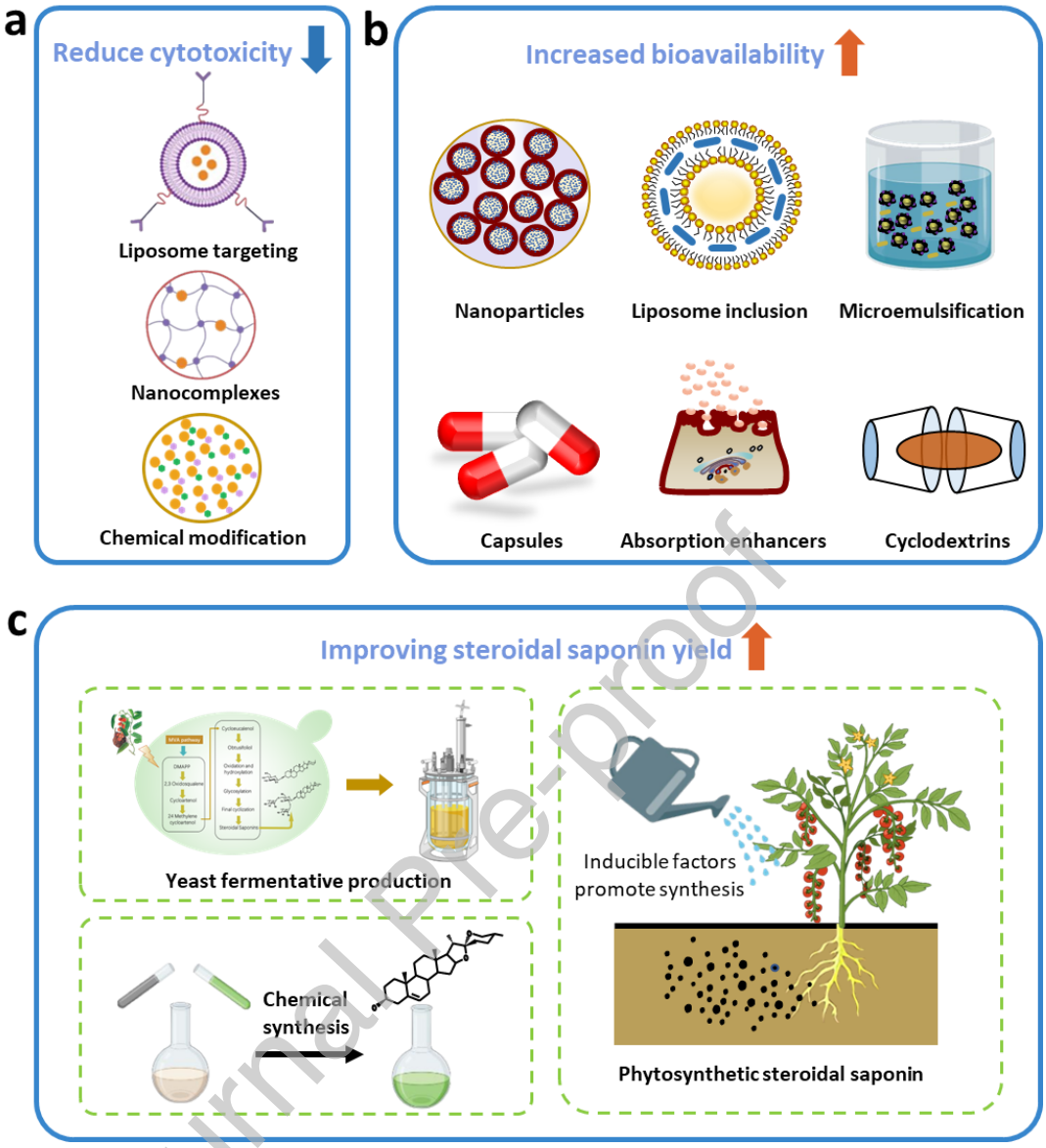

Figure 9

Declaration of Interest Statement

We declare that there are no conflicts of interest in this article